

https://dspace.org/

Synthesis of dimethyl ether using natural gas as a feed via the C-H-O ternary diagram

Masindi, Andisani

2017

http://hdl.handle.net/10539/22960

Masindi, Andisani (2017) Synthesis of dimethyl ether using natural gas as a feed via the C-H-O ternary diagram, University of the Witwatersrand, Johannesburg, <http://hdl.handle.net/10539/22960>

Downloaded from a DSpace repository. https://dspace.org/

SYNTHESIS OF DIMETHYL ETHER USING NATURAL GAS AS A FEED VIA THE C-H-O TERNARY DIAGRAM

Andisani Masindi (301241)

A dissertation submitted to the faculty of Engineering and the Built Environment, University of the Witwatersrand, in fulfilment of the requirements for the degree of Master of Science in Engineering – Chemical Engineering

Johannesburg, 2017

Declaration

I declare that this dissertation submitted for masters in chemical engineering (part time) is my own unaided work except for where I have explicitly indicated otherwise. I have followed the required conventions in referencing the thoughts and ideas of others and understand that the University of Witwatersrand may take disciplinary action against me if there is belief that this is not my own aided work or that I have failed to acknowledge the source of the ideas or words in my writing.



(Signature of candidate)

On the 6th day of February 2017

Abstract

In this research, the C, H and O bond equivalent diagram was used to design processes for DME synthesis using natural gas as a feed. This research proposes alternative ways of producing DME using natural gas (a cleaner gas) compared to the traditional routes.

The different feed combinations were assessed for the production of syngas. The crucial step is the H_2:CO ratio in each feed which determines the DME synthesis process route and yield.

The syngas process was developed under equilibrium and non-equilibrium conditions (assuming 100% methane conversion). The region of operation on the ternary bond diagram was limited by mass and energy balance and carbon deposition boundaries. The feed composition was as follows,

(1) Feed 1: methane, steam and oxygen

(2) Feed 2: methane, oxygen and carbon dioxide

(3) Feed 3: methane, oxygen, carbon dioxide and water.

Feed (2) had the highest DME yield. The most optimal reaction route produced DME via the JFE reaction route (H_2:CO =1). The yield of DME was 0.67 moles of DME per mole methane processed under non-equilibrium conditions. The proposed route does not emit CO_2, excess CO_2 is recycled back to the reforming reactor. Under equilibrium, the yield of DME was 0.25 mole DME per mole methane processed. The results indicate that a combination of partial oxidation and dry reforming produces a syngas composition which results in a high DME yield compared to (1) and (3).

Acknowledgements

I would like to express my deepest appreciation to the following persons:

- Shell SA refining for financing the dissertation and allowing me the opportunity to study part-time.
- Dr. Shehzaad Kauchali – my supervisor for his guidance, motivation and providing research insights
- My family and close friends for their motivation and fostering a spirit of hard work and perseverance during the entire duration of the research

Contents

Declaration i
Abstract ii
Acknowledgements iii
List of Figures vii
List of Tables ix
List of Symbols x
1. Introduction 1
1.1 Background 1
1.2 Aims and Objectives 2
2.Literature review 4
2.1 Natural Gas Reforming Technologies 4
2.1.1 Steam Reforming 5
2.1.2 Partial Oxidation (POx) 5
2.1.3 Auto thermal Reforming (ATR) 7
2.1.4 Dry gas reforming 8
2.2 DME Synthesis 10
2.2.1 Properties of Dimethyl Ether 10
2.2.2 Direct and Indirect DME synthesis 11
2.2.3 Effect of nature and type of catalyst on DME synthesis 17
2.2.4 Effect of operating conditions and feed composition on DME synthesis and yield 19
2.3 Summary 22
3. The Ternary Bond Equivalent Diagram 24
3.1 History of Ternary Bond Equivalent Diagram 24
3.2 Constructing the Ternary Bond Equivalent diagram 25
4. Graphical representation of the different reforming reaction routes 28
4.1 Graphical representation of the stoichiometric region for each feed 30
4.1.1 Stoichiometric region for Feed 1 30
4.1.2 Stoichiometric region for feed 2 31
4.1.3 Stoichiometric region for feed 3 32
4.2 Thermally balanced operation 33
4.2.1 Thermal balance line of operation for feed 1 33
4.2.2 Thermal balance line of operation for feed 2 34
4.2.3 Thermal balanced line of operation for feed 3 35

4.3 Summary 36
5. The DME synthesis process 37
5.1 DME synthesis using Feed 1 37
5.1.1 DME synthesis process routes 39
5.1.2 Summary of all reaction routes 43
5.2 DME synthesis using Feed 2 45
5.2.1 DME synthesis process routes 47
5.2.2 Summary of all reaction routes 56
5.3 Summary 58
6. Carbon Deposition Boundaries 60
6.1 Carbon deposition boundary – feed 1 61
6.2 Carbon deposition boundary – Feed 2 63
6.3 Summary 65
7. Modelling Chemical Equilibrium 66
7.1 Modelling Equilibrium – Feed 1 66
7.1.1 Analysing Equilibrium for feed 1 66
7.1.2 DME synthesis using feed 1 70
7.1.3 Summary of all reaction routes 73
7.2 Modelling Equilibrium feed 2 74
7.2.1 Analysing Equilibrium for feed 2 74
7.2.2 DME synthesis using feed 2 77
7.2.3 Summary of all reaction routes 83
7.3 Modelling Equilibrium Feed 3 84
7.3.1 Analyzing Equilibrium for feed 3 84
7.3.2 DME synthesis using feed 3 86
7.4 Comparison of Equilibrium results to Non-Equilibrium results 88
7.4.1 Comparing results for feed 1 88
7.4.2 Comparing results for feed 2 90
8. Conclusion 92
References 94
Appendix 98
Appendix A: Bond Equivalent percentages and using the CHO diagram 98
A1: Calculating the Bond Equivalent percentages 98
A2: Using the CHO diagram to represent a separation process 98
Appendix B: The thermal balanced lines 100

B1: Determining the thermal balanced line for Feed 1 100
B2: Thermal Balance points feed 2 102
B3: Thermal Balance points feed 3 102
Appendix C: Testing for the value of alpha to adjust the H_2:CO ratio for each feed within the stoichiometric region 103
Appendix D: Carbon Deposition Boundaries 104

List of Figures

Figure 2 : Synthesis gas production by adiabatic pre-reforming and Autothermal reforming (Aasberg-Petersen *et al.*, 2002) 8
Figure 3: DME Production (Azizi et al., 2014) 12
Figure 4: Process Flow Diagram of DME synthesis – The JFE 100 tpd pilot plant (Yotaro, et al., 2006) 12
Figure 5: Indirect DME synthesis (Azizi et al.,2014) 16
Figure 1 : Dual type reactor configuration (Vakili, et al., 2012) 22
Figure 6 : C, H and O diagram and reaction trajectories (Battaerd & Evans, 1979) 26
Figure 7 : Stoichiometric region for feed 1 30
Figure 8 : Ternary Diagram for Feed 2 31
Figure 9 : Ternary Diagram for Feed 3 32
Figure 10: Thermal balance line for feed 1 34
Figure 11: Thermal balance line for feed 2 35
Figure 12: Thermal balance line for feed 3 36
Figure 13 : DME synthesis using Feed 1 39
Figure 14 : Process Flow diagram for DME synthesis using feed 1 – Option 1a 40
Figure 15 : Process flow diagram for DME synthesis using feed 1 option 1b 41
Figure 16 : Process Flow diagram for DME synthesis using feed 1 – Option 2a 42
Figure 17 : Process Flow diagram for DME synthesis using feed 1 – Option 2b 43
Figure 18 : DME synthesis using Feed 2 46
Figure 19 : Process Flow diagram for DME synthesis using feed 2 – Option 1a 48
Figure 20 : Process Flow diagram for DME synthesis using feed 2 – Option 1b 49
Figure 21 : Process Flow diagram for DME synthesis using feed 2 – Option 1c 50
Figure 22 : Process Flow diagram for DME synthesis using feed 2 – Option 2a 51
Figure 23 : Process Flow diagram for DME synthesis using feed 2 – Option 2b 52
Figure 24 : Process Flow diagram for DME synthesis using feed 2 – Option 2c 53
Figure 25 : Process Flow diagram for DME synthesis using feed 2 – Option 3a 54
Figure 26 : Process Flow diagram for DME synthesis using feed 2 – Option 3b 55
Figure 27: Comparison of reaction routes for feed 2 - Option 1 57
Figure 28 : Carbon-deposition boundaries – Feed 1 @ 1 atm represented as BE percentages of the equilibrium state 61

Figure 29 : Carbon Deposition Boundary – Feed 2 @ 1 atm represented as BE percentages of the equilibrium state 63
Figure 30 : Conversion of methane over a temperature range 500K to 1300K at a steam to carbon ratio of 2. 68
Figure 31 : Conversion of methane over a temperature range 500K to 1300K at an oxygen to carbon ratio of 1. 69
Figure 32 : Modelling Equilibrium – Feed 1 70
Figure 33 : Modelling Equilibrium - Process flow diagram for DME synthesis using feed 1 option 1.....72
Figure 34 : Conversion of methane over a temperature range 500K to 1300K at an oxygen to carbon ratio of 1.5 75
Figure 35 : Modelling Equilibrium – Feed 2 77
Figure 36 : Modelling Equilibrium - Process flow diagram for DME synthesis using feed 2 option 1.....79
Figure 37 : Modelling Equilibrium - Process flow diagram for DME synthesis using feed 2 option 1b.....80
Figure 38 : Modelling Equilibrium - Process flow diagram for DME synthesis using feed 2 option 2.....81
Figure 39 : Modelling Equilibrium - Process flow diagram for DME synthesis using feed 2 option 3.....82
Figure 40 : Conversion of methane over a temperature range 500K to 1300K at an oxygen to carbon ratio of 0.5. 85
Figure 41 : Conversion of methane over a temperature range 500K to 1300K at a carbon dioxide to methane ratio of 1. 86
Figure 42 : Modelling Equilibrium – Feed 3 87
Figure 43 : Using the CHO diagram to represent a separation process.....98
Figure 44 : Carbon deposition boundaries at 1 atm, represented as BE percentages of the equilibrium state.....104

List of Tables

Table 1 : Typical Natural Gas composition 4
Table 2 : Reaction species for each feed 28
Table 3 : TBL point A-D and their respective H_2:CO ratio for feed 1 38
Table 4 : A Summary of all Options for Feed 1 43
Table 5 : Point A, D and E on TBL for Feed 2 together with their respective H_2:CO ratios 45
Table 6: Summary of all reaction routes for feed 2 56
Table 7 : A Summary of all Options for Feed 1 and Feed 2 59
Table 8 : H_2:CO ratio for feed 1 at Chemical Equilibrium vs. H_2:CO ratio @ 100% CH_4 conversion 67
Table 9 : Thermal balance point A-D and amount excess hydrogen required 71
Table 10 : Modelling Equilibrium Summary of options for feed 1 73
Table 11 : H_2:CO ratio for feed 2 at Chemical Equilibrium vs. H_2:CO ratio @ 100% CH_4 conversion 76
Table 12 : Modelling equilibrium summary of options for feed 2 83
Table 13 : H_2:CO ratio for feed 3 at Chemical Equilibrium vs. H_2:CO ratio @ 100% CH_4 conversion 84
Table 14: Comparison of equilibrium and non-equilibrium results for feed 1 89
Table 15: Comparison of equilibrium and non-equilibrium results for feed 2 90
Table 16 : BE % for point D – Feed 2 99
Table 17 : BE% for point K after removing 0.58 moles water from the composition at point D 99
Table 18 : Balancing endothermic reactions with exothermic reactions for feed 1 100
Table 20 : Calculating BE percentage for Feed 1-point D 101
Table 21: Thermal balance points for feed 1 101
Table 22 : Thermal balance points for feed 2 102
Table 23 : Thermal balance points for feed 3 102
Table 24 : Carbon deposition boundaries at 1 atm and temperature range 800K to 1500K (Tay, et al., 2011) 105

List of Symbols

CH_4	Methane
H_2	Hydrogen
O_2	Oxygen
CO	Carbon Monoxide
CO_2	Carbon dioxide
H_2O	Water
DME	Dimethyl Ether
CH_3OCH_3	Dimethyl Ether
GTL	Gas to liquid
GTG	Gas to Gas
Mb/day	Million barrels per day
CHO	Carbon, Hydrogen and Oxygen system
H_2:CO	Hydrogen to carbon monoxide molar stoichiometric ratio
H_2:CO_2	Hydrogen to carbon dioxide molar stoichiometric ratio
WGS	Water-Gas-Shift reaction
RWGS	Reverse Water-Gas-Shift reaction
Syngas	Synthesis gas
ΔHrn	Heat of reaction of products – heat of reaction of reactants

1. Introduction

1.1 Background

Coal, oil and natural gas account for 85% of the world's primary energy (Economides & Wood, 2009). These fossil fuels can be used interchangeably but with varying efficiencies. Coal is the cheapest of these fossil fuels and has been the primary energy source for power generation for centuries. Coal contributes 72% of the total energy consumption in South Africa followed by crude oil (BP, 2012). Energy utility, Eskom generates 85% of its electricity from coal. Other players such as Sasol also use coal intensively in their synthesis gas production processes. This contributes to making South Africa the largest emitter of carbon dioxide on the African continent.

On the other hand, crude oil plants contribute 72% of South Africa's total refining capacity, and all the crude oil is imported. This makes South Africa vulnerable to oil price fluctuations. Furthermore, environmental regulations on the allowable sulphur content on both petrol and diesel have become stricter requiring refineries to upgrade their process units or install new hydro treating units which require a high capital expenditure and a high cost of operating the unit (Eduardo, et al., 2005)

Based on the above there is a growing need to pursue cleaner energy sources and natural gas provides a cleaner and better alternative. The synthetic fuels produced from natural gas have a zero sulphur content compared to the products obtained from crude oil eliminating the need for further treatment. Furthermore, natural gas results in low carbon dioxide emissions compared to coal when processed. If natural gas can be gradually introduced, it can reduce SA's dependence on imports and also contribute to a cleaner environment.

Southern Africa has an opportunity to shift towards increasing the use of natural gas because of the recent shale gas discovery in the Karoo, coal-bed methane in the Kalahari basin in 2006 and new licenses awarded in 2012 for oil and gas exploration in the Orange River basin.(ATKearney, 2013)

Natural gas can be transformed into synthesis gas via different reforming technologies such as steam reforming, partial oxidation as well as dry reforming. The synthesis gas can either follow a route traditionally known as gas to liquid (GTL), where liquid fuels equivalent to products

obtained from a crude oil refinery are produced or it can follow the gas to gas route (GTG) where the syngas produced reacts to form other gases – e.g. dimethyl ether (DME).

The focus of this research will be on the synthesis of DME using syngas obtained from natural gas reforming. A graphical technique method known as the CHO ternary bond equivalent diagram will be used to develop a conceptual process for natural gas conversion to produce syngas which meets the ratio of hydrogen to carbon monoxide (H_2:CO) required for DME synthesis. The different routes will be assessed on the amount of carbon dioxide emissions produced, the yield of DME per mole methane processed, heat requirement, as well as any other waste products in the system.

1.2 Aims and Objectives

The aim of this research is therefore to:

Use a conceptual and systematic method of process design to develop a process which utilises natural gas as a feed to produce DME (gas to gas transformation). The objectives are to:

- Use the ternary bond equivalent diagram to analyse a combination of different feeds which contain methane for syngas production
- Identify the feasible region of operation for each feed using mass balances
- Determine the thermal balance line of operation for each feed by balancing endothermic and exothermic reactions
- Use the feasible region of operation to design processes for DME synthesis taking into consideration the syngas composition, in particular the stoichiometric ratio of H_2:CO
- Test the obtained results under conditions of carbon formation by using carbon-deposition boundaries to identify regions of no carbon formation (At certain temperatures carbon may form affecting the product yield and may also block catalyst sites)
- Analyse a separate system which considers chemical equilibrium and compare the yield of DME under equilibrium and non-equilibrium conditions
- Different processes for each feed will be compared and analysed based on the yield of DME per mole of methane, carbon dioxide emissions, energy requirement as well as the complexity of the process (need for one or more separators, recycle stream etc.).

To achieve the objectives, the initial chapter (literature review) discusses different natural gas reforming technologies for synthesis gas production. This is followed by the DME synthesis process covering the direct and indirect method. The research will expand to cover developments and progress made in improving the synthesis of DME using the direct synthesis method. This will cover (i) areas in catalysis to show progress made (ii) effect of reactor feed composition and operating conditions on DME synthesis. The latter will be the main focus of the research.

The methodology applied will be introduced (chapter 3) together with a graphical representation of reforming reactions to determine the feasible region of operation (chapter 4). Chapter 5 focuses on developing processes for DME synthesis from syngas assuming 100% methane conversion whereas chapter 6 considers the formation of solid carbon further restricting the feasible region of operation obtained in chapter 4. Chapter 7 models the results under equilibrium conditions.

2. Literature review

DME can be produced from different sources such as biomass, coal and natural gas etc. This chapter introduces the different natural gas reforming technologies as well as developments in the Direct and Indirect DME synthesis methods.

2.1 Natural Gas Reforming Technologies

Natural gas is formed when layers of plants and animals are exposed to intense heat and pressure over thousands of years, the layers of plant and animal matter continue to build up until intense pressure and heat turns them into oil and natural gas. Natural gas can be used for combined heat and power (CHP) cycle turbines during electricity generation with improved efficiencies and low carbon dioxide emissions, it can also be used as a transportation fuel and heating fuel.

Natural gas treating/ processing is an important step before using the gas. The gas usually contains element Hydrogen (H), Carbon(C) and Oxygen (O), and a small amount of contaminants (Nitrogen (N), Sulphur (S) and rare gases). Table 1 shows typical Natural gas composition.

Typical Natural Gas composition		
Methane	CH_4	70-90%
Ethane	C_2H_6	
Propane	C_3H_8	0-20%
Butane	C_4H_{10}	
Carbon Dioxide	CO_2	0-8%
Oxygen	O_2	0-0.2%
Nitrogen	N_2	0-5%
Hydrogen sulphide	H_2S	0-5%
Rare gases	A,He, Ne, Xe	Trace

Table 1 : Typical Natural Gas composition

Natural Gas can be converted to useful products by using the following well established technologies:

2.1.1 Steam Reforming

The predominant commercial technology for syngas generation has been and continues to be steam methane reforming (SMR) (Wilhelm et al., 2001; Barelli et al., 2008; Al-Sayari, 2013; Lyubovsky, 2005). Steam reforming is widely used for Methanol and ammonia synthesis (Vernon *et al.*, 1990). Natural gas is reacted with steam in the presence of a catalyst to produce syngas with the ratio of H_2:CO of 3: 1 via the following chemical reaction:

$$\mathbf{CH_4 + H_2O \leftrightarrow 3H_2 + CO} \qquad \mathbf{206\,\frac{kJ}{mol}} \qquad \text{Equation 2.1}$$

$$\mathbf{CH_4 + 2H_2O \leftrightarrow 4H_2 + CO_2} \qquad \mathbf{165\ \frac{kJ}{mol}} \qquad \text{Equation 2.2}$$

The reaction is highly endothermic and takes place at temperatures of 800 degrees to 900 degrees Celsius and pressures of 15-30 atm. The effluent gas from the reformer normally contains 76% H_2, 13% CH_4, 12% CO and 10% CO_2- on a molar basis (Barelli et al., 2003). The steam reformer is usually followed by the water-gas shift reaction in order to adjust the H_2:CO ratio depending on the synthesis gas end use. (Lyubovsky, 2005).

$$\mathbf{H_20 + CO \leftrightarrow CO_2 + H_2} \qquad \mathbf{-41\ \frac{kJ}{mol}} \qquad \text{Equation 2.3}$$

The reaction is exothermic and is favoured by low temperatures. The water-gas shift reactor is kept at temperatures around 300-400 degrees Celsius to favour the reaction. The ratio can be reduced by recycling carbon-dioxide and removing excess hydrogen by means of membranes. However, for hydrogen production a high H_2:CO ratio in the syngas is desired.

The advantage of using SMR technology is that there is no oxygen requirement and has the lowest process temperature requirement (below 900 degrees Celsius). On the other hand, the disadvantage of having a maximum operating temperature of below 900 degrees is that it limits methane conversion. It is common practice to add a secondary reforming stage in which oxygen or carbon dioxide can be used as oxidants to improve the methane conversion and reduce the hydrogen content (Vernon et al., 1990).

2.1.2 Partial Oxidation (POx)

This is the exothermic reaction of methane and oxygen to produce a mixture of hydrogen and carbon monoxide at a stoichiometric ratio of 2:1 in a single step reaction.

$$\mathbf{CH_4 + 1/2\,O_2 \rightarrow CO + 2\,H_2} \qquad \mathbf{36\ \frac{kJ}{mol}} \qquad \text{Equation 2.4}$$

This reaction is favoured thermodynamically at temperatures greater than 900 degrees in excess methane. However, the selectivity is affected by the formation of water and carbon dioxide in total oxidation reactions which are more exothermic (Bharadwaj & Schmidt, 1995). Therefore, the product composition at the reactor exit is determined by the thermodynamic equilibrium of all participating species in the process.

$$\mathbf{CH_4 + 3/2\,O_2 \rightarrow 2H_2O + CO} \qquad \mathbf{-519\ \frac{kJ}{mol}} \qquad \text{Equation 2.4}$$

$$\mathbf{CH_4 + 2O_2 \rightarrow 2H_2O + CO_2} \qquad \mathbf{-802.5\ \frac{kJ}{mol}} \qquad \text{Equation 2.5}$$

The partial oxidation of methane has been applied in catalytic and non-catalytic environments. The non-catalytic reaction has excessive temperatures, long residence times as well as excessive coke formation. The coke formation makes the reaction uncontrollable (Vosloo, 2001; Al-Sayari, 2013; Bharadwaj & Schmidt, 1995). On the other hand, the catalytic reaction has low residence times and is relatively inexpensive (Lyubovsky, 2005).

Shell produces syngas by partial oxidation of natural gas with pure oxygen in the Shell Gasification Process (SGP), the technology is based on non-catalytic thermal partial combustion with pure oxygen without any steam injection, achieving a carbon efficiency greater than 95% and a high conversion with a methane slip of about 1% and a high selectivity in the formation of the valuable product (about 2% carbon formation) (Overtoom et al., 2009).

Lyubovsky et al., (2005) demonstrated the catalytic partial oxidation of methane into syngas at pressures up to 0.8 MPA, power densities up to 15 MW/land selectivity greater than 85%. The product composition profiles indicated high initial selectivity to carbon monoxide and low initial selectivity to hydrogen. This suggests that direct partial oxidation of methane is primarily into carbon monoxide, the selectivity to hydrogen occurs during steam reforming of methane. This supports why POx has a low natural H_2:CO stoichiometric ratio than SMR. The two technologies can be combined to achieve the required H_2:CO ratio for a wide range of applications using Autothermal Reforming (ATR).

The advantage of POx is that it produces syngas with a H_2:CO ratio of 2:1, which is close to the ratio required for F-T reaction and methanol synthesis (Zhu & Flytzani- Stephanopoulos, 2001). In order to use this technology for other applications, the H_2:CO stoichiometric ratio

needs to be adjusted. This can be achieved by a combination of different steam reforming technologies.

Bharadwaj & Schmidt (1995) demonstrated that direct oxidation process in Autothermal reactors has a low residence time (requiring small reactors and can save investment costs). The oxygen requirement and very high process operating temperatures is however a disadvantage. The technology has also not been commercialized yet because it involves pre-mixing of methane and oxygen mixtures which do not provide for safe operation; they can be flammable or explosive. On the other hand, Steam reforming is a mature technology; the disadvantage is that it requires large heat exchange reactors demanding large initial investments (Lyubovsky et al., 2005).

2.1.3 Auto thermal Reforming (ATR)

The technology uses both steam and oxygen to produce syngas in the presence of a catalyst. The reaction automatically happens by virtue of the internal heat brought in by oxidation of the feed hydrocarbons (Bao et al., 2010). ATR has been identified as the preferred option for large scale, safe and economic synthesis gas production (Aasberg-Petersen *et al.*, 2002). ATR makes it possible to adjust the H_2:CO ratio. The ratio is achieved by re-circulating carbon-dioxide and reducing the amount of steam added to the hydrocarbon feedstock.

The reactions carried on ATR are shown below:

$$\mathbf{CH_4 + H_2O \leftrightarrow 3H_2 + CO} \qquad \mathbf{206\,\frac{kJ}{mol}} \qquad \text{Equation 2.6}$$

$$\mathbf{CH_4 + 2H_2O \leftrightarrow 4H_2 + CO_2} \qquad \mathbf{165\,\frac{kJ}{mol}} \qquad \text{Equation 2.8}$$

$$\mathbf{H_20 + CO \leftrightarrow CO_2 + H_2} \qquad \mathbf{-41.2\,\frac{kJ}{mol}} \qquad \text{Equation 2.7}$$

$$\mathbf{CH_4 + 3/2\,O_2 \rightarrow 2H_2O + C} \qquad \mathbf{-519\,\frac{kJ}{mol}} \qquad \text{Equation 2.8}$$

Figure 1 shows the autothermal reforming process for syngas production. In the pre-reformer stage, chemical reactions similar to SMR take place. At higher temperatures, less methane and more carbon monoxide are present in the equilibrium gas. Increasing the ratio of steam to carbon decreases the methane content (Dybkjaer, 1995). When operating at low steam to carbon ratios, the risk of soot formation is higher in the ATR reactor and whisker carbon

formation in pre-reformer stage (Aasberg-Petersen et al., 2002). Steam to carbon ratio limits depend on a number of factors: operating temperature, catalyst type, feed gas composition etc.

In the Autothermal reformer stage (see Figure 1), the unconverted methane is combined with carbon dioxide and reacted with oxygen to produce synthesis gas.

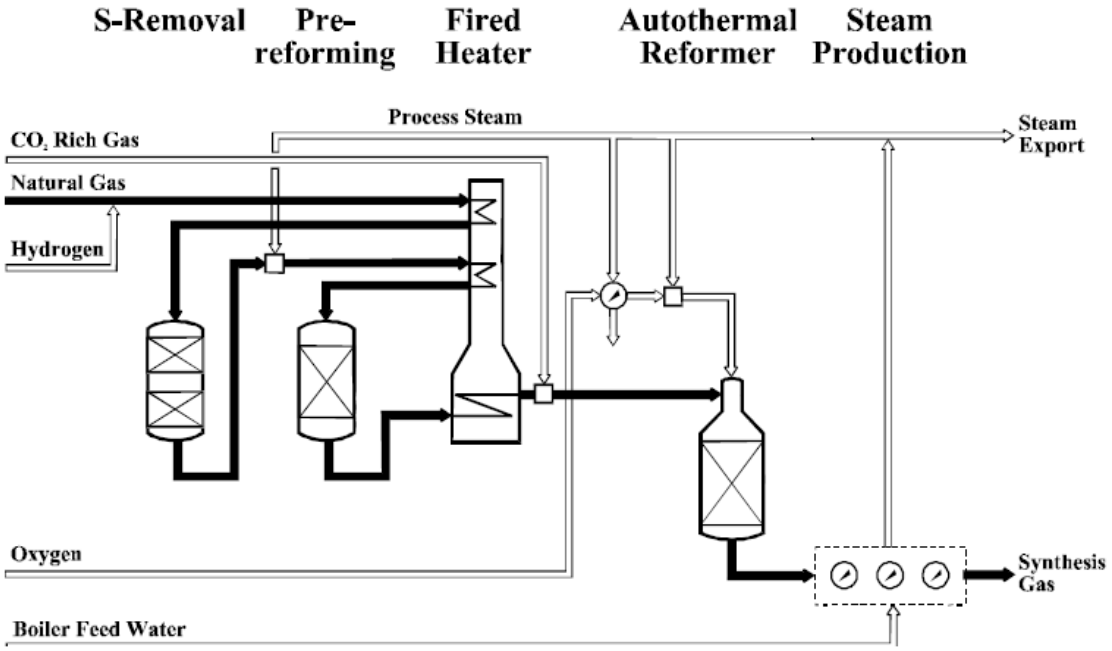


Figure 1 : Synthesis gas production by adiabatic pre-reforming and Autothermal reforming (Aasberg-Petersen *et al.*, 2002)

2.1.4 Dry gas reforming

In dry gas reforming, carbon dioxide is reacted with natural gas to produce a syngas mixture with a stoichiometric ratio of H_2:CO of 1:1. This ratio is much lower than that of steam reforming however suitable for the direct DME synthesis. The ratio is not suitable for methanol synthesis which requires a stoichiometric ratio of 2:1. The carbon dioxide methane reaction can be used for energy storage and transmission application.

Reforming methane using carbon dioxide as an oxidant has been used in many processes with other methane reforming technologies such as SMR. This is done to lower the H_2:CO ratio to that desired (Ashcroft et al., 1991; Edwards & Maitra, 1995).

Methane reaction with CO_2 as an oxidant follows the following reaction:

$$\mathbf{CH_4 + CO_2 \leftrightarrow 2H_2 + 2CO} \qquad \mathbf{247\,\frac{kJ}{mol}} \qquad \text{Equation 2.9}$$

However, this reaction is prone to carbon deposition (Ashcroft et al., 1991; Edwards and Maitra, 1995) via the following side reactions:

$$\mathbf{CH_4 \rightarrow C + 2H_2} \qquad \mathbf{75\,\frac{kJ}{mol}} \qquad \text{Equation 2.10}$$

$$\mathbf{2CO \rightarrow C + CO_2} \qquad \mathbf{-171\,\frac{kJ}{mol}} \qquad \text{Eqution 2.11}$$

(Boudouard reaction)

$$\mathbf{H_2 + CO_2 \rightarrow H_2O + CO} \qquad \mathbf{40\,\frac{kJ}{mol}} \qquad \text{Equation 2.12}$$

$$\mathbf{C + H_2O \leftrightarrow H_2 + CO} \qquad \mathbf{131\,\frac{kJ}{mol}} \qquad \text{Equation 2.13}$$

If reaction **12** is faster than the carbon removal reactions there will be a net build-up of carbon which will result in catalyst deactivation and reactor blockages (Edwards &Maitra, 1995).

Reforming methane using carbon dioxide as an oxidant has not been commercialised as a stand-alone technology however it has potential applications. The 1:1 ratio of H_2:CO enables the direct production of Dimethyl Ether (DME) via the following chemical reaction:

$$\mathbf{3CO + 3H_2 \leftrightarrow CH_3OCH_3 + CO_2} \qquad \text{Equation 2.14}$$

2.2 DME Synthesis

2.2.1 Properties of Dimethyl Ether

Dimethyl Ether (DME) belongs to the class of organic compounds that contain an ether group i.e. an oxygen atom connected to two alkyl groups given by the general formula R-O-R. It is a symmetrical ether and is the simplest ether with the chemical formula CH_3OCH_3. The boiling point of DME is -25 degrees Celsius (relatively low compared to that of other alcohols, this is because ether molecules cannot form hydrogen bonds with each other) and a vapour pressure of 5.1 atmosphere at 25 degrees. It is a volatile highly flammable liquid with physical properties similar to that of liquefied petroleum gases but different thermal properties. (Troy, et al., 2006) . DME is a gas at standard temperature and pressure and can be liquefied and handled similar to LPG hence new infrastructure is not required to transport and store DME because of its similarity to LPG.

DME is produced from a variety of sources such as biomass, landfills, and waste from paper and pulp mills, coal and natural gas making it a multi-feedstock product. An important process step in DME production is synthesis gas (CO and $H_{2)}$ production. Synthesis gas is obtained from various sources such as gasification of coal or biomass and natural gas reforming. Various technologies have been investigated over the years and DME has been traditionally produced by means of a two-step process: firstly, synthesis gas first converted to methanol and secondly, the dehydration of methanol to DME.

The total world production of DME was at 9 million tons per annum in 2010 and was primarily by means of methanol dehydration. (International Association of DME, 2010). China has the majority of DME production facilities. In Trinidad and Tobago, Indonesia and Uzbekistan constructions are underway. Sweden has the first bioDME plant.

DME has desirable combustion properties for use as a fuel and is considered to emit low emissions of particulate matter (NOx and SOx) compared to conventional diesel, it also has a high cetane number (55-60) compared to that of diesel obtained from petroleum (40-53) making it an excellent alternative to the present transportation fuel (Azizi, et al.,2014). Its boiling point of -25 degrees provides fast fuel and air mixing enabling easy starting and acceptable driveability when the engine is cold. Other advantages include a better thermal efficiency than diesel, multi-source and multi-purpose fuel, ignition characteristics better than

diesel, high wheel-wheel efficiency **(**Troy, et al., 2006**,** Sorenson, 2001**,** Zoha, et al., 2014, (International Association of DME, 2010)**.**

On the other hand, DME's physical properties will need to be changed in order for DME to be used in traditional diesel fuel injection systems. **(**Sorenson, 2001**,** Troy, et al., 2006). DME has a lower liquid density when compared to diesel fuel leading to the requirement of a fuel tank almost double the size in order to achieve the same driving distance. Its viscosity is also low by a factor of 20 (Sorenson, 2001, Troy, et al., 2006) which can cause leakage in pumps and fuel ejectors. Another challenge with DME is its low lubricity resulting in early wear and tear of pumps and fuel injectors. To address these issue additives have been used to increase the lubricity of DME and still further developments are required in the field.

Currently DME is used in heavy-duty trucks with diesel engines designed specifically for DME use. In China (Shanghai) this technology has been employed in the transportation sector in some of the bus routes, in Europe there is a fleet of Volvo trucks running on DME made from renewable feedstock. This demonstrates that DME is starting to gain acceptance for use as a fuel for trucks and it is only a matter of time until it gains acceptance in other vehicle fleets.

DME is used for a variety of other applications as well such as chemical feedstock, it can also be used as a fuel in rail and marine applications, hydrogen production for use in fuel cells (an advantage due to a high hydrogen content compared to methanol). DME can also be used as residential fuel for heating and cooking (as a substitute for LPG).

2.2.2 Direct and Indirect DME synthesis

DME is produced in two different ways, the indirect route (the traditional route and commercially proven technology) as well as the direct route (considered the most efficient). In the indirect route DME is produced in a two-step process, methanol synthesis followed by the dehydration of methanol. On the other hand, direct route produces DME directly from synthesis gas in one process step. The companies which own the technologies for indirect DME synthesis are Udhe, Lurgi, Toyo and MGC and the ones for direct synthesis are; Haldor Topsoe, JFE holdings, Korea Gas Corporation, air products and NKK.

Figure **2** shows the difference between the two routes.

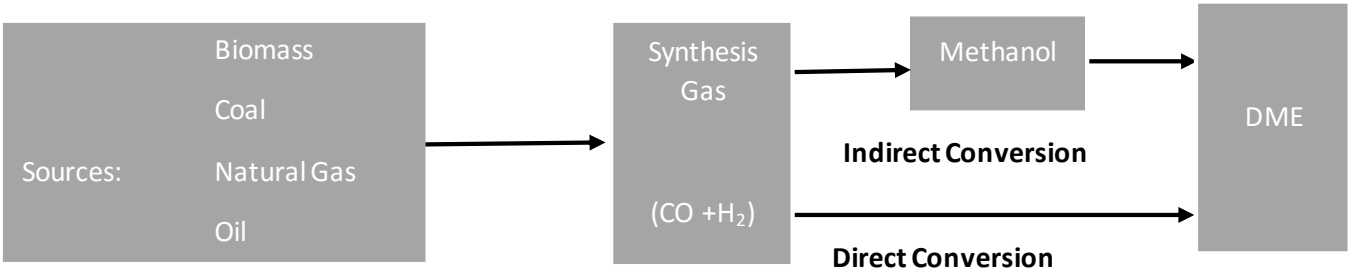


Figure 2: DME Production (Azizi et al., 2014)

2.2.2.1 Direct DME synthesis

Direct DME synthesise can take place via two main routes: a route which produces carbon-dioxide as a by-product – JFE process and a route which produces water as a by-product – Haldor Topsoe and others.

Reaction path 1: The JFE direct DME synthesis process

In this process, synthesis gas is produced by the auto thermal reforming (ATR) unit which combines partial oxidation of methane and dry reforming in order to obtain the H_2:CO stoichiometric ratio of 1:1. The carbon dioxide used is recycled from downstream processes. This is represented by the following reaction:

$$\mathbf{2CH_4 + O_2 + CO_2 \rightarrow 3CO + 3H_2 + H_2O} \qquad \text{Equation 2.15}$$

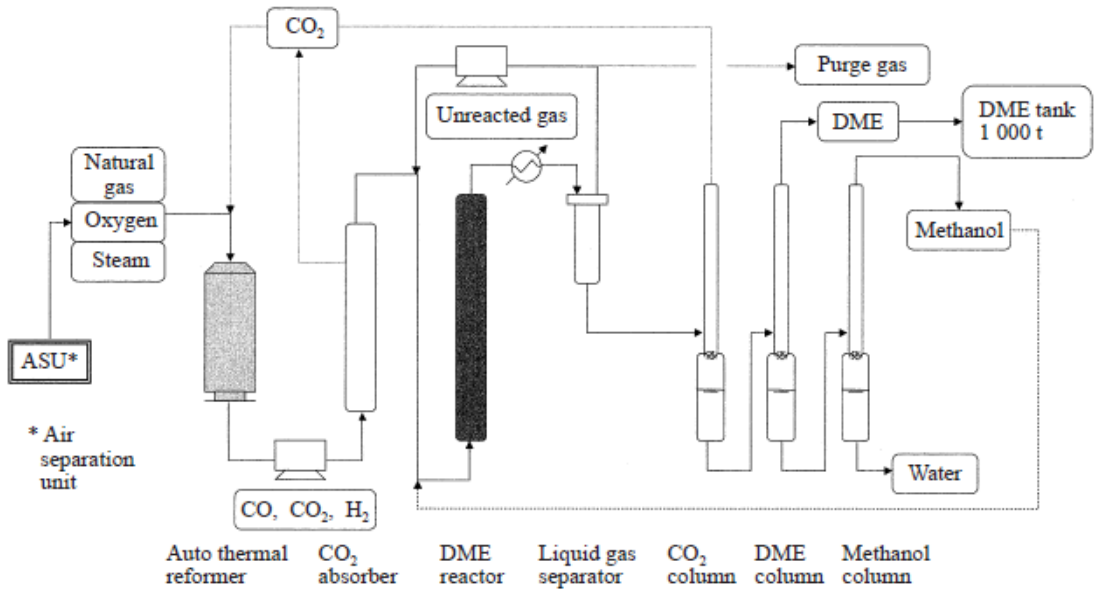


Figure 3: Process Flow Diagram of DME synthesis – The JFE 100 tpd pilot plant (Yotaro, et al., 2006)

The operating pressure on the ATR is 2.3 MPa. The product outlet from the auto thermal reformer is H_2, CO and CO_2 with an H_2:CO ratio of 1. Carbon dioxide is removed from the synthesis gas product by the carbon dioxide absorber before sending the syngas to the DME reactor. The DME reactor operates at a pressure of 5 MPa and a temperature of 260 degrees Celsius, the reaction takes place in the presence of bifunctional catalysts. The product of the reaction is DME and by-product is carbon dioxide. The unreacted gas is separated by the gas-liquid separator and recycled back to the ATR, the liquid component is sent to a stripper in order to separate carbon dioxide formed during the reaction and recycle it back to the ATR. The remaining products (DME and methanol) are sent to the DME column to remove methanol. The product DME is then stored in the tank. The process is shown on Figure 3. The following reactions take place in the DME reactor:

Methanol synthesis:

$$\mathbf{2CO + 4H_2 \leftrightarrow 2CH_3OH} \qquad \mathbf{-181.6\ \frac{kJ}{DME\ mol}} \qquad \text{Equation 2.16}$$

Methanol Dehydration:

$$\mathbf{2CH_3OH \leftrightarrow CH_3OCH_3 + H_2O} \qquad \mathbf{-23.4\ \frac{kJ}{DME\ mol}} \qquad \text{Equation 2.17}$$

Water- Gas Shift reaction:

$$\mathbf{CO + H_2O \leftrightarrow CO_2 + H_2} \qquad \mathbf{-41\ \frac{kJ}{DME\ mol}} \qquad \text{Equation 2.18}$$

Overall Reaction:

$$\mathbf{3CO + 3H_2 \leftrightarrow CH_3OCH_3 + CO_2} \qquad \mathbf{-258.6\ \frac{kJ}{DME\ mol}} \qquad \text{Equation 2.19}$$

The JFE direct DME synthesis step involves 3 reaction steps, Methanol Synthesis, Methanol dehydration and the water-gas shift reaction. Methanol is synthesised from synthesis gas with the stoichiometric ratio of H_2:CO = 2:1. This is the optimum ratio where the equilibrium conversion of syngas is at its maximum (Takashi, et al., 2003).The dehydration reaction takes place simultaneously in order to remove methanol thereby increasing the conversion of syngas. The Water-Gas shift reaction removes water formed during the dehydration reaction in order to prevent the accumulation of water on the catalyst active sites. Water has an inhibiting effect on the reaction rate by competing with methanol molecules over acid sites and therefore the

removal of water during DME synthesis is beneficial for achieving high selectivity towards DME. For the overall reaction the equilibrium conversion reaches its maximum when the stoichiometric ratio of H_2:CO is 1:1 **(**Takashi, et al., 2003, Zoha, et al., 2014, George, et al., 2009)

The variation of H_2:CO ratio can change the direction of the water-gas shift reaction thereby also affecting the selectivity to DME. In a reaction where the ratio of H_2:CO is high the reverse water-gas shift reaction is favoured thereby reducing the production of carbon dioxide and consequently reducing DME production, on the other hand a low H_2:CO ratio increases the production of carbon dioxide and favours the effective removal of methanol due to the elimination of water formed via the water-gas shift reaction.

Carbon dioxide content of the feed also plays a critical role in determining the direction of the water-gas shift reaction and thereby affecting DME yield. A syngas feed which is rich in carbon monoxide favours the effective removal of methanol due to the elimination of water via the water-gas shift reaction. Conversely feed rich in carbon dioxide favours the reverse water gas shift reaction thereby producing more water inhibiting methanol dehydration resulting in a low DME selectivity.

The overall reaction for the JFE process is given by:

$$\mathbf{2CH_4 + O_2 \rightarrow CH_3OCH_3 + H_2O} \qquad \text{Equation 2.20}$$

The reaction represents the partial oxidation of methane to DME and water.

Reaction path 2: Haldor Topsoe and others

This path involves only two reaction steps – methanol synthesis and methanol dehydration resulting in the following overall reaction.

Overall Reaction:

$$\mathbf{2CO + 4H_2 \rightarrow CH_3OCH_3 + H_2O} \qquad \mathbf{-205\ \frac{kJ}{DME\ mol}} \qquad \text{Equation 2.21}$$

Reaction path 2 results in DME and by-product water compared to JFE process where the by-product is carbon dioxide. For this process the equilibrium conversion reaches its maximum when the H_2:CO ratio is equal to 2:1. The maximum equilibrium conversion for the JFE process is higher than that of reaction path 2**, (**Takashi, et al., 2003**,** Kaoru, et al., 1984 George, et al.,

2009**)** this is because the water-gas shift reaction in reaction path 1 allows for the continuous removal of water thereby preventing accumulation on the catalyst site. Water plays an inhibiting role by competing with methanol molecules over acid sites and can also lead to catalyst degradation. The other advantage of reaction path 1 is the easy separation of carbon dioxide from DME compared to the separation from water. Reaction path 1 consumes less energy.

Alternatively, for a syngas feed which contains CO_2, H_2 and CO, Carbon-dioxide hydrogenation to methanol is another option for DME synthesis. This option has gained significant recognition because it promotes the recycling of carbon dioxide which could have been emitted to the atmosphere.

Methanol synthesis from CO_2 takes place via the reaction below:

$$\mathbf{CO_2 + 3H_2 \leftrightarrow CH_3OH + H_2O} \qquad \mathbf{-49.4\ \frac{kJ}{DME\ mol}} \qquad \text{Equation 2.22}$$

$$\mathbf{CO_2 + H_2 \leftrightarrow CO + H_2O} \qquad \mathbf{41.4\ \frac{kJ}{DME\ mol}} \qquad \text{Equation 2.23}$$

$$\mathbf{CO + 2H_2 \rightarrow CH_3OH} \qquad \mathbf{-181.6\ \frac{kJ}{DME\ mol}} \qquad \text{Equation 2.24}$$

$$\mathbf{2CH_3OH \rightarrow CH_3OCH_3 + H_2O} \qquad \mathbf{-23.4\ \frac{kJ}{DME\ mol}} \qquad \text{Equation 2.25}$$

Overall reaction:

$$\mathbf{2CO_2 + 6H_2 \rightarrow CH_3OCH_3 + 3H_2O} \qquad \text{Equation 2.26}$$

Thermodynamically methanol synthesis from Carbon Dioxide is less favoured compared to synthesis from CO (Shen et al., 2000). The hydrogenation of carbon dioxide produces large amounts of water from the methanol synthesis reaction as well as RWGS reaction, blocking the catalyst sites. Moreover, carbon dioxide molecules can also have an inhibiting effect on methanol synthesis by adsorbing onto the catalyst sites faster than carbon monoxide and hydrogen thereby reducing the production of methanol. Furthermore, other by products are formed during the hydrogenation of carbon dioxide such as carbon monoxide, hydrocarbons and higher alcohols. A highly selective catalyst is therefore required to avoid the formation of undesired products (Wei, et al., 2011)

3.2.2.2 Indirect DME synthesis

Indirect DME synthesis is a simple process in which methanol is first produced from synthesis gas from different sources such as coal, biomass, natural gas and oil etc. and then converted to DME in a separate reactor. This process has been commercialised however thermodynamically DME production from syngas is more favourable than the indirect route and methanol itself is an expensive chemical feedstock (Mingting, et al., 1997). The indirect route also has a lower carbon monoxide conversion than the direct route and requires high capital costs for the reactor design. (Mingting, et al., 1997, Azizi, et al., 2014)

The process flow diagram is shown below:

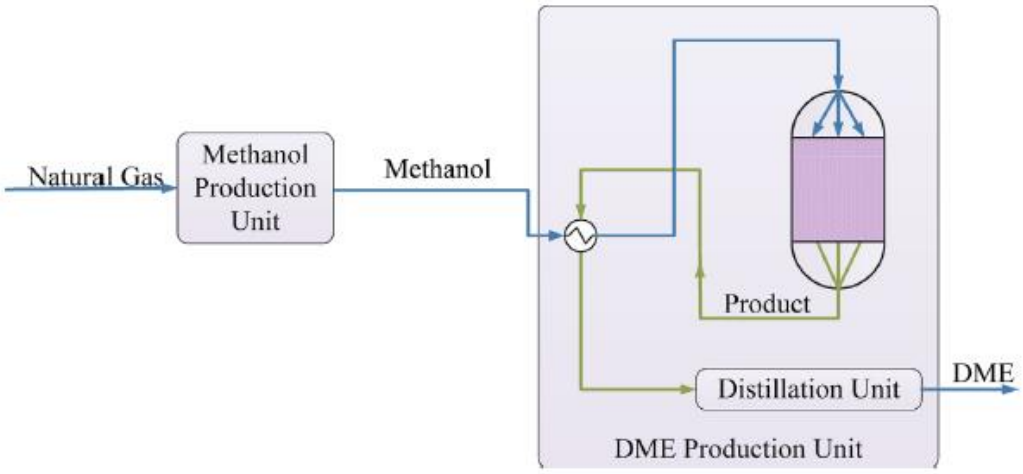


Figure 4: Indirect DME synthesis (Azizi et al.,2014)

The reaction for the indirect method is the dehydration of methanol shown below:

$$\mathbf{2CH_3OH \leftrightarrow CH_3OCH_3 + H_2O} \qquad \mathbf{-23.4\ \frac{kJ}{DME\ mol}} \qquad \text{Equation 2.27}$$

Both DME and water are reaction inhibitors (Azizi, et al., 2014). As soon as the water accumulates on the surface of the synthesis catalysts it blocks the active sites and limits the conversion of methanol to DME. The reaction is also favoured at low temperatures, since the reaction is exothermic any increase in temperature will affect DME yield as well as result in coke formation and yield of other by-products such as ethylene, carbon monoxide and hydrogen (Azizi, et al., 2014, Ki-Won, et al., 2002).

2.2.3 Effect of nature and type of catalyst on DME synthesis

Dennis et al. (1991) developed a novel process for producing DME from synthesis gas derived from coal in a one-step reaction sequence. The process used a slurry reactor with methanol synthesis, dehydration and the water-gas shift reaction all happening in the same reactor. They investigated the effect of the different catalyst compositions or ratios on DME selectivity. The catalysts, which are used, can be a mixture of methanol, water-gas shift reaction and dehydration catalysts.

Dennis et al. (1991) found that an improvement in selectivity to DME was achieved by increasing the concentration of acid dehydration catalyst. The concentration of the acid dehydration catalyst was increased by reducing the concentration of methanol catalyst. As a result, as methanol was being produced, the dehydration reaction was promoted and the selectivity to DME improved. The advantage achieved by a one-step reaction sequence is overcoming the thermodynamic constraints of the methanol reaction when it takes place in a two-step process. The authors concluded that the type of catalysts used, their ratios and the operating conditions affect productivity and selectivity of DME and methanol. Adding or removing steam and carbon dioxide in the process was found to also affect the product distribution as well as the rate of the reactions.

Ki-Won et al. (2002) carried out the conversion of methanol to DME over solid acid catalysts in order to investigate the effect of water in a one step synthesis of DME from carbon dioxide hydrogenation.The authors found that the catalyst is active and stable in methanol dehydration to DME however the presence of water deactivates the catalyst and this is because water blocks the catalyst sites.

Takashi et al. (2003) developed an innovative process for direct DME synthesis called the JFE direct DME synthesis process. A pilot plant with the capacity of 5 tons per day DME. This is part of the scale up research that was conducted for 15 years to commercialise the technology. The process consisted of 3 sections, syngas preparation, DME synthesis in a slurry reactor and separation or purification of the products and by-products (DME, carbon dioxide and methanol distillation columns). In the process natural gas is converted to syngas with oxygen, steam and by-product carbon dioxide in an auto thermal reactor (ATR). The DME slurry reactor allows for the control of the reaction temperature at high syngas conversion by providing homogenous liquid phase mixing and thereby preventing catalyst deactivation – the syngas conversion to

DME is highly exothermic. To successfully achieve significant DME synthesis results, the catalyst was also modified to promote methanol synthesis, dehydration and the water-gas shift reaction. Based on their results they conducted a 100TPD demo plant in Hokkaido Japan to pave the way for commercial DME production technology. In 2005 JFE completed the development of Direct DME synthesis process on an ATR with a carbon dioxide recycle. They developed their own efficient catalyst and mass production technology. They are now ready for licensing and catalyst supply.

In 2005 Eduardo et al. published a paper, which presented the possibilities of natural gas as a clean raw material to replace oil. Eduardo et al. (2005) discussed the main options of catalytic chemical transformation, amongst others is gas to gas transformation yielding DME. During the direct DME synthesis reaction, methanol synthesis is the intermediary step and the water-gas shift reaction (which displaces the water formed during methanol dehydration) is a critical reaction for DME synthesis. The catalyst must favour the selectivity to DME, for that to happen it should have multiple sites (methanol synthesis characteristics metallic sites) as well as containing sufficient acidity for the dehydration reaction to occur. The sites should also promote the water gas shift reaction which becomes significant for the removal of water being generated from the dehydration reaction and the formation of carbon dioxide. Such catalysts are termed bifunctional catalysts.

The greater acidity favours the formation of DME; the oxygen atom is more electronegative than the carbon, which makes the hydrogen alpha to ethers more acidic than in simple hydrocarbons. On the other hand, a high concentration of metallic sites favours the conversion to methanol. The water gas shift reaction occurs as an indication that the water formed during dehydration continues to react with carbon dioxide (Eduardo, et al., 2005). There is still a lot of work to be done in the development of catalysts for Direct DME synthesis.

Miriam, et al., 2011studied various dehydration catalysts in the synthesis of DME directly from CO rich syngas under different reaction conditions. The catalysts investigated were a combination of methanol catalysts. The degree of acidity of the catalyst determines the rate of conversion of carbon monoxide to DME. In low acidic environments, dehydration of methanol is less efficient whereas in very high acidic environments the DME formed is catalysed further to hydrocarbons. γ-Al_2O_3 was identified as a suitable dehydration catalyst. The effect of temperature, water and carbon-dioxide was also investigated. The authors found that a high carbon monoxide conversion can be achieved by a longer residence time, high H_2 content in

the syngas as well as increasing temperature up to 280 degrees Celsius. When more than 10 vol. % of water is added to the feed, the WGSR becomes dominant enhancing carbon dioxide formation and thereby decreasing the selectivity to DME. A feed which contains more than 8 vol. % carbon dioxide also decreases carbon monoxide conversion and lowers DME selectivity compared to a feed which does not contain any carbon dioxide.

2.2.4 Effect of operating conditions and feed composition on DME synthesis and yield

Shen et al. (2000) investigated the thermodynamics involved in the catalytic hydrogenation of carbon dioxide to produce DME and methanol. The authors analysed the efffect of temperature on methanol and carbon monoxide yields at equilibrium for different pressures at a H_2:CO_2 ratio of 3:1, the exact stoichiometric ratio for the reaction. This was compared to DME and carbon monoxide yield at the same operating conditions. They found that both reactions have the same dependence on temperature and pressure, the equilibrium conversion of carbon dioxide to oxygenates increases with pressure and decreases with increasing temperature. On the other hand, the formation of carbon monoxide via the reverse water gas shift reaction has an opposite dependence.

When comparing the yield of DME and methanol at equilibrium the yield of DME is higher than that of methanol. The equilibrium conversion of carbon dioxide to DME was observed to be much higher than the equilibrium conversion of carbon dioxide to methanol.

The effect of intial carbon dioxide concentration or H_2:CO_2 ratio was also investigated for both DME and methanol yield. The yield for both increases with decreasing concentration of carbon dioxide.

Wang, et al (2006) studied the effect of carbon dioxide concentration on the syngas feed for DME synthesis. The authors identified that there is a tipping point for the reaction to be favoured by a certain concentration of carbon dioxide in the feed.This study is also conducted under a different reaction route - DME synthesis via the hydrogenation of carbon monoxide as the main reaction. The authors analysed three different feed compositions with different space velocities.

- Feed A with a high hydrogen (63.5 vol.%) and carbon monoxide concentration (35.3 vol.%) and a very low carbon dioxide concentration (1.2 vol.%)

- Feed C with a low concentration of hydrogen (51.8 vol.%) and carbon monoxide (24.7 vol.%) and a high concentration of carbon dioxide (23.5 vol.%) and feed B in the middle. The different feeds are in the order of increasing H_2:CO ratio.

The authors found that increasing the concentration of carbon dioxide in the feed results in a low DME selectivity compared to cases where the concentration is low. This is because the presence of carbon dioxide can restrict hydrogenation of carbon monoxide by competing over the active sites with carbon monoxide, while the other two reactions remain unaffected (carbon dioxide hydrogenation and WGS). Hence, carbon dioxide selectivity increases with reducing DME/carbon dioxide ratio.

On the other extreme side, when the carbon dioxide content is very high (23.5 vol.%) the opposite is observed. Carbon dioxide hydrogenation is still promoted but the rate of the water gas shift reaction (where carbon dioxide is the product) is much lower than carbon dioxide hydrogenation resulting in low carbon dioxide concentration in the outlet stream and hence DME/carbon dioxide ratio is higher for this carbon dioxide content. This suggests that there exists a carbon dioxide concentration where the yield of DME is optimum. The authors concluded that adding a suitable amount of carbon dioxide to the syngas can enhance the yield of DME as well as applying low reaction space velocity.

Florian et al. (2011) studied the conversion of carbon dioxide with hydrogen to methanol over a commercial Cu/ZnO catalyst with the aim to test the applicability of conventional catalyst system for the carbon dioxide hydrogenation reaction system. The syngas based methanol synthesis process e.g. the Lurgi Mega Methanol process has been in use for many years using the standard synthesis gas process conditions however, the use of carbon dioxide as a feedstock instead of carbon monoxide has posed many challenges when using the conventional catalysts system and identifying the optimum operating conditions. As a result, the authors tested the carbon dioxide based methanol under two different process conditions for accurate comparison of results. The carbon monoxide syngas process conditions (syngas at 70 bar, 250 degrees and recycle ratio (RR) =3.6) and the carbon dioxide syngas process conditions (syngas at 80 bar, 250 degrees and RR= 4.5). They compared the following cases:

i. Base case process condition comparing carbon dioxide syngas at carbon dioxide process conditions and carbon monoxide syngas at carbon monoxide process conditions
ii. Carbon monoxide syngas at carbon monoxide process conditions and carbon dioxide syngas at carbon monoxide process conditions

iii. Carbon monoxide syngas at carbon dioxide process conditions and carbon dioxide syngas at carbon dioxide process conditions.

The authors found that for all cases the productivity (given as space time yield) of the process with standard carbon monoxide syngas is higher than for carbon dioxide hydrogenation for all cases. The base case showed a significant difference in productivity between the carbon monoxide process conditions and the carbon dioxide process conditions (carbon monoxide syngas had 50% higher productivity than carbon dioxide syngas). However, for the third case when operating at carbon dioxide conditions the difference between the productivity between carbon monoxide syngas and carbon dioxide syngas is only 25%, which shows an improvement, compared to the base case results. From these the authors concluded that methanol synthesis from carbon monoxide is more productive than methanol synthesis from carbon dioxide however, the productivity difference can be significantly decreased by the selection of process conditions which favour the methanol synthesis reaction. Moreover, they found that carbon dioxide hydrogenation, although slower than carbon monoxide hydrogenation, it is more selective and produces high purity product that is beneficial for DME synthesis.

Vakili et al. (2012) designed an industrial dual reactor with the objective of optimizing DME production by overcoming equilibrium reaction limitations of direct DME synthesis. Reaction kinetics are rate limiting at the beginning of the reaction, requiring high temperatures to drive the reaction. However, due to the exothermicity of the reaction as the reaction proceeds, high temperatures reduce the equilibrium conversion. As a result to increase the conversion, the temperature profile should show declining temperatures as the reaction continues. Consequently, the authors designed a dual type reactor which follows the temperature profile of an optimum DME synthesis process where high temperatures promote the reaction in the beginning and low temperatures at the end. The designed system has a water-cooled reactor (the first reactor) as well as a gas-cooled reactor (the second reactor). On the first reactor A bifunctional catalyst is loaded on the tube side of the first reactor and on the shell side of the second reactor. The cold syngas feed enters the second reactor where it is heated by heat from the reacting gas which flows on the shell side. The hot syngas is then fed to the tubes of the first reactor where DME reaction is initiated. The reaction is completed on the second reactor on the shell side in order to progress it at lower temperatures.

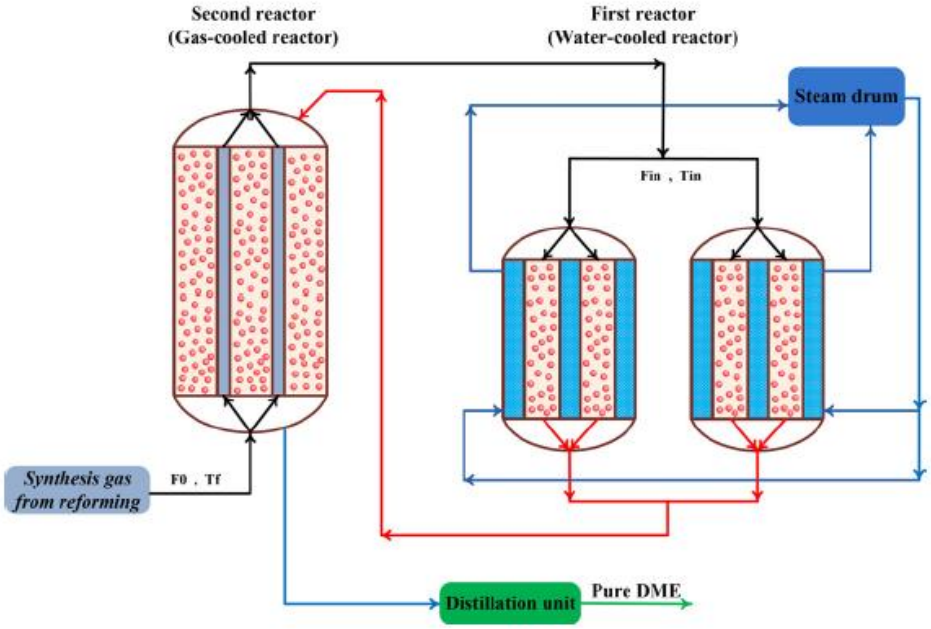


Figure 5 : Dual type reactor configuration **(Vakili, et al., 2012)**

The authors investigated the effect of flow patterns on the reactor performance between counter-current flow and co-current flow. They identified counter-current flow as the best flow pattern for the dual reactor due to a high DME production rate when this flow pattern is applied. The simulated results indicated an enhanced DME production rate up to 60 t/day compared to the conventional industrial DME synthesis reactor (which uses the indirect DME synthesis process).

2.3 Summary

In this chapter different natural gas reforming technologies are discussed, together with their respective syngas ratios as well as their applications. Steam methane reforming has the highest H_2:CO ratio, and can be used together with partial oxidation in order to reduce the ratio to that applicable for DME synthesis. Dry gas reforming produces a syngas with a ratio of H_2:CO = 1:1, which is suitable for direct DME synthesis.

Traditionally DME was produced following an indirect process; focus has been given to develop catalysts with multiple sites, which promote both the dehydration reaction and the water-gas shift reaction. A high DME yield is obtained when DME is produced in a one-step reaction sequence, because it overcomes the thermodynamic limitations of the methanol synthesis reaction. The syngas composition of the feed has an impact on DME yield, a feed with a syngas ratio (H_2:CO) of 1:1, has a higher DME yield than a feed with a syngas ratio

(H_2:CO) of 2:1 at equilibrium. Temperature, initial carbon dioxide concentration, hydrogen and water content of the feed also has an impact on the yield of DME.

3. The Ternary Bond Equivalent Diagram

Many reactions occur during natural gas reforming depending on the reforming technology applied as discussed in chapter 3.1. The reactions can be represented on the ternary bond diagram as long as the reaction species are constrained to C, H and O. These reactions can produce a broad range of products depending on the reaction pathways and technologies.

In this research a graphical approach will be used for the evaluation of natural gas reforming technologies and consequently the production of synthesis gas for further downstream processing. This approach will enable the determination of the feasible region of operation by considering mass and energy balances only. Furthermore, based on the optimum region of operation a conceptual design for DME synthesis can be developed. The optimum region of operation is determined by reaction stoichiometry, then constrained by the thermal balance line between exothermic and endothermic reactions. The feasible region of operation is obtained before considering (Wei, 1979):

- Thermodynamic equilibrium
- Reaction kinetics and extent of reaction
- Reactor design and operation

3.1 History of Ternary Bond Equivalent Diagram

Coal composition charts showing the range of known compositions with respect to three major elements (C, H and O) have been used for a long time for coal classification and to provide understanding of the coalification process (Battaerd & Evans, 1978). The first established coal chart (Seyler coal chart) had a limitation, in that it could not show the feasible processes which occur during coalification. The chart was mainly used to classify coal into ranks. Van Krevelen developed a chart which showed reaction trajectories by plotting atomic H/C and O/C ratio on rectangular coordinates. They used this to identify the main chemical changes in coalification.

Cairns &Tavebaugh (1964) used the C, H, O ternary diagram to determine carbon deposition boundaries. They considered the C, H, O gas phase composition in equilibrium with graphite over a temperature range 298 – 1500 K at a pressure of 1 atm. They used the C: H: O ratios of the system to determine whether or not carbon will form from a given reactant composition.

Battaerd & Evans (1978) explored the use of Ternary Bond Equivalent diagram to express the possibilities and limitations of processes for converting coal to liquids using hydrogenation. To demonstrate they considered the conversion of brown coal to oil and the problem of oxygen removal. This was based only on reaction stoichiometry.

Wei (1979) extended this by considering reaction stoichiometry and thermodynamic equilibrium. They analysed a coal gasification process where the feed consisted only of fixed carbon, steam and oxygen. A consideration of the thermal balance line between exothermic and endothermic reactions constrains the results to a thermal balanced line (Wei, 1979).

Tay, et al. (2011) used the ternary C-H-O diagram to evaluate the gas phase equilibrium composition of biomass gasification. They used this to design an integrated biorefinery. The graphical approach enabled them to determine the optimum operating parameters of biomass gasification such as the gasification agent, temperature and pressure as well as the optimum ratios of multiple feed stocks.

Pillay,2013 used the ternary bond equivalent diagram to evaluate processes for landfill gas utilization. Processes evaluated where electricity generation, synfuels production, DME production etc. The graphical approach enabled Pillay, 2013 to develop processes which not only use landfill gas as an alternative source to coal, oil etc. but also to develop processes with low carbon dioxide emissions.

3.2 Constructing the Ternary Bond Equivalent diagram

The ternary bond equivalent diagram is constructed by placing element C, H and O on the apex of the equilateral triangle (Figure 6Figure **4**). At each apex the bond- equivalent percentage of the respective element is 100%. Lines radiating from Hydrogen in all directions represent – dehydrogenation, similarly lines radiating from oxygen in all directions represent de-oxidation trajectories etc.

Reactions involving all three elements are determined by lines radiating from the appropriate point (Battaerd & Evans, 1978). To determine the position of a compound containing C, H and O on the diagram the bond equivalent percentages are determined by multiplying the mole fraction of each element by the number of valence electrons each atom contains. For carbon the number of valence electrons is equal to 4, oxygen 2 and hydrogen 1.

$$C = \frac{4x_c}{4x_c + x_{H_2} + 2x_{O_2}}$$

$$O = \frac{2x_{O_2}}{4x_c + x_{H_2} + 2x_{O_2}}$$

$$H = \frac{2x_{H_2}}{4x_c + x_{H_2} + 2x_{O_2}}$$

The bond equivalent percentages of CO, CO_2 and H_2O can be represented by:

CO

$$C = \frac{4x_c}{4x_c + x_{H_2} + 2x_{O_2}} = \frac{4*1}{4*1+0+2*1} = 0.67$$

$$O = \frac{2x_{O_2}}{4x_c + x_{H_2} + 2x_{O_2}} = \frac{2*1}{4*1+0+2*1} = 0.33$$

Similarly, the BE for CO_2 = 0.5 and H_2O also 0.5. The full calculations are shown on appendix A.

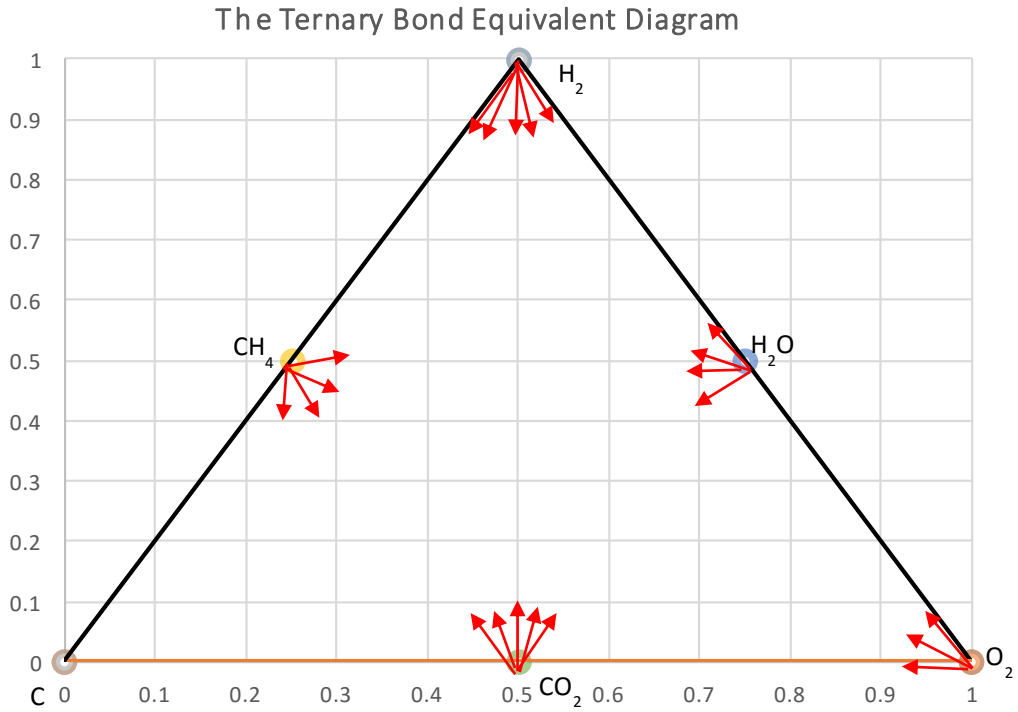


Figure 6 : C, H and O diagram and reaction trajectories (Battaerd & Evans, 1979)

Carbon dioxide is represented by a point midway between carbon and oxygen, methane represented by the point midway between Hydrogen and Carbon. See the respective positions of methane, water and carbon dioxide on figure 6 above.

The C, H, and O bond equivalent diagram will be shown to form the basis of the stoichiometrically feasible region, further constrained by the thermally balanced operation. These regions will thus form the basis for flowsheet design as discussed in the next chapter.

4. Graphical representation of the different reforming reaction routes

This chapter will make use of the ternary bond equivalent diagram to analyse different reaction systems based on three different feeds which follow different natural gas reforming technologies or a combination of natural reforming technologies. The results will be constrained by mass and energy balance to a feasible region of operation.

Furthermore, in chapter 5 the diagram will be used to develop a process, which produces DME from the syngas composition obtained from each feed satisfying a syngas stoichiometric ratio (H_2:CO) of 1:1 or 2:1. Chapter 6 will further restrict the results to a region of no carbon formation by using the carbon deposition boundaries.

The following reaction feeds were considered for natural gas reforming assuming the gas is 100% methane with no impurities.

Reaction species	**Feed 1**	**Feed 2**	**Feed 3**
CH_4	×	×	×
H_2O	×		×
O_2	×	×	×
CO_2		×	×

Table 2 : Reaction species for each feed

i. ***Feed 1***: Methane, steam and oxygen – A combination of steam reforming and partial oxidation of methane
ii. ***Feed 2***: Methane, carbon dioxide and oxygen– A combination of dry reforming and partial oxidation
iii. ***Feed 3***: Methane, carbon dioxide, steam and oxygen – a combination of all 3 reforming technologies.

For each feed, the resultant products should not be part of the original feed or consume products. In other words,

i. Feed 1: The reactants, oxygen and water should not be part of the resultant products or consume the products formed during the reaction
ii. Feed 2: The reactants oxygen and carbon dioxide should not be part of the resultant products or consume the products formed during the reaction
iii. Feed 3: The reactants carbon dioxide, steam and oxygen should not be part of the resultant products or consume the products formed during the reaction.

In this section, we determine the important reactions that will form the stoichiometric region; the important reactions are at the intersections of the H_2-CO, H_2-CO_2 and H_2O-CO line. The following reactions were selected because they intersect with each other on the C,H and O diagram and the products formed can be represented on the ternary diagram. All the reactions which do not intersect with each other were omitted for the determination of the feasible region of operation.

Reforming reactions for **feed 1** are obtained by a linear combination of the following reactions:

$$\mathbf{CH_4 + 2H_2O \rightarrow 4H_2 + CO2} \qquad \mathbf{165\ \frac{kJ}{mol}} \qquad \text{Equation 5.1}$$

$$\mathbf{CH_4 + H_2O \rightarrow 3H_2 + CO} \qquad \mathbf{206\ \frac{kJ}{mol}} \qquad \text{Equation 5.2}$$

$$\mathbf{CH_4 + 0.5O_2 \rightarrow CO + 2H_2} \qquad \mathbf{-35.7\ \frac{kJ}{mol}} \qquad \text{Equation 5.3}$$

$$\mathbf{CH_4 + O_2 \rightarrow CO_2 + 2H_2} \qquad \mathbf{-318.6\ \frac{kJ}{mol}} \qquad \text{Equation 5.4}$$

For **feed 2** the following important reactions determine the stoichiometric region

$$\mathbf{CH_4 + 3CO_2 \rightarrow 4CO + 2H_2O} \qquad \mathbf{329.6\ \frac{kJ}{mol}} \qquad \text{Equation 5.5}$$

$$\mathbf{CH_4 + CO_2 \rightarrow 2H_2 + 2CO} \qquad \mathbf{247\ \frac{kJ}{mol}} \qquad \text{Equation 5.6}$$

$$\mathbf{CH_4 + 1.5O_2 \rightarrow CO + 2H_2O} \qquad \mathbf{-519\ \frac{kJ}{mol}} \qquad \text{Equation 5.7}$$

$$\mathbf{CH_4 + 0.5O_2 \rightarrow CO + 2H_2} \qquad \mathbf{-35.7\ \frac{kJ}{mol}} \qquad \text{Equation 5.8}$$

Feed 3 is represented by a linear combination of the following reactions:

$$\mathbf{CH_4 + CO_2 \rightarrow 2H_2 + 2CO} \qquad \mathbf{247.3\ \frac{kJ}{mol}} \qquad \text{Equation 5.9}$$

$$CH_4 + H_2O \rightarrow 3H_2 + CO \qquad 206.2\ \frac{kJ}{mol} \qquad \text{Equation 5.10}$$

$$CH_4 + 0.5O_2 \rightarrow CO + 2H_2 \qquad 35.7\ \frac{kJ}{mol} \qquad \text{Equation 5.11}$$

4.1 Graphical representation of the stoichiometric region for each feed

4.1.1 Stoichiometric region for Feed 1

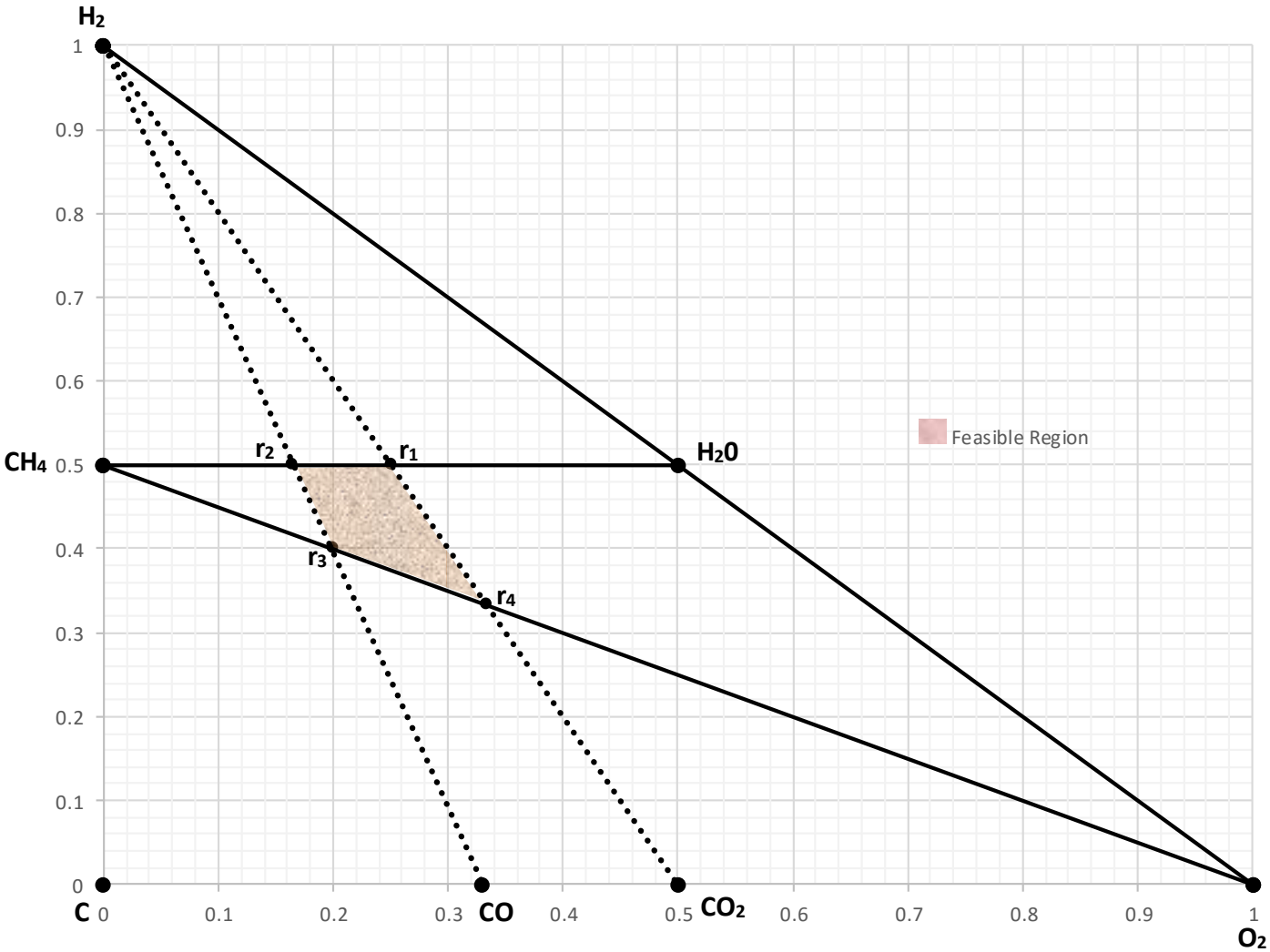


Figure 7 : Stoichiometric region for feed 1

For this feed, methane is reacted with oxygen and steam to produce a syngas mixture of H_2, CO and CO_2 as shown by the reactions in the section above. To represent the reaction pathway in the C, H, O diagram for all reactions $\mathbf{r_1} - \mathbf{r_4}$ a solid straight-line is extended from methane first to the vertex of the equilateral triangle representing oxygen for reactions $\mathbf{r_3}$ and $\mathbf{r_4}$ and then

to water for reactions r_1 and $\mathbf{r_2}$. The resultant products are represented by dotted lines intersecting the reaction line**.** The point $\mathbf{r_2}$ represents the reaction between methane and water to produce H_2 and CO, $\mathbf{r_3}$ the reaction between methane and oxygen to produce the same products but at a different point on the diagram (point $\mathbf{r_3}$). Similarly, $\mathbf{r_1}$ represents the reaction between methane and water to form the reaction products H_2 and CO_2, and r_4 methane and oxygen to form the same reaction products but at a different point (point $\mathbf{r_4}$), see Figure 7.

The different points $\mathbf{r_1}$, $\mathbf{r_2}$, $\mathbf{r_3}$ and $\mathbf{r_4}$ represent different syngas compositions. The stoichiometric region is the region bound by $\mathbf{r_1}$, $\mathbf{r_2}$, $\mathbf{r_3}$ and $\mathbf{r_4}$, see Figure 7. Any point within the region can be obtained by a linear combination of the above reactions.

4.1.2 Stoichiometric region for feed 2

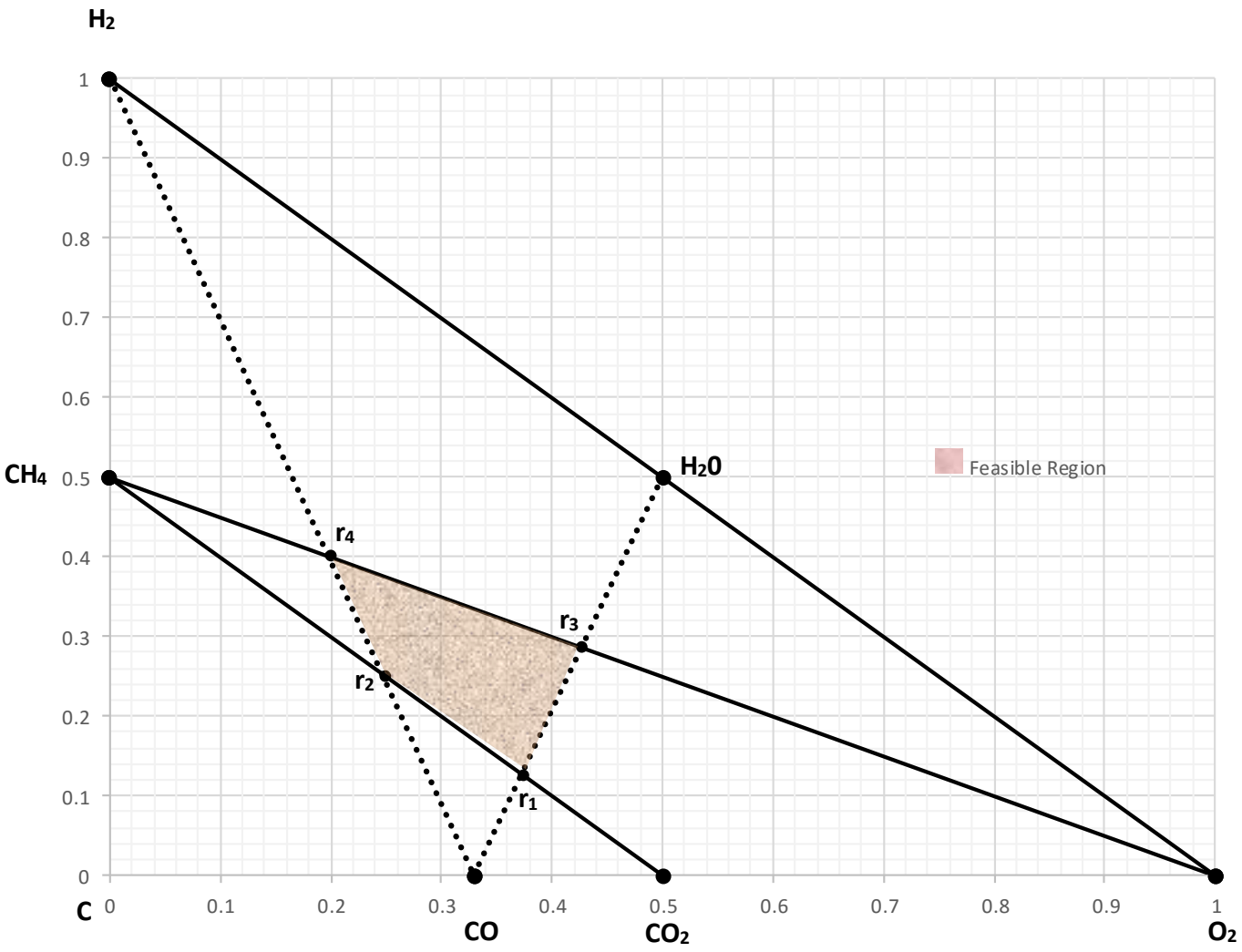


Figure 8 : Ternary Diagram for Feed 2

In this case methane is reacted with oxygen and carbon dioxide to produce a synthesis gas mixture of H_2, CO and H_2O. The stoichiometric region is bound by the point $\mathbf{r_1}$-$\mathbf{r_4}$, see Figure 8.

The point $\mathbf{r_2}$ (dry gas reforming) and $\mathbf{r_4}$ has a stoichiometric ratio H_2:CO =1:1, H_2:CO = 2:1 (partial oxidation of methane) suitable for DME synthesis via the JFE process and Haldor Topsoe process respectively.

4.1.3 Stoichiometric region for feed 3

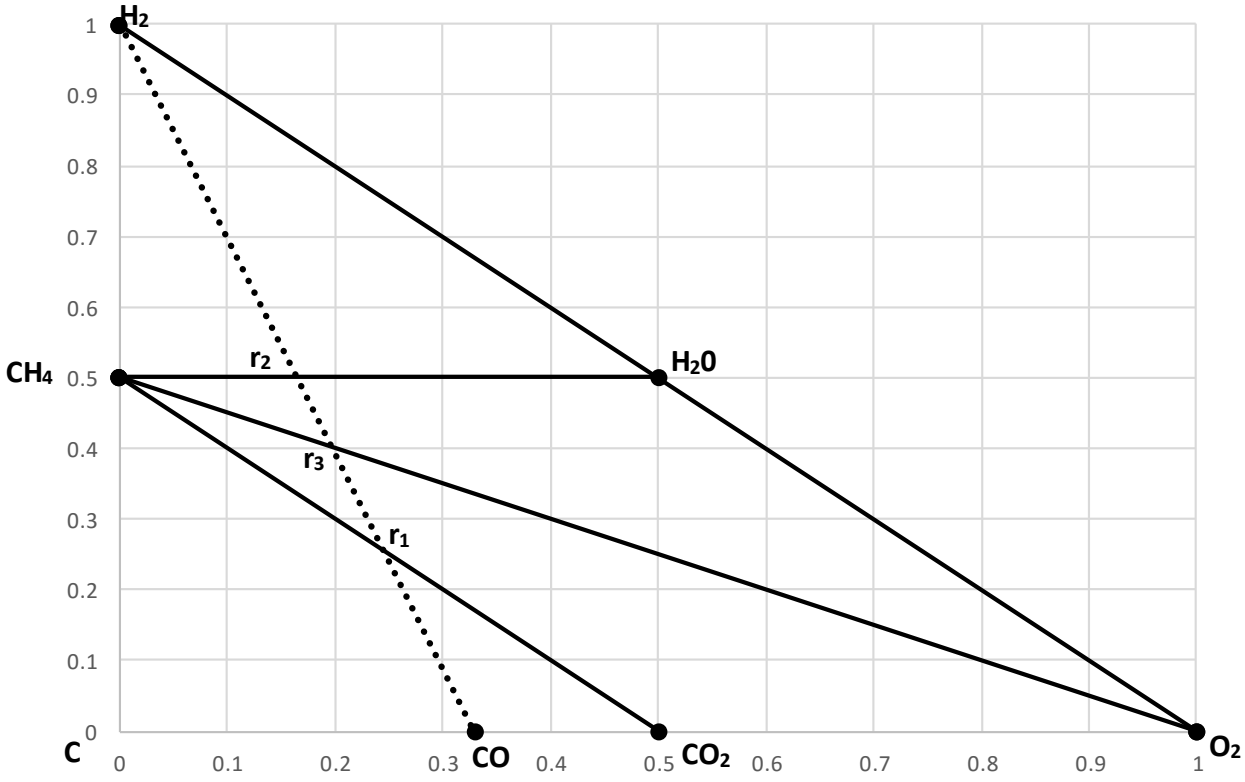


Figure 9 : Ternary Diagram for Feed 3

Methane is reacted with oxygen, carbon dioxide and water to produce a synthesis gas mixture of H_2 and CO. The point $\mathbf{r_1}$, $\mathbf{r_2}$, and $\mathbf{r_3}$ represent dry reforming, steam reforming and partial oxidation of methane respectively. Similarly applying the same rule that the resultant products should not appear in the original feed results in the product distribution lying on the straight-line H_2-CO unlike for feed 1 and feed 2. As a result, the stoichiometric region for this feed does not exist, it lies in a straight line (Figure 9).

4.2 Thermally balanced operation

The feasible region is further constrained by the thermal balanced line between exothermic and endothermic reaction. For an adiabatic system, each mole of heat produced per mole of methane can be used to balance the energy required for the endothermic reaction.

4.2.1 Thermal balance line of operation for feed 1

For feed 1 the thermal balance line is obtained by balancing the endothermic reaction $\mathbf{r_1}$ (165 kJ/kmol) with exothermic reaction $\mathbf{r_3}$ (-35.7 kJ/kmol) and $\mathbf{r_4}$ (-318.6) kJ/kmol. Similarly, $\mathbf{r_2}$ (206 kJ/kmol) balances $\mathbf{r_3}$ and $\mathbf{r_4}$.

The points on the thermal balanced line are represented by the following equations:

A: $\mathbf{CH_4 + 0.15H_2O + 0.43O_2 \rightarrow 2.15H_2 + CO}$ $\mathbf{0\ \frac{kJ}{mol}}$ Equation 5.12

B: $\mathbf{CH_4 + 0.36H_2O + 0.41O_2 \rightarrow 2.36H_2 + 0.18CO_2 + 0.82CO}$ $\mathbf{0\ \frac{kJ}{mol}}$ Equation 5.13

C: $\mathbf{CH_4 + 0.61H_2O + 0.39O_2 \rightarrow 2.61H_2 + 0.39CO_2 + 0.61CO}$ $\mathbf{0\ \frac{kJ}{mol}}$ Equation 5:14

D: $\mathbf{CH_4 + 1.32H_2O + 0.34O_2 \rightarrow 3.32H_2 + CO_2}$ $\mathbf{0\ \frac{kJ}{mol}}$ Equation 5.15

Point B and C can be obtained by a linear combination of A and D.

Point A to Point C are in the order of increasing H_2:CO ratio. Point A is represented by the stoichiometric ratio H_2:CO =2.15:1, B = 2.87:1, C = 4.27:1, D with an H_2:CO_2 ratio of 3.32:1. The points within the thermal balanced line (B and C) represent syngas very rich in hydrogen, this is because this points represent a combination of partial oxidation and steam reforming (ATR), see Figure 10.

By operating at the thermal balance line, the ratio obtained is higher than that obtained at point r_3 (ratio of 2) away from the thermal balanced line. Operating away from the thermal balanced line requires energy input/ removal making the process less efficient.

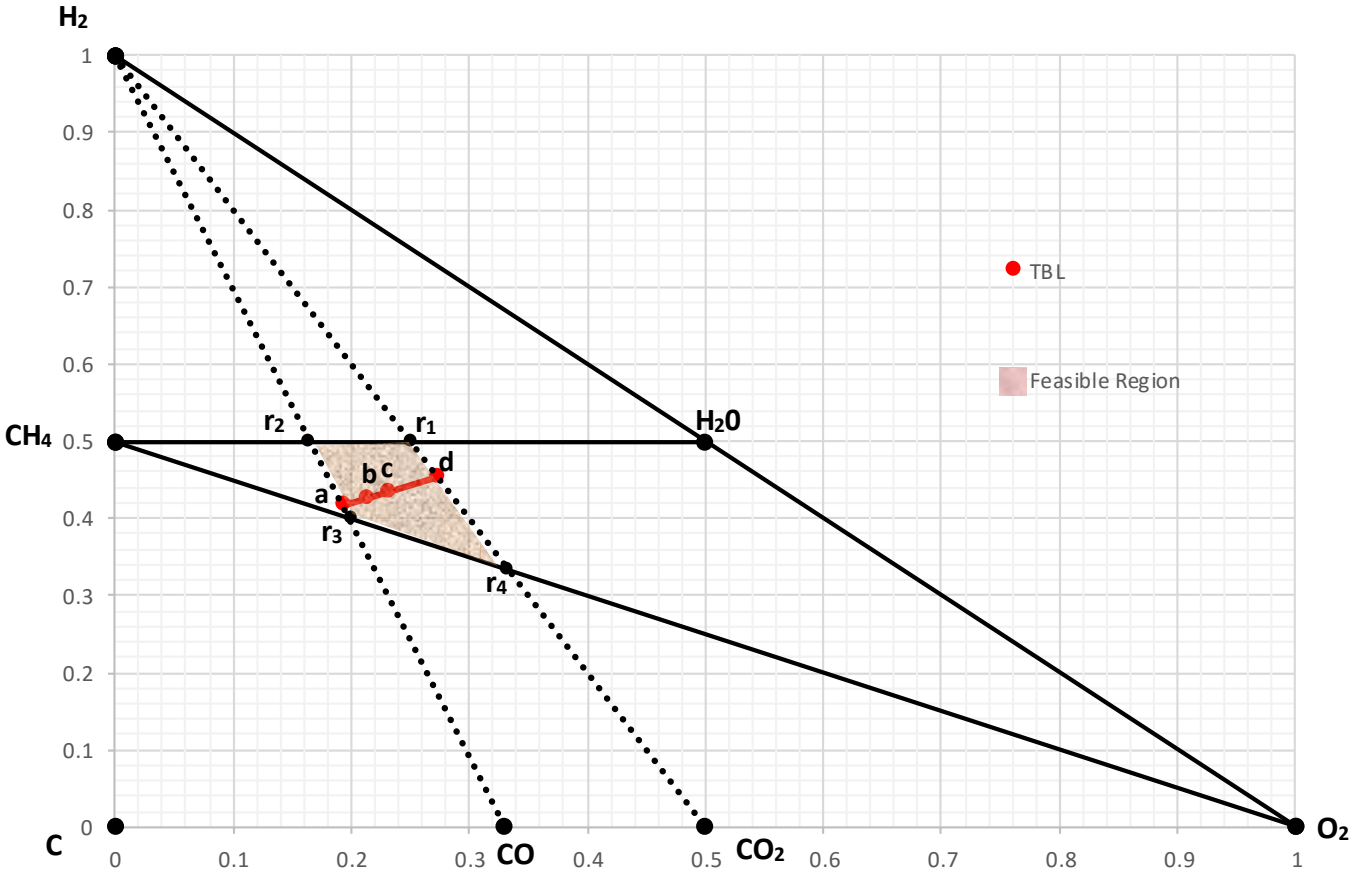


Figure 10: Thermal balance line for feed 1

The line a-d represents the thermal balanced line, above the line products emerge colder and below the line products emerge hotter due to the endothermic reactions r_1 and r_2.

4.2.2 Thermal balance line of operation for feed 2

Similarly, the thermal balance line for feed 2 is represented by the equations below and is obtained by balancing $\mathbf{r_1}$ and $\mathbf{r_2}$ (endothermic) with $\mathbf{r_3}$ and $\mathbf{r_4}$ (exothermic). Above the thermal balanced line products emerge hotter and below the line colder, see Figure 11. The points within the thermal balance line can be represented by linear combinations of A, B, C, and D. The point A, B and C are in the order of decreasing H_2:CO ratio from 1.87:1 to 0.8:1.

$$\mathbf{A:\ CH_4 + 0.07CO_2 + 0.47O_2 \rightarrow 2H_2 + 1.07CO} \qquad \mathbf{0\ \frac{kJ}{mol}} \qquad \text{Equation 5.16}$$

$$\mathbf{B:\ CH_4 + 0.29CO_2 + 0.45O_2 \rightarrow 1.80H_2 + 1.29CO + 0.2H_2O} \qquad \mathbf{0\ \frac{kJ}{mol}} \qquad \text{Equation 5.17}$$

$$\mathbf{C:\ CH_4 + 0.68CO_2 + 0.48O_2 \rightarrow 1.35H_2 + 1.68CO + 0.65H_2O} \qquad \mathbf{0\ \frac{kJ}{mol}} \qquad \text{Equation 5.18}$$

D: $\mathbf{CH_4 + 1.84CO_2 + 0.58O_2 \rightarrow 2.84CO + 2H_2O}$ $\quad \mathbf{0\ \frac{kJ}{mol}}$ Equation 5.19

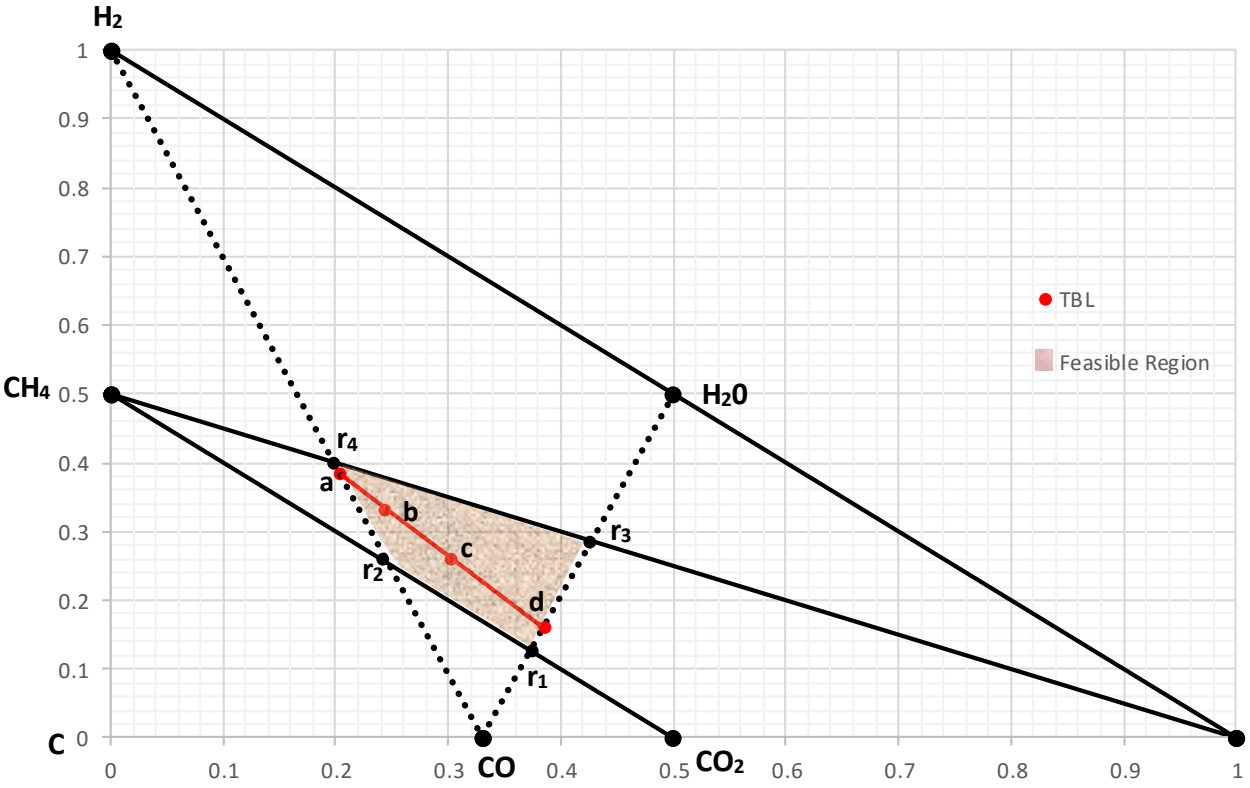


Figure 11: Thermal balance line for feed 2

4.2.3 Thermal balanced line of operation for feed 3

Similarly, for feed 3 the thermal balance line of operation is obtained by balancing the exothermic reaction r_3 with r_1 and r_2. The thermal balance line lies on the straight line H_2- CO (Figure 12).

The following points represent the thermal balance line:

A: $\mathbf{CH_4 + 0.13CO_2 + 0.44\ O_2 \rightarrow 2H_2 + 1.12\ CO}$ $\quad \mathbf{0\ \frac{kJ}{mol}}$ Equation 5.20

B: $\mathbf{CH_4 + 0.15\ H_2O + 0.43O_2 \rightarrow 2.15H_2 + CO}$ $\quad \mathbf{0\ \frac{kJ}{mol}}$ Equation 5.21

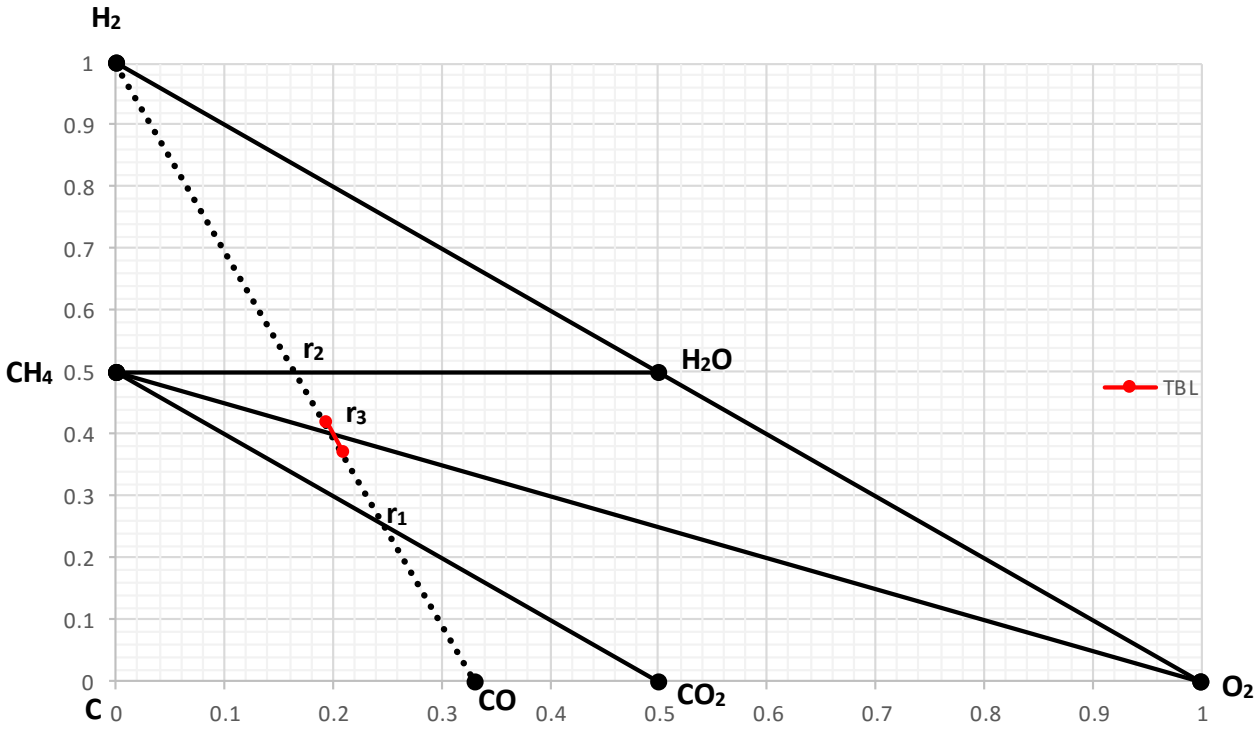


Figure 12: Thermal balance line for feed 3

4.3 Summary

Here, a mass balance region (stoichiometric region) was developed wherein reforming reactions occur for the various feeds chosen. The mass balance region is further constrained by the application of the overall energy balance. This resulted in a straight-line relationship on the phase diagram indicating thermally neutral operation.

5. The DME synthesis process

Chapter 4 developed the constrained region for syngas production by considering mass and energy balances. The aim of natural gas reforming or gasification of biomass and coal is obtaining the right syngas composition for the desired end use. The composition, especially the ratio of H_2 to CO is very important when the syngas is used in downstream processes. In this section, we apply the diagram developed in chapter 4 to develop a flow sheet for the production of DME at different syngas compositions. The feasible region for feed 3 does not exists as discussed in chapter 4 and hence feed 3 will not be considered for DME synthesis.

5.1 DME synthesis using Feed 1

Feed 1 is bound by the stoichiometric region, which is very rich in hydrogen as discussed in the previous chapter. The point $\mathbf{r_2}$ on the C, H, O diagram corresponds to an H_2:CO ratio of 3:1 obtained via steam reforming. The point r_3 corresponds to the H_2:CO ratio of 2:1 obtained via partial oxidation of methane. Steam reforming produces syngas too rich in hydrogen (Azizi, et al.,2014) whereas partial oxidation a ratio close to that for DME synthesis.

The JFE DME synthesis process requires the H_2:CO ratio of 1:1 which cannot be satisfied by either of the points on the stoichiometric region. This hypothesis can be verified by testing the points on the stoichiometric region, which lie on the line H_2 – CO. The value alpha can be determined using the following equation on the line $\mathbf{r_2}$-$\mathbf{r_3}$:

$$\alpha r_2 + (1-\alpha) r_3 \rightarrow H_2(1-\alpha) + CO$$

For the ratio $\frac{H_2}{CO} = 1$, the equation must satisfy the condition: $0 < \alpha < 1$

In this case for the ratio to be met, $\alpha = -1$, therefore the solution does not exist and the feed is not suitable for the production of DME via JFE process. The same test was applied for all the linear combinations of r_1-r_4 as well as on the thermal balance line. This feed follows the Haldor Topsoe process (satisfying the ratio of 2).

Therefore, it can be concluded that DME can only be produced via the Haldor Topsoe process for this feed type within the stoichiometric region as well as on the thermal balance line. Therefore, the reaction by-product using this feed type is water and the product will lie on the line joining H_2:CO=2:1 and water as shown in Figure 13. This process will require an additional

water-gas shift in order to obtain the desired H_2:CO ratio. Variation of the H_2:CO ratio changes the direction of the water gas shift reaction.

To adjust the ratio would require more carbon dioxide in order to drive the WGS reaction to produce CO. Moreover, the WGS reaction takes place outside the stoichiometric region for this feed type, operating outside the feasible region is not allowed. An alternative would be to remove excess hydrogen or to operate away from the thermal balance line in order to meet the ratio requirement. Excess hydrogen can be removed by using a membrane, however the separation of gases using a membrane is expensive.

Table **3** shows the points A and D on the thermal balance line together with their respective H_2:CO ratios, CO_2 produced and excess hydrogen.

Point	**H_2:CO**	**CO_2 produced**	**Alternative: remove extra Hydrogen**
A	2.15	0	0.15
B	2.87	0.18	0.72
C	4.27	0.39	1.39
D	-	1	0.32

Table 3 : TBL point A-D and their respective H_2:CO ratio for feed 1

Point **A** is more favourable because it uses the least amount of hydrogen and the remove stream also contains the least amount of hydrogen, therefore results in less process waste. Point **D** provides an interesting picture, the amount of CO contained in the syngas mixture at this point is zero. There are two options for the synthesis of DME at point D, one option would be to synthesise methanol-using carbon dioxide and remove any additional hydrogen. The separation of hydrogen from carbon monoxide can be done by using membranes (Peer, et al., 2007).

Another option would be to use additional CO_2 to produce CO via the water-gas shift reaction and consequently produce DME via methanol dehydration. However, this option requires an additional carbon dioxide stream as well as operating outside the stoichiometric region. Because of the above findings, focus will be given to point A and D on the thermal balanced line and any point within the stoichiometric region. Figure 13 shows DME synthesis reaction path for feed 1.

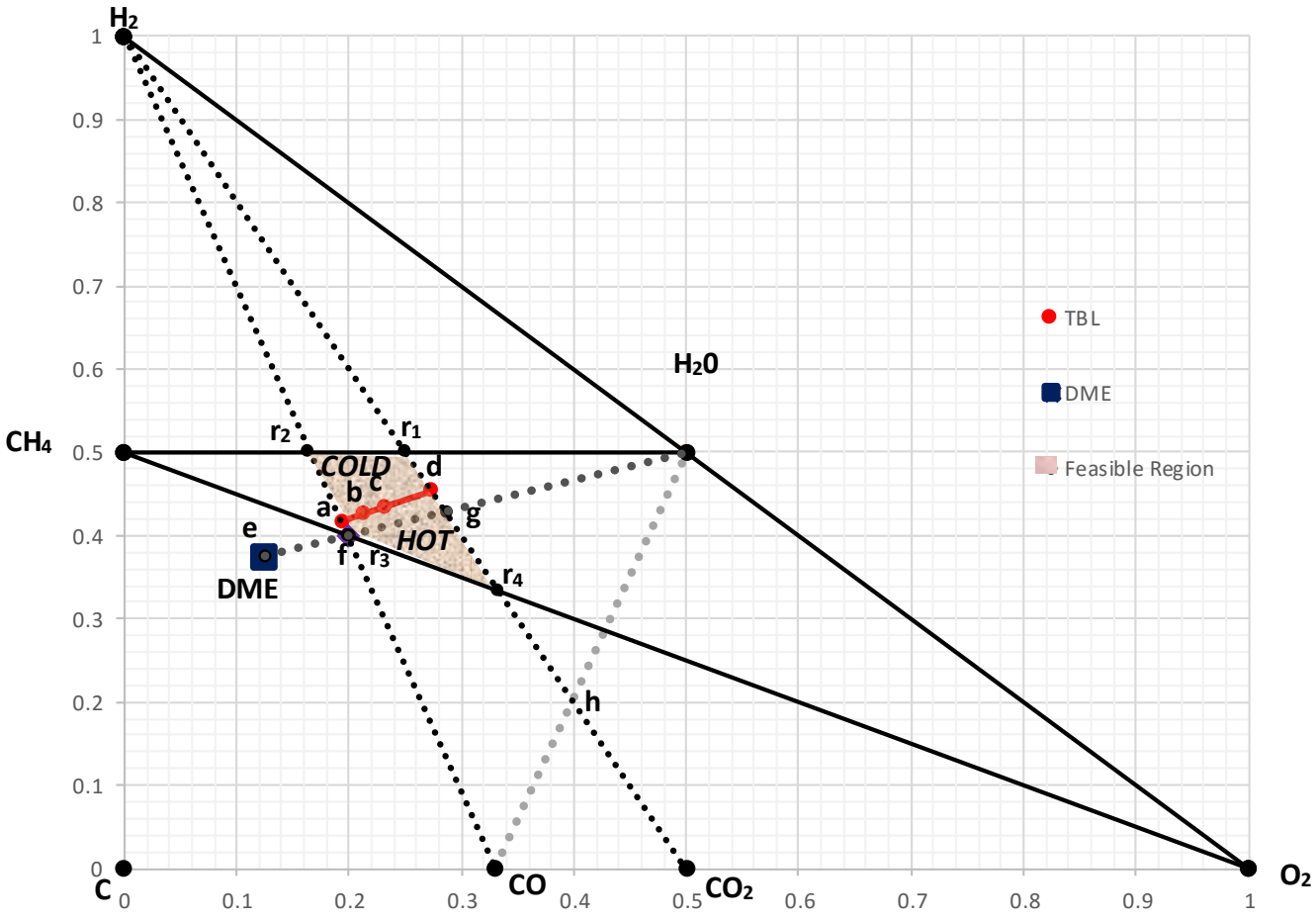


Figure 13 : DME synthesis using Feed 1

5.1.1 DME synthesis process routes

Option 1: DME synthesis from point A on the thermal balanced line

Reaction A which occurs on the TBL (point a) produces syngas in the ratio, H_2:CO = 2.15:1

$$\mathbf{A:\ CH_4 + 0.15H_2O + 0.43O_2 \rightarrow 2.15H_2 + CO} \qquad \mathbf{0\ \frac{KJ}{MOL}} \qquad \text{Equation 6.1}$$

To reduce the ratio to **2, 0.15 moles of hydrogen** is removed and the following reaction takes place for methanol synthesis to get to point **f** on the graph. This point is slightly away from the TBL on the hot side. A sample calculation for representing a separation process on the C, H and O diagram is shown on appendix A1.

Methanol synthesis from **CO:**

$$\mathbf{2H_2 + CO \rightarrow CH_3OH} \qquad \text{Equation 6.2}$$

DME is produced by the dehydration of methanol, here the reaction by-product is water which gets recycled and some of it removed from the system. This is represented by the point **e** (DME) and the dotted product line DME and water.

$$\mathbf{CH_3OH \rightarrow 0.5CH_3OCH_3 + 0.5H_20} \qquad \text{Equation 6.3}$$

Overall Reaction:

$$\mathbf{CH_4 + 0.43O_2 \rightarrow 0.5CH_3OCH_3 + 0.35H_2O + 0.15H_2} \qquad \text{Equation 6.4}$$

Process flow diagram is shown below:

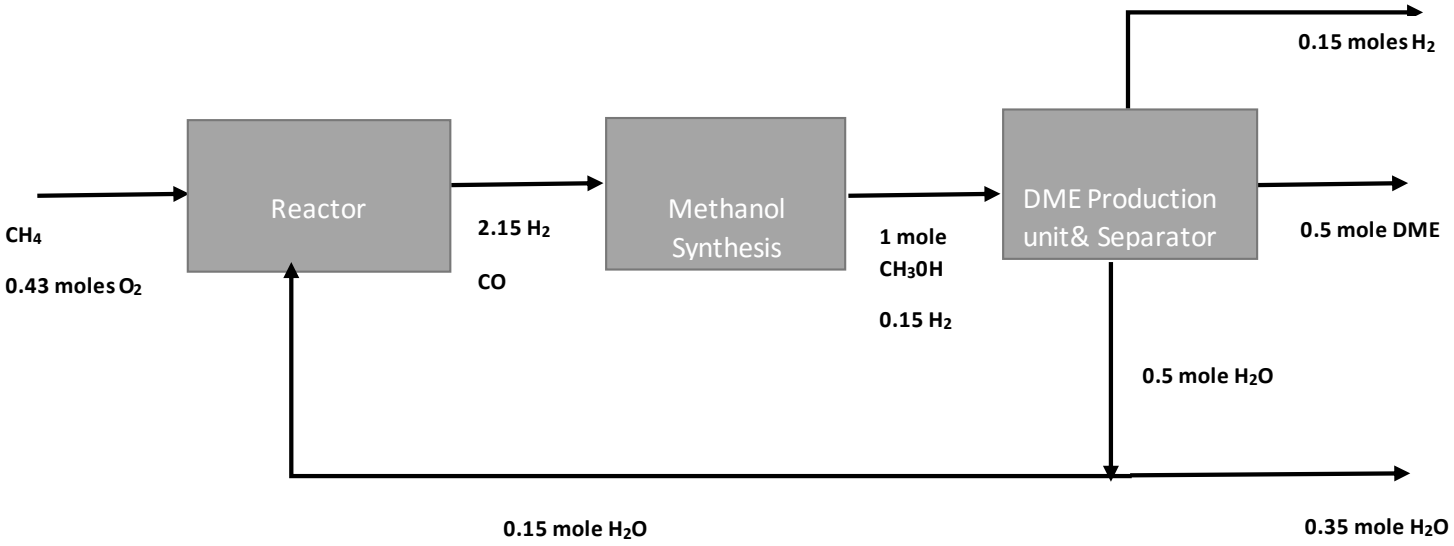


Figure 14 : Process Flow diagram for DME synthesis using feed 1 – Option 1a

The yield of DME per mole of methane is 0.5. This process requires the separation of DME from water and excess hydrogen. 0.15 moles of water is also recycled back to the syngas reactor. The separation of hydrogen from DME and water would require the use of a membrane which is costly making the reaction route less preferable compared to other possible routes.

An alternative will be to operate directly from point **f** or point $\mathbf{r_3}$ with an H_2:CO ratio of 2:1 away from the thermal balance line on the hot side. This option does not require any hydrogen remove and proceeds directly to form DME and water. However, this requires the removal of excess heat from the system.

Option 1b: Operating from point **f** or point $\mathbf{r_3}$

$$\mathbf{r_3 : CH_4 + 0.5O_2 \rightarrow CO + 2H_2} \qquad \mathbf{-35.67\ \frac{kJ}{mol}} \qquad \text{Equation 6.5}$$

$$\mathbf{CO + 2H_2 \rightarrow 0.5CH_3OCH_3 + 0.5H_2O}$$ Equation 6.6

Overall Reaction:

$$\mathbf{CH_4 + 0.5O_2 \rightarrow 0.5CH_3OCH_3 + 0.5H_2O}$$ Equation 6.7

Process flow diagram is shown below:

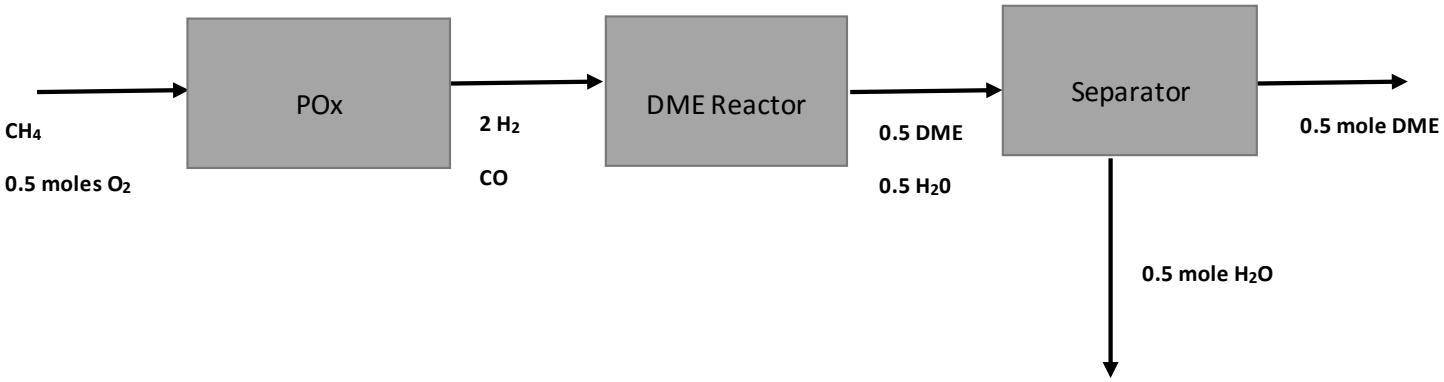


Figure 15 : Process flow diagram for DME synthesis using feed 1 option 1b

Option 2a: DME synthesis from point D on the thermal balanced line

$$\mathbf{D: CH_4 + 1.32H_2O + 0.34O_2 \rightarrow 3.32H_2 + CO_2} \qquad \mathbf{0\frac{KJ}{MOL}}$$ Equation 6.8

At this point DME can be synthesised from carbon dioxide and hydrogen with methanol synthesis as an intermediate step by removing **0.32 moles of hydrogen** to get to point **g** where **3** moles of hydrogen react with **1** mole of carbon dioxide to form methanol and water. This reaction is taking place at the extreme hot side of the stoichiometric region compared to **option 1.** The resultant by-product is still water obtained from the dehydration of methanol. The yield of DME per mole of methane is still the same as that of option 1. The process also requires separation of DME from water and hydrogen. There is an internal water recycle stream for synthesis gas production, the remaining excess water is removed from the system.

Methanol synthesis from Carbon dioxide

$$\mathbf{3H_2 + CO_2 \rightarrow CH_3OH + H_2O}$$ Equation 6.9

Methanol Dehydration:

$$\mathbf{CH_3OH \rightarrow 0.5CH_3OCH_3 + 0.5H_20}$$ Equation 6.10

Overall Reaction:

$$\mathbf{CH_4 + 0.34O_2 \rightarrow 0.5CH_3OCH_3 + 0.32H_2 + 0.18H_2O}$$ Equation 6.11

Process flow diagram is shown below:

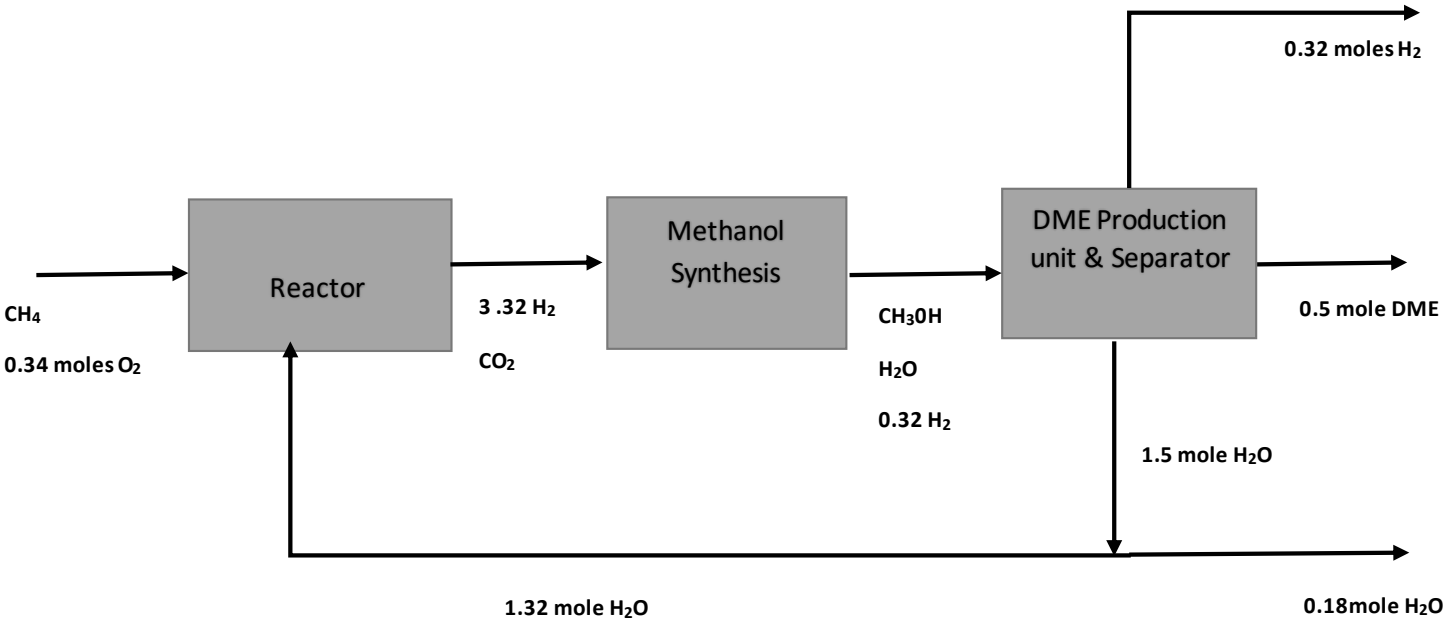


Figure 16 : Process Flow diagram for DME synthesis using feed 1 – Option 2a

Option 2b: Operating from point **g**

Similarly, a more direct route can be obtained by operating on the line $\mathbf{r_1}$ to $\mathbf{r_4}$ which satisfies the ratio H_2:CO_2 = 3:1 away from the thermal balance line to produce DME and water directly.

$$\alpha r_1 + (1-\alpha) r_4 \rightarrow 2H_2(1+\alpha) + CO_2$$

α = 0.25 satisfies the ratio =3 and the point lies on **g** as shown on the graph above given by the following equation:

$$\mathbf{CH_4 + H_2O + 0.5O_2 \rightarrow 3H_2 + CO_2} \qquad \mathbf{-76.82\ \frac{kJ}{mol}}$$ Equation 6.12

Produce DME directly from point **g**

$$\mathbf{3H_2 + CO_2 \rightarrow 0.5CH_3OCH_3 + 1.5H_2O}$$ Equation 6.13

Overall reaction:

$$\mathbf{CH_4 + 0.5O_2 \rightarrow 0.5CH_3OCH_3 + 0.5H_2O}$$ Equation 6.14

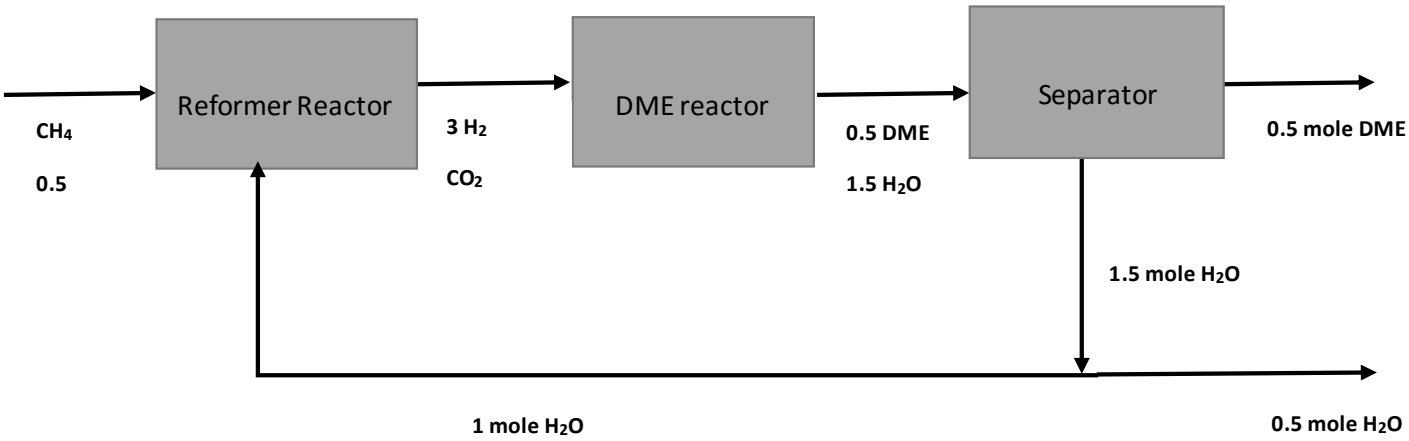


Figure 17 : Process Flow diagram for DME synthesis using feed 1 – Option 2b

5.1.2 Summary of all reaction routes

Table 4 represents a summary of all the options.

	DME yield/mole methane	**CO_2 recycle**	**CO_2 emissions**	**H_2O waste stream**	**Waste streams (H_2, CO)**	**ΔHrn (syngas step) (kJ/mol)**	**H_2:CO ratio**
1a	0.5	-	-	0.35	0.15	0	2:1
1b	0.5	-	-	0.5	-	-35.67	2:1
2a	0.5	-	-	0.18	0.32	0	2:1
****2b***	0.5	-	-	0.5	-	-76.82	3:1

*H_2:CO_2 ratio

Table 4 : A Summary of all Options for Feed 1

From the above it can be concluded that for all reaction routes for feed 1 the yield of DME per mole methane remains the same (0.5 moles per mole methane). However, option 1b and 2b are the optimal reaction routes due to the following:

i. Option 1b and 2b operate in the exothermic region, therefore the reaction does not require energy input into the system.

ii. The syngas (H_2 and CO) is also used up when producing DME via these process routes and therefore no separation is required to remove the gases from the DME produced compared to reaction routes 1a and 2a.

5.2 DME synthesis using Feed 2

The syngas mixture obtained for feed 2 has a relatively low H_2:CO ratio within the stoichiometric region as well as on the thermal balanced line compared to the syngas mixture for feed 1. The thermal balance points A-D are in the order of decreasing ratio as discussed in section 4.2.2 from a H_2:CO ratio of 1.87:1 to 0.8:1 (see *Obtained by a linear combination of thermal balanced point A and D to satisfy the H2:CO ratio of 1

Table **5**). In low H_2:CO mixture a strong synergy is obtained by the removal of water via the water-gas shift reaction and the conversion of carbon monoxide to methanol.

Point	**H_2:CO**
A	1.87
B	1.40
C	0.8
D	-
**E*	1

*Obtained by a linear combination of thermal balanced point A and D to satisfy the H_2:CO ratio of 1

Table 5 : Point A, D and E on TBL for Feed 2 together with their respective H_2:CO ratios

Table 5 is a very interesting point, it has a high H_2:CO ratio, close to 2:1. This is because it lies close to the point r_4 (Figure 18) on the stoichiometric region. To increase the ratio to 2 will require the removal of 0.07 moles of CO in order to operate at point r_4 or j (Figure 18).

On the other hand, another point D exists with a CO:H_2O ratio = 1.42, to synthesise DME at this point will require the removal of 0.575 moles of water to operate at the point $\mathbf{r_1}$ away from the thermal balance line. Otherwise, the reaction can also take place away from the thermal balance line at point **h** obtained by a linear combination of $\mathbf{r_1}$ and $\mathbf{r_3}$. Fortunately, unlike feed 1 the WGS reaction occurs within the stoichiometric region at the hot side of the thermal balance line.

There exists a point on the TBL obtained by a linear combination of point A and D which satisfies the ratio H_2:CO = 1:1.

$$\alpha A + (1-\alpha)D \rightarrow H_2(2\alpha) + CO\ (\ 2.84 - 1.77\alpha\ ) + 2H_2O\ (1-\alpha)$$

For H_2:CO ratio = 1:1, **alpha = 0.25,** the equation for point E on Figure 18 is as follows; equation 6.16.

$$\mathbf{CH_4 + 0.5CO_2 + 0.5O_2 \rightarrow 1.5H_2 + 1.5CO + 0.5H_2O} \qquad \text{Equation 6.16}$$

The value of alpha to satisfy the ratio H_2:CO = 2:1 is negative and hence the solution does not exist on the TBL.

Apart from the above discussed thermal balanced points, the reaction can also take place at any point on the line r_1-r_3 (Figure 18) and the line r_3-r_4 (Figure 18) obtained by a linear combination of r_1 and r_3; r_3 and r_4 reactions which satisfies the ratio H_2:CO of 1:1.

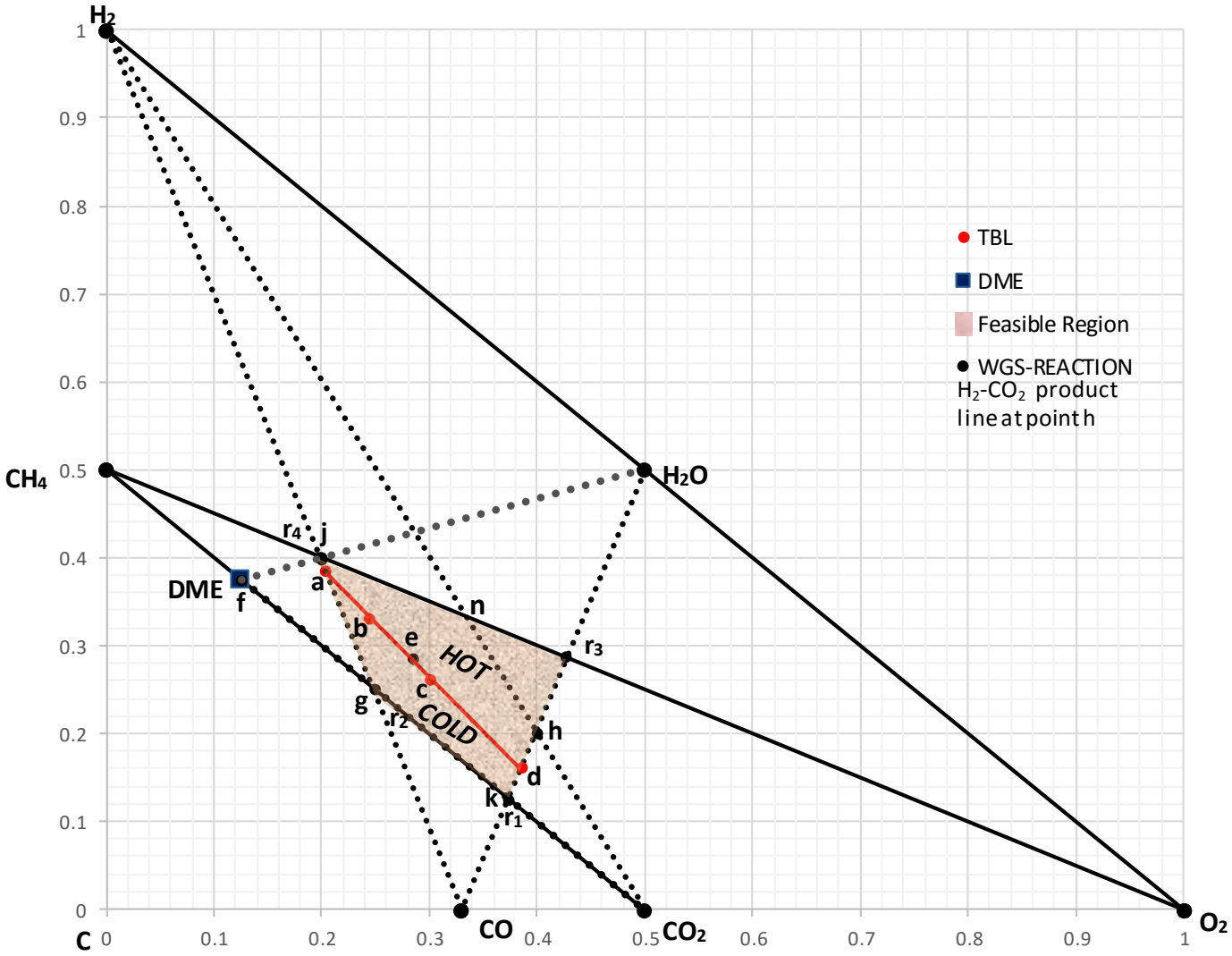


Figure 18 : DME synthesis using Feed 2

Moreover, the reaction can also satisfy the ratio H_2:CO =2:1 at point r_4 away from the TBL. The process is however more expensive to carry out because it is more energy intensive than when operating at the thermal balanced line (point A). Therefore, it can be concluded that Feed 2

follows the production of DME via the JFE process when operating at the thermal balanced line; it also follows the Haldor Topsoe process when operating away from the thermal balance line at point $\mathbf{r_4}$ or point **j** on Figure 18.

As a result, the results will focus on exploring points A, D and E and any points within or on the stoichiometric region.

5.2.1 DME synthesis process routes

Option 1a: Operating within the stoichiometric region at point **n**

Point **n** is obtained by the linear combination of r_3 and r_4 to satisfy the ratio H_2:CO =1:1.

$$\propto \boldsymbol{r_3} + (\mathbf{1}-\propto)\boldsymbol{r_4} \rightarrow \boldsymbol{CO} + \mathbf{2} \propto \boldsymbol{H_2O} + \mathbf{2}\boldsymbol{H_2}\ (\mathbf{1}-\propto) + \mathbf{2} \propto \boldsymbol{H_2O}$$

For the value of alpha = 0.5, Point n is given by:

$$\mathbf{CH_4 + O_2 \rightarrow CO + H_2 + H_2O} \qquad -\mathbf{277.5}\,\frac{\mathbf{KJ}}{\mathbf{MOL}} \qquad \text{Equation 6.17}$$

In this case in order to get to point **g** (figure 18), 1 mole of water is removed from the system, H_2 and CO react to form DME and carbon dioxide. The reaction begins at the extreme hot side of the TBL and runs to completion at the extreme cold side of the TBL.

$$\mathbf{CO + H_2 \rightarrow 0.33CH_3OCH_3 + 0.33CO_2} \qquad \text{Equation 6.18}$$

Overall reaction:

$$\mathbf{CH_4 + O_2 \rightarrow 0.33CH_3OCH_3 + 0.33CO_2 + H_2O} \qquad \text{Equation 6.19}$$

Process flow diagram is shown on figure 19.

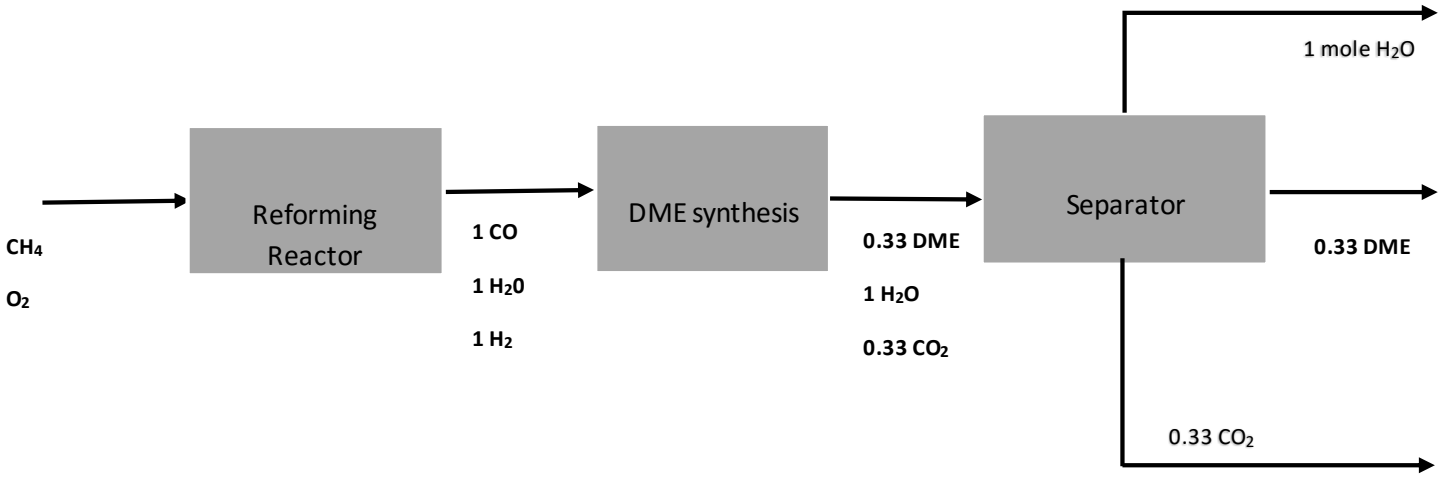


Figure 19 : Process Flow diagram for DME synthesis using feed 2 – Option 1a

The process results in 0.33 moles of carbon dioxide being emitted to the atmosphere per mole of methane processed. An alternative will be to operate at thermal balance point E which results in less emissions.

Option 1b: Operating at thermal balance point E

Point **e** is given by the equation below obtained by using alpha = **0.25** to obtain a linear combination of point A and D which gives H_2:CO ratio of 1:1.

$$\mathbf{E: CH_4 + 0.5CO_2 + 0.5O_2 \rightarrow 1.5H_2 + 1.5CO + 0.5H_2O} \qquad \mathbf{0\ \frac{KJ}{MOL}} \quad \text{Equation 6.20}$$

Remove 0.5 moles of water to get to point **g** where 1.5 moles H_2 and 1.5 moles CO react together to form DME and CO_2 via the following reaction:

$$\mathbf{1.5H_2 + 1.5C0 \rightarrow 0.5CH_3OCH_3 + 0.5CO_2} \qquad \text{Equation 6.21}$$

Overall Reaction:

$$\mathbf{CH_4 + 0.5O_2 \rightarrow 0.5CH_3OCH_3 + 0.5H_2O} \qquad \text{Equation 6.22}$$

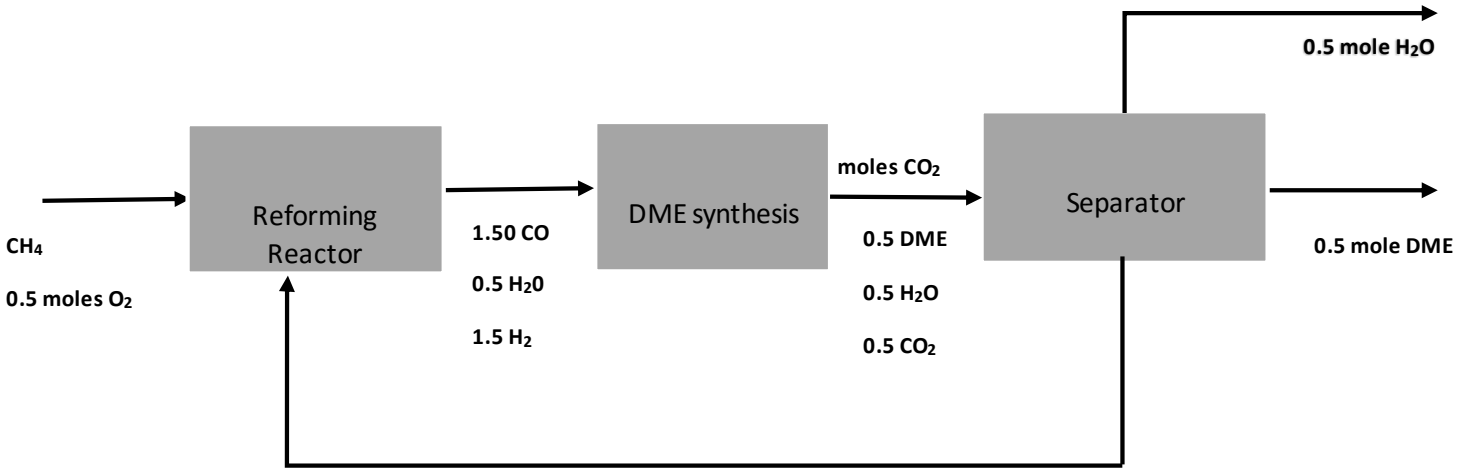


Figure 20 : Process Flow diagram for DME synthesis using feed 2 – Option 1b

This reaction has an internal carbon dioxide recycle stream obtained from downstream processes (DME synthesis reaction). Carbon dioxide is used in the reformer reactor to produce a syngas mixture of H_2, CO and H_2O. The DME reaction occurs on the extreme cold side of the thermal balance line. The yield of DME is **0.5** mole per mole of methane.

Alternatively, to eliminate the water removal step, the reaction can operate at the stoichiometric region $\mathbf{r_2}$ or point **g** away from the thermal balance line on the hot region

Option 1c: Operating at point $\mathbf{r_2}$ within the stoichiometric region

Point $\mathbf{r_2}$ or point **g** is given by the following equation:

$$\mathbf{r_2 : CH_4 + CO_2 \rightarrow 2H_2 + 2CO} \qquad \mathbf{247.3\ \frac{KJ}{MOL}} \qquad \text{Equation 6.23}$$

$$\mathbf{2H_2 + 2C0 \rightarrow 0.67CH_3OCH_3 + 0.67CO_2} \qquad \text{Equation 6.24}$$

Overall reaction:

$$\mathbf{CH_4 + 0.33CO_2 \rightarrow 0.67CH_3OCH_3} \qquad \text{Equation 6.25}$$

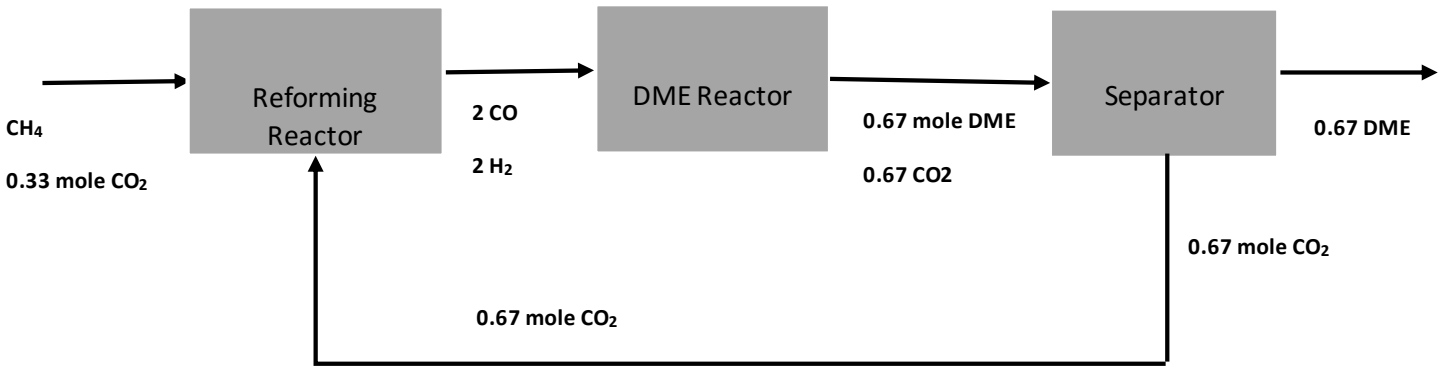


Figure 21 : Process Flow diagram for DME synthesis using feed 2 – Option 1c

The above options 1a,1b and 1c represent the possible processes which can take place along the line g – n. As can be seen the yield of DME decreases as we move further from point $\mathbf{r_2}$ on the cold side of the TBL towards the hot side to point **n**. This is because the concentration of water in the syngas increases as we move towards point **n.** The concentration of water increases towards point **n** due to the RWGS at point **h**.

Option 2

Option 2 provides an option of producing DME along the line r_1-r_3 via the water gas shift reaction. This reaction takes place when all the reactants are in stoichiometric proportions, otherwise the product stream will contain unreacted species. There lies a point **h** on this line where the shift reaction occurs in stoichiometric proportions with no unreacted species

Option 2a: From point **h** on the stoichiometric region.

Point **h** (on the line r_1-r_3) on Figure 18 is obtained by a linear combination of $\mathbf{r_1}$ and $\mathbf{r_3}$**.** It produces gas with a high water content and DME is produced via the following equation.

$$\mathbf{h}: \mathbf{CH_4 + CO_2 + O_2 \rightarrow 2CO + 2H_2O} \qquad \mathbf{-236.4\ \frac{kJ}{mol}} \qquad \text{Equation 6.26}$$

Produce hydrogen via the WGS reaction by reacting 1 mole of water with 1 mole of carbon monoxide.

$$\mathbf{H_2O + CO \rightarrow H_2 + CO_2} \qquad \text{Equation 6.27}$$

The unreacted CO reacts with hydrogen at point **g** on the cold side of the TBL to form DME and carbon dioxide. Remove water (1 mole) and carbon dioxide (1 mole) via path h-k-g on figure above to get to point **g**.

$$H_2 + CO \rightarrow 0.33CH_3OCH_3 + 0.33CO_2$$ Equation 6.28

Overall reaction:

$$CH_4 + O_2 \rightarrow 0.33CH_3OCH_3 + H_2O + 0.33CO_2$$ Equation 6.29

Process flow diagram is shown below

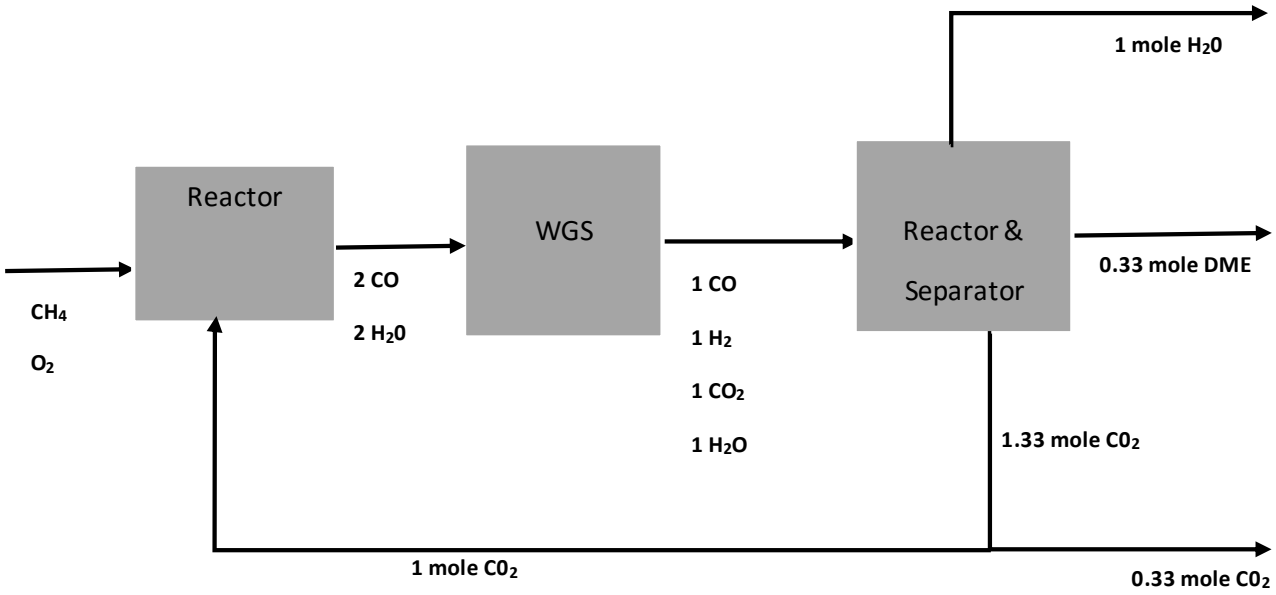


Figure 22 : Process Flow diagram for DME synthesis using feed 2 – Option 2a

The yield of DME per mole methane for this process is 0.33. The process has a carbon dioxide recycle stream as well as a remove stream to remove the excess carbon dioxide. The amount of water produced from the process is 1 mole per mole methane processed.

Option 2b: From point D on the thermal balanced line:

$$\mathbf{D:}\ CH_4 + 1.84CO_2 + 0.58O_2 \rightarrow 2.84CO + 2H_2O \quad 0\frac{KJ}{MOL}$$ Equation 6.30

At this point 2.84 moles of carbon dioxide react with 2 moles of water to form hydrogen and carbon dioxide via the following reaction:

$$2.84\,CO + 2\,H_2O \rightarrow 1.42CO_2 + 1.42CO + 0.58\,H_2O + 1.42\,H_2$$ Equation 6.31

Remove carbon dioxide and unreacted water via reaction pathway d-k-g to get to point g where unreacted carbon monoxide and hydrogen react to form DME and water

$$1.42CO + 1.42\,H_2 \rightarrow 0.473\,CH_3OCH_3 + 0.473CO_2$$ Equation 6.32

Overall reaction

$$\mathbf{CH_4 + \ 0.58O_2 \ \rightarrow 0.473\ CH_3OCH_3 + 0.053CO_2 + 0.58\ H_2O} \qquad \text{Equation 6.33}$$

Process diagram shown below:

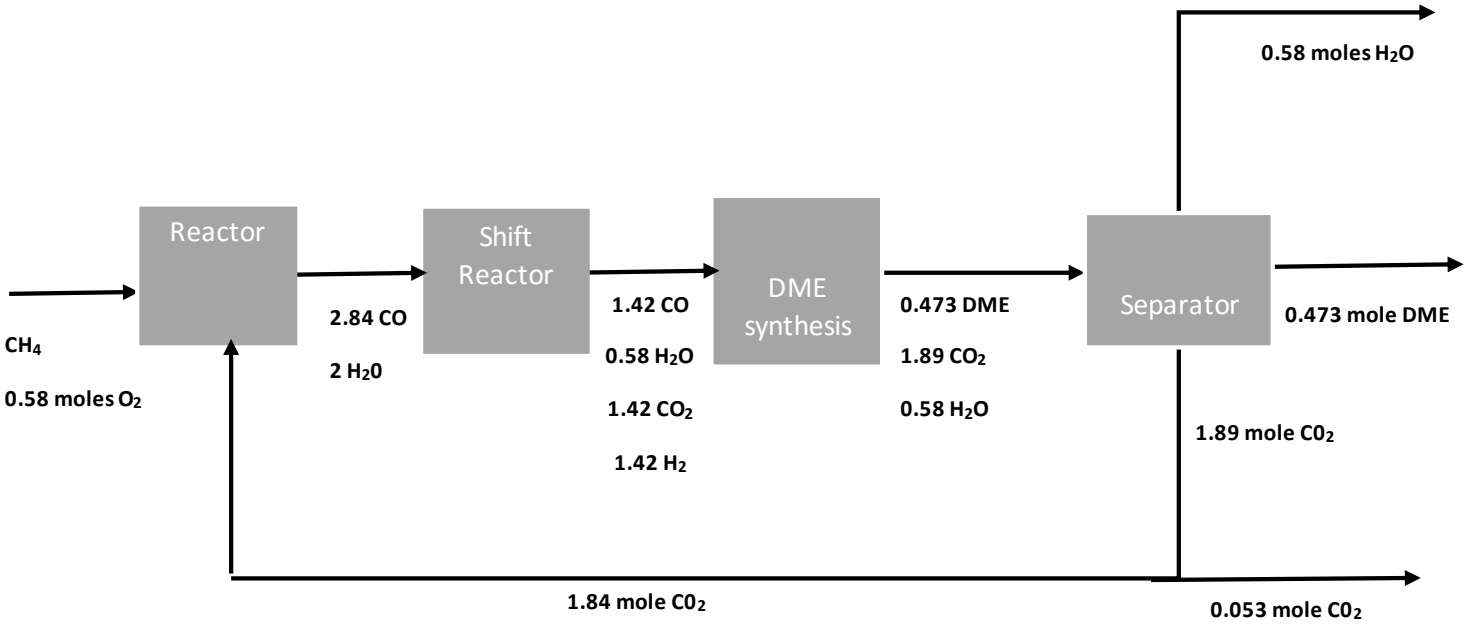


Figure 23 : Process Flow diagram for DME synthesis using feed 2 – Option **2b**

The amount of DME produced per mole methane is **0.473**, slightly higher than option 2a. The process also requires two reactors, one for syngas production and another for the shift reaction. A separator is required to separate both water and carbon dioxide from DME, separation of water from DME is more difficult than separation of carbon dioxide from DME. There is an internal carbon dioxide recycle stream as well as a separator to remove excess carbon dioxide from the system.

Alternatively, to reduce the amount of waste produced when operating along the water-gas shift reaction line r_1-r_3, the point r_1 on the stoichiometric region allows for a process, which uses up all reactants.

Option 2c: Operating at point **k** or point $\mathbf{r_1}$ via the following chemical reaction:

$$\mathbf{r1: CH_4 + 3CO_2 \rightarrow 4CO + 2H_2O} \qquad \mathbf{329.6\ \frac{KJ}{MOL}} \qquad \text{Equation 6.34}$$

$$\mathbf{4CO + 2H_2O \rightarrow 2H_2 + 2CO_2 + 2CO} \qquad \text{Equation 6.35}$$

Remove all the carbon dioxide via reaction pathway **k-g** to get to point **g** where unreacted carbon monoxide reacts with hydrogen to form DME and carbon dioxide

$$\mathbf{2CO + 2H_2 \rightarrow\ 0.67\ CH_3OCH_3 + 0.67CO_2}$$ Equation 6.36

Overall Reaction

$$\mathbf{CH_4 + 0.33CO_2 \rightarrow\ 0.67\ CH_3OCH_3}$$ Equation 6.37

Process diagram is shown below

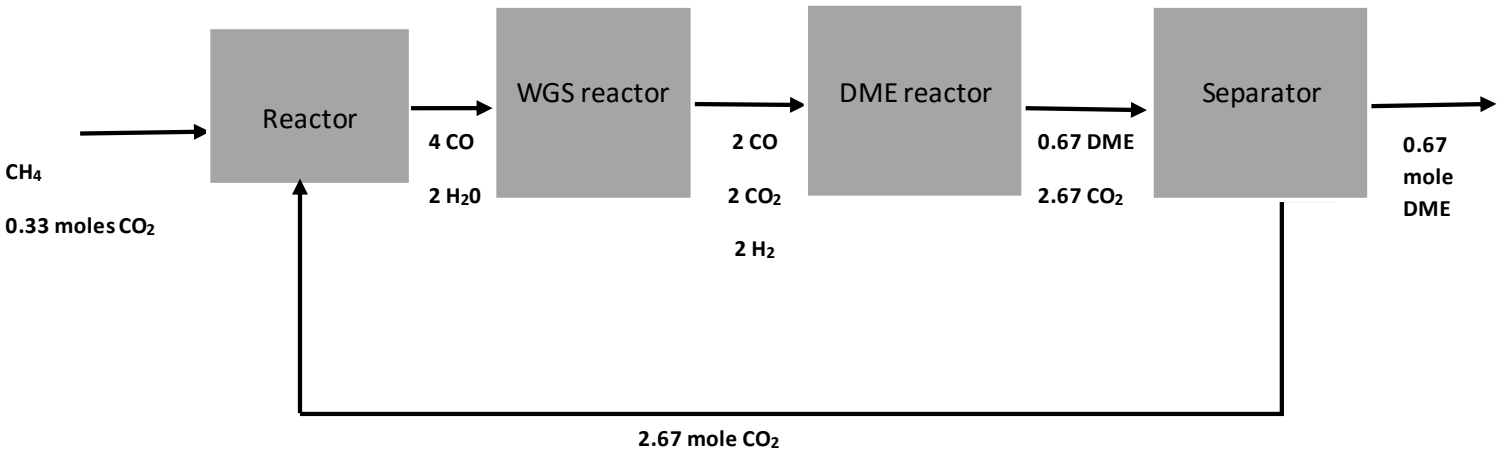


Figure 24 : Process Flow diagram for DME synthesis using feed 2 – Option 2c

The above reaction requires an additional carbon dioxide feed of 0.33 moles, the internal recycle stream does not satisfy the required amount (3 moles) for syngas production. The yield of DME per mole of methane for this reaction is **0.67 moles**.

As we move along the line r_1-r_3 (from the cold side of the thermal balance to the hot side) the yield of DME decreases, if we proceed towards point r_3 on the line r_1-r_3, the yield of DME at stoichiometric point r_3 is the lowest. At this point DME is produced by reacting 0.5 mole CO with 0.5 moles H_2O to produce 0.5 mole H_2 which then reacts with unreacted CO to produce 0.167 mole DME. Separation is also required to remove 1.5 moles of water from the system and the formed carbon dioxide. This indicates that as we move down the line r_1-r_3 the water content in the syngas increases decreasing the yield of DME as observed for option 1.

$$\mathbf{r3 : CH_4 + 1.5O_2 \rightarrow CO + 2H_2O}$$ Equation 6.38

$$\mathbf{0.5CO + 0.5H_2\ \rightarrow\ 0.167CH_3OCH_3 + 0.67CO_2}$$ Equation 6.39

Option 3

Option 3 involves the production of DME via the Haldor Topsoe process with a ratio of H_2:CO = 2:1.

Option 3a: Point A on the thermal balance line

$$\mathbf{A: CH_4 + 0.07CO_2 + 0.47O_2 \rightarrow 2H_2 + 1.07CO} \qquad \mathbf{0\frac{KJ}{MOL}} \qquad \text{Equation 6.40}$$

Introduce a separator to remove 0.07 moles of CO in order to adjust the H_2:CO ratio to 2:1, this moves to point **j** on the stoichiometric region. DME synthesis will takes place via 2 reaction steps at point **j**, methanol synthesis using CO and then the dehydration of methanol to form DME. In this case the by-product is water and the product line is shown by the dotted line DME-H_2O.

Overall reaction can be represented by:

$$\mathbf{CH_4 + 0.07CO_2 + 0.47O_2 \rightarrow 0.5CH_3OCH_3 + 0.5H_2O + 0.07CO} \qquad \text{Equation 6.41}$$

Some form of partial oxidation and dry reforming of methane to produce DME and water. With a CO remove stream. Process flow diagram is shown in figure 25.

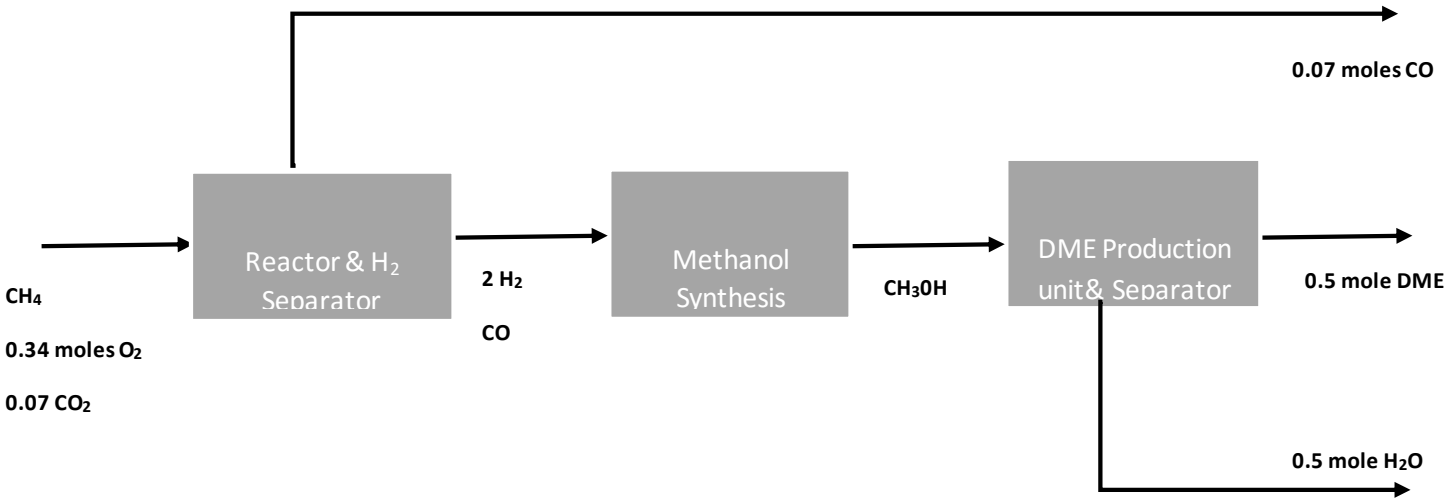


Figure 25 : Process Flow diagram for DME synthesis using feed 2 – Option 3a

This process is similar to that of feed 1, the yield of DME per mole of methane is 0.5 with by-product water. Alternatively, can operate at point $\mathbf{r_4}$ or point **j** away from the thermal balance line at the extreme hot side. Here H_2 and CO react in the ratio 1:2 to form methanol. For this case DME is produced via the Haldor Topsoe process. This process is better than the one above because it eliminates the CO removal step but operates in a region where heat is not balanced.

Option 3b: Operate at stoichiometric region $\mathbf{r_4}$ or point **j**

$$\mathbf{r4}: \mathbf{CH_4 + 0.5O_2 \rightarrow CO + 2H_2} \qquad \mathbf{-35.67\frac{KJ}{MOL}} \qquad \text{Equation 6.42}$$

Methanol synthesis from CO

$$\mathbf{CO + 2H_2 \rightarrow CH_3OH} \qquad \text{Equation 6.43}$$

Methanol Dehydration:

$$\mathbf{CH_3OH \rightarrow 0.5CH_3OCH_3 + 0.5H_2O} \qquad \text{Equation 6.44}$$

Overall Reaction:

$$\mathbf{CH_4 + 0.5O_2 \rightarrow 0.5CH_3OCH_3 + 0.5H_2O} \qquad \text{Equation 6.45}$$

The yield of DME per mole of methane is still the same as the one above and similar to that of feed 1. Process flow diagram is shown in figure 26.

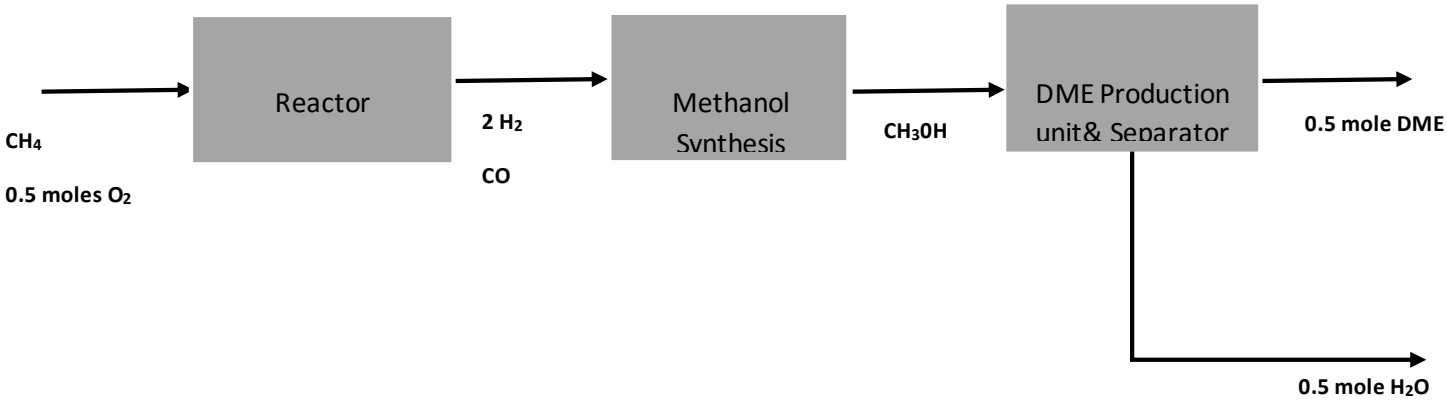


Figure 26 : Process Flow diagram for DME synthesis using feed 2 – Option 3b

5.2.2 Summary of all reaction routes

The yield of DME varies for this feed type depending on whether the process follows the Haldor Topsoe reaction route (H_2:CO = 2:1) or the JFE process (H_2:CO =1:1). Table 6 shows a summary of all reaction routes.

	DME yield/mole methane	**CO_2 recycle**	**CO_2 emission**	**H_2O waste stream**	**Waste streams (H_2, CO**)**	**ΔHrn (kJ/MOL)**	**H2:CO ratio**
	Feed 2						
	Option 1						
Option 1a	0.33	-	0.33	1	-	-277.5	1
Option 1b	0.5	0.5	-	0.5	-	0	1
Option 1c	0.67	0.67	-	-	-	247.3	1
	Option 2						
Option 2a	0.33	1	0.33	1	-	-236.4	1
Option 2b	0.473	1.84	0.053	0.58	-	0	1
**Option 2c*	0.67	2.67	-	-	-	329.6	1
	Option 3						
Option 3a	0.5	-	-	0.5	0.07**	0	2
Option 3b	0.5	-	-	0.5	-	-35.67	2

*Option 2c requires an additional carbon dioxide feed of 0.33 moles

Table 6: Summary of all reaction routes for feed 2

The reaction routes for feed 2 have varying DME yields, from 0.33 to 0.67. Reaction route 1a, 1b and 1c represent the reactions which take place along the point n, e and g respectively. This points lie on the straight line NEG as shown on the figure 27.

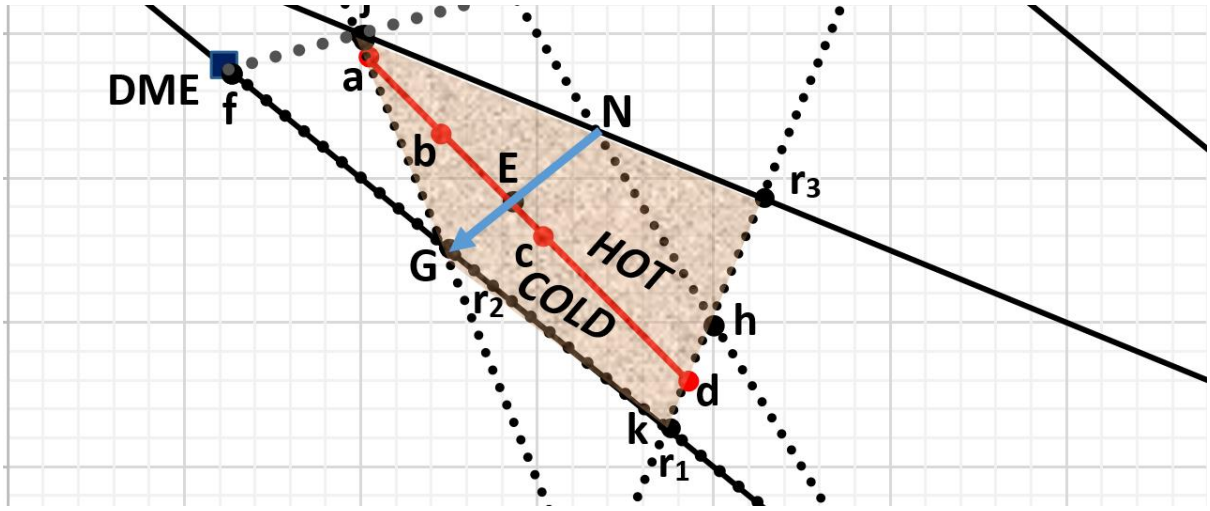


Figure 27: Comparison of reaction routes for feed 2 - Option 1

As we move from the point N to the point G (from the hot side of the thermal balance line to the cold side of the thermal balance line) the yield of DME increases with the consequent removal of water. Note the amount of water decreases from 1 to 0 as we approach point G. However, operating at point G requires energy input into the system. A trade-off between DME yield and energy requirement.

Similarly, the reaction routes for option 2 (2a, 2b and 2c) are in the order of increasing DME yield, the yield of DME increases with the consequent removal of carbon dioxide and water. However, option 2c requires an external carbon dioxide feed in order to drive the formation of DME as well as energy input into the system. Option 2c is thus not a feasible option for DME synthesis.

Option 3 produces DME via the same route as feed 1, the yield of DME is 0.5 per mole methane with by-product water. It is worth noting that in order to produce DME via option 3b, it requires the removal of excess carbon monoxide and water. On the other hand, Option 3b only requires the removal of water from the product stream however, removing water from DME requires more energy than removing gases.

From the above it can be concluded that for all reaction routes for feed 2 the yield of DME per mole methane varies depending on the process route. However, option 1b and 1c are the optimal reaction routes due to the following:

i. Option 1b has a carbon dioxide recycle stream and hence no carbon dioxide emissions.
ii. Option 1c has a high DME yield and a carbon dioxide recycle stream although energy is required for the reaction to take place

5.3 Summary

Feed 1 produces DME via the Haldor Topsoe reaction route (H_2:CO = 2:1). The yield of DME for this feed for all options is 0.5 mole DME/ mole methane with by-product water. Feed 2 produces DME via the JFE process on the TBL and some points within or on the stoichiometric region. It also follows the Haldor Topsoe reaction routes on some points within the stoichiometric region. The yield of DME ranges from **0.**33 mole DME/mole methane to **0.67 mole DME/mole methane**. Reactions which follow the JFE reaction route (H_2:CO =1:1) are known to give high syngas conversion than the reactions which follow the Haldor Topsoe reaction routes at the same temperature. The advantage for feed 2 is that most reaction routes follow the JFE process and thus have carbon dioxide as a by-product. Carbon dioxide is easier to separate from DME than water because it requires less energy for separation than separating DME from water. Table 7 shows a summary of all the options.

	DME yield/mole methane	**CO_2 recycle**	**CO_2 emissions**	**H_2O waste stream**	**Waste streams (H_2, CO**)**	**ΔHrn (KJ/MOL)**	**H2:CO ratio**
	Feed 1						
	Option 1						
Option 1a	0.5	-	-	0.35	0.15	0	2
Option 1b	0.5	-	-	0.5	-	-35.67	2
	Option 2						
Option 2a	0.5	-	-	0.18	0.32	0	2

Option 2b	0.5	-	-	0.5	-	-76.82	2
	Feed 2						
	Option 1						
Option 1a	0.33	-	0.33	1	-	-277.5	1
Option 1b	0.5	0.5	-	0.5	-	0	1
Option 1c	0.67	0.67	-	-	-	247.3	1
	Option 2						
Option 2a	0.33	1	0.33	1	-	-236.4	1
Option 2b	0.473	1.84	0.053	0.58	-	0	1
**Option 2c*	0.67	2.67	-	-	-	329.6	1
	Option 3						
Option 3a	0.5	-	-	0.5	0.07**	0	2
Option 3b	0.5	-	-	0.5	-	-35.67	2

Table 7 : A Summary of all Options for Feed 1 and Feed 2

*Option 2c requires an additional carbon dioxide feed of 0.33 moles

The table above compares all options for both feed 1and feed 2. The highlighted options have a high yield of DME per mole methane compared to the rest, less process waste as well as zero carbon dioxide emissions. The proposed option for DME synthesis is option 1b and 2b for **feed 1** and option 1b and 1c for **feed 2**. These options will be further explored in the next chapter when the effect of carbon formation is considered.

6. Carbon Deposition Boundaries

The results in chapter 4 and 5 were based on the assumption that all the reactions go to completion and the feasible region is only limited by mass and energy balance. This is an overestimation of the actual yield obtained under equilibrium. In this chapter thermodynamic equilibrium on the C,H,O diagram will be considered. The formation of solid carbon is represented by using carbon deposition boundaries obtained from Tay, et al., 2011.

Thermodynamic equilibrium on the C, H, and O ternary diagram is obtained at a temperature range 400K to 1500K at different pressures. The main species to consider at equilibrium are C, H_2, CO_2, H_2O, CO and CH_4. Among the main species to consider in equilibrium, carbon is the only species present in the solid phase. (Prins et al, 2003, Tay et al, 2011).

It is desirable to operate in regions were solid carbon is not formed to avoid deposition on the catalysts as well as the reactor walls etc. Operating away from this region will also ensure that solid carbon is not present in the syngas.

In the ternary diagram the carbon-deposition boundaries are plotted by specifying the O/H ratio, the remaining independent variable. Other parameters can be specified, Cairns & Tevebaugh, 1964 chose to use oxygen and hydrogen ratios. The carbon deposition boundaries presented on Figure 28 and Figure 29 are at 1 atm and temperature range 800K-1500K. The region below the carbon deposition boundary towards the apex of the triangle, where element C is located, represents all syngas compositions where carbon deposition may occur. Similarly the region above, away from the apex of the triangle towards H and O represent a region of no carbon deposition. It is worth noting that the formation of carbon under chemical equilibrium has no effect on the gaseous composition.

The carbon deposition boundaries at low temperature start much closer to CH_4 at the bond equivalent just above 0.5. At low temperature, the dominant products are CH_4, H_2O and CO_2 and the lines start at this point on the C-H line towards the C-O line on the region between CO and CO_2. At higher temperatures, the lines approaches H_2 and it becomes a straight line joining H_2 and CO (1500K and 1200K). This is because the reactions which favor the formation of CH_4, H_2O and CO_2 are exothermic and are favored by lower temperatures. On the other hand, the CO reactions (the reverse reactions) are highly endothermic. The carbon reaction which results in solid carbon formation is moderately endothermic.

If the pressure is increased to beyond 1 atm, the starting point of the lines shift towards CH_4 (Li, et al., 2001, Tavebaugh & Cairns, 1965) and the deposition boundaries become less temperature dependent.

6.1 Carbon deposition boundary – feed 1

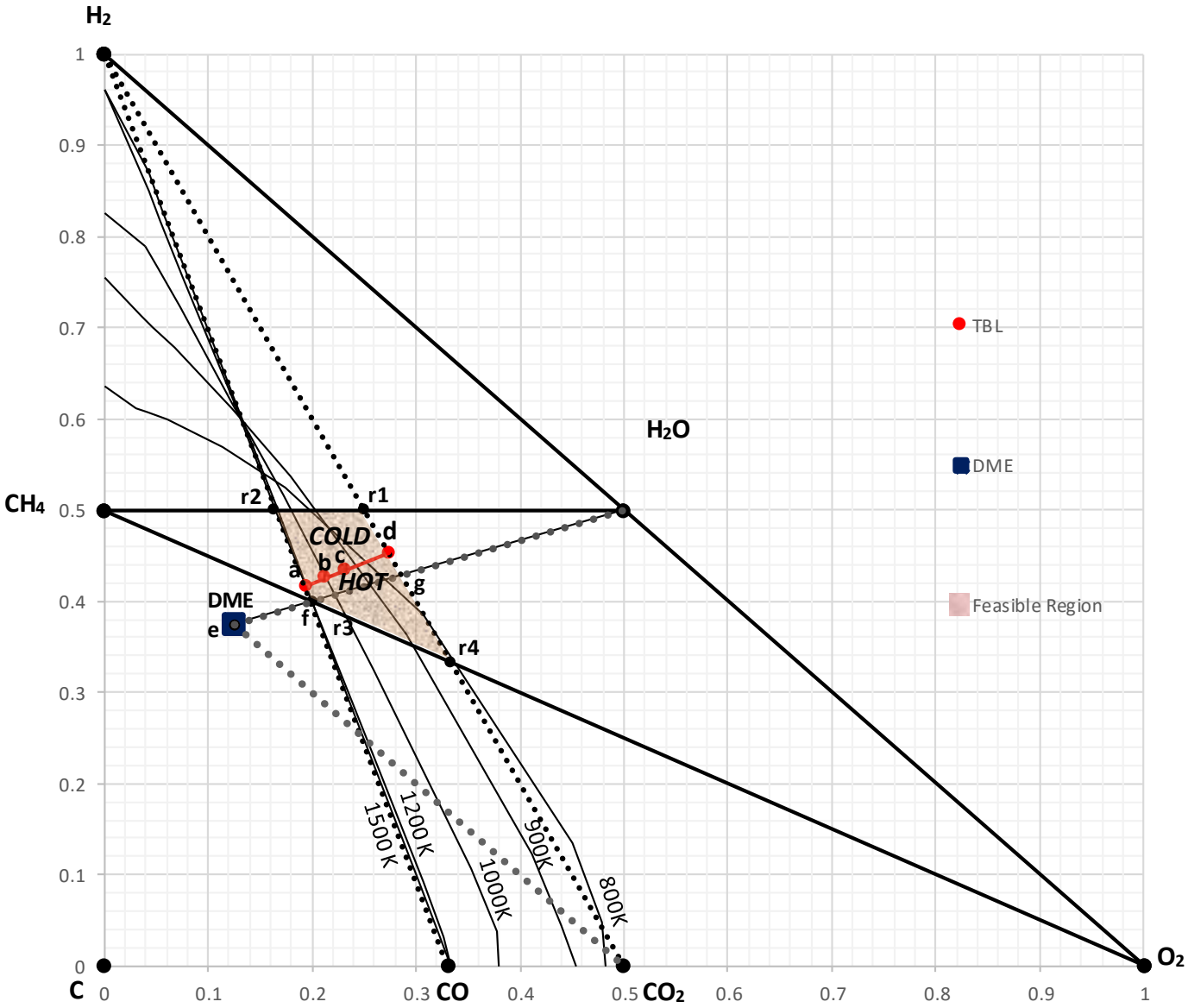


Figure 28 : Carbon-deposition boundaries – Feed 1 @ 1 atm represented as BE percentages of the equilibrium state

For feed 1 the most feasible options for DME synthesis were **options 1b** and **2b** as discussed in the previous chapter. Therefore, the options will be discussed with a new restriction – carbon deposition. Option **1b** operates at point **f** or point $\mathbf{r_3}$ away from the thermal balanced line on the hot side. Point **f** lies on the carbon deposition boundary at 1500 K, therefore the syngas at

point **f** has no solid carbon present if the reaction occurs at 1500K, however most partial oxidation reactions occur around 1200K, therefore carbon may deposit!

On the other hand, option **2b** operates at point **g** where **3** moles of hydrogen react with **1** mole of carbon dioxide to form DME and water. Point **g** lies above the carbon deposition boundary at 800K, towards H-O line. Above the carbon deposition boundary, no solid carbon is present. However, operating below 800K will result in the process operating outside the stoichiometric region and away from the thermal balance line.

6.2 Carbon deposition boundary – Feed 2

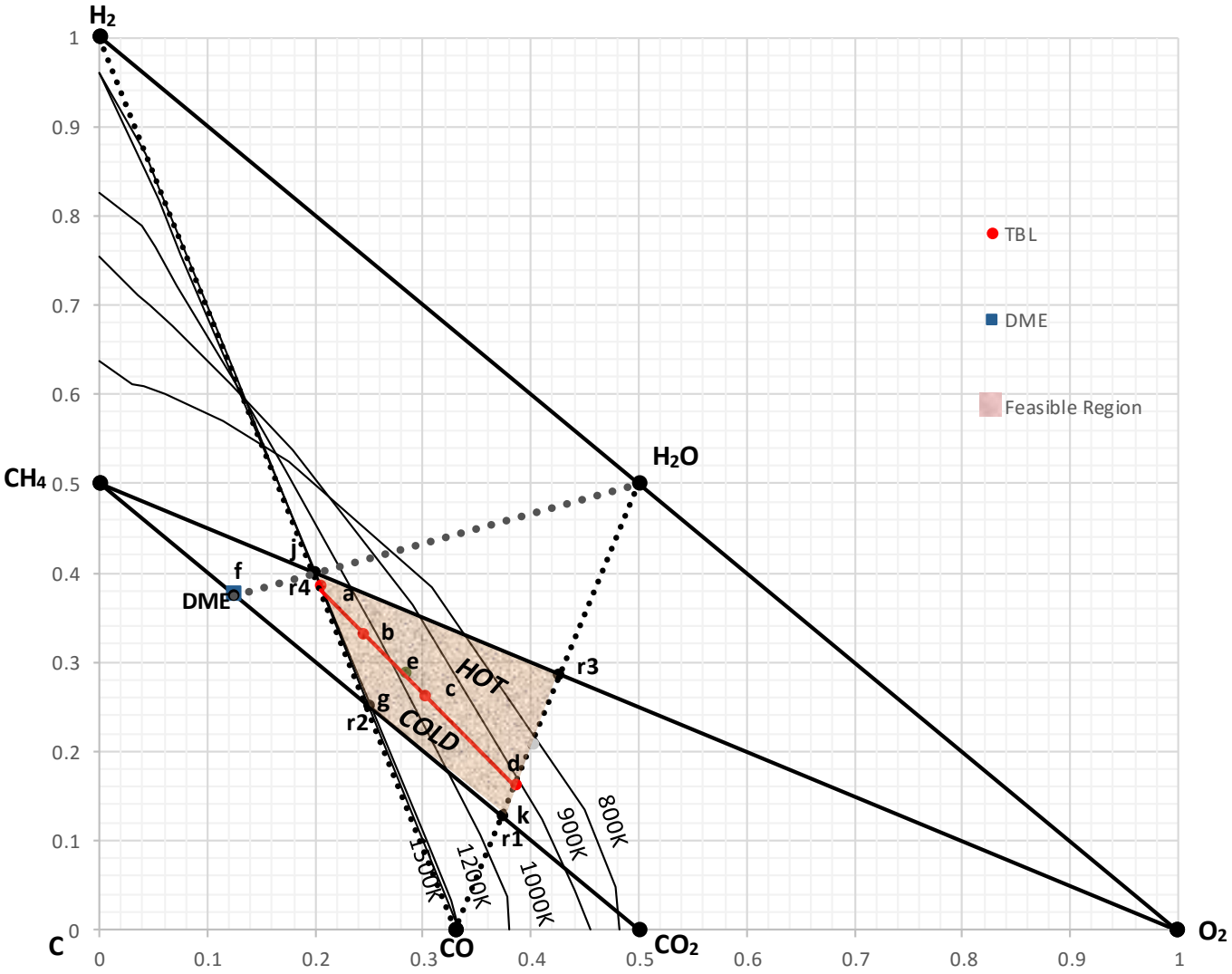


Figure 29 : Carbon Deposition Boundary – Feed 2 @ 1 atm represented as BE percentages of the equilibrium state

For feed 2 the most feasible options for DME synthesis were option **1b and 1c** as discussed in chapter 6 above. The above options will be further explored by taking in consideration carbon deposition. **Option 1c** operates at point $\mathbf{r_2}$ or point **g** with the following syngas composition; $2H_2$, 2CO. Point **g** lies on the carbon deposition boundary at 1500K and therefore there is no solid carbon formed

Option 1b operates at the thermal balance point **E** with the syngas composition; 1.5CO, $1.5H_2$ and 0.5 H_2O. This point lies on the carbon deposition boundary at 1200K, therefore there is no solid carbon formed**.**

It can therefore be concluded that **option 1c** is the most feasible option with the highest DME yield per mole methane, a smaller carbon dioxide recycle stream and operates at a region with no carbon formation.

6.3 Summary

The purpose of the carbon deposition study was to further restrict the region of operation to one where carbon deposition does not take place. The feasible regions of operation for both feed 1 and feed 2 where tested against this restriction. For feed 2 all the optimal reaction routes operate in regions of no solid carbon formation therefore it is feasible to produce DME via this reaction route. However, for feed 1 both the optimal reaction routes identified in chapter 6 did not satisfy this condition. Instead to avoid carbon formation:

i. The temperature should be 1500K, most partial oxidation reactions take place at 1200K.
ii. The temperature should be below 800K – however this is outside the feasible region of operation

In conclusion mass and energy balances alone cannot be used to determine an optimal reaction route, the possibility of carbon formation should also be considered, which then limits the reaction to a new set of operating conditions.

The next chapter considers chemical equilibrium when modelling reaction routes for both feed 1 and feed 2.

7. Modelling Chemical Equilibrium

The thermal balanced line for all feeds 1-3 was obtained by balancing the heat of reaction for exothermic and endothermic reactions for each feed at 650K assuming 100% conversion. At this conversion the syngas composition was determined and used for the conceptual design of a DME process.

In this chapter chemical equilibrium for all species CO, CO_2, H_2O, H_2 and CH_4 is considered and a new feasible region is obtained by considering equilibrium conversion. The reactions for each feed are simulated on Aspen Plus using the Gibbs reactor and Peng-Robinson equation of state. The Peng-Robinson equation of state accurately represents the relationship between temperature and pressure. A new TBL line is then obtained based on equilibrium. The results are then compared to the TBL obtained by only considering mass and energy balance. The operating temperature and pressure for the Gibbs reactor is specified at 973 K and 8 bar. The operating conditions typical for different syngas production methods (Rostrup-Nielsen & Rostrup-Nielsen, 2001; Lutz et al., 2004; Simpson & Lutz, 2007).

7.1 Modelling Equilibrium – Feed 1

7.1.1 Analysing Equilibrium for feed 1

Feed 1 involves the reaction of methane with water and oxygen. The feed undergoes steam reforming and oxidation reactions.

The equilibrium reactions are shown below and expressed per mole methane.

$$\mathbf{CH_4 + 2H_2O \leftrightarrow 1.89H_2 + 0.27CO_2 + 0.27CO + 0.46\,CH_4 + 1.19H_2O} \qquad \mathbf{99.8\,\frac{kJ}{mol}} \qquad \text{Equation 8.1}$$

$$\mathbf{CH_4 + H_2O \leftrightarrow 1.26H_2 + 0.14CO_2 + 0.23CO + 0.63CH_4 + 0.49H_2O} \qquad \mathbf{70.6\,\frac{kJ}{mol}} \qquad \text{Equation 8.2}$$

$$\mathbf{CH_4 + 0.5O_2 \rightarrow 0.72H_2 + 0.2CO_2 + 0.31CO + 0.49CH_4 + 0.29H_2O} \qquad \mathbf{-145.6\,\frac{kJ}{mol}} \qquad \text{Equation 8.3}$$

$$\mathbf{CH_4 + O_2 \rightarrow 0.85H_2 + 0.47CO_2 + 0.33CO + 0.21CH_4 + 0.74H_2O} \qquad \mathbf{-339.06\,\frac{kJ}{mol}} \qquad \text{Equation 8.4}$$

The equilibrium TBL is shown by the points below.

$$\mathbf{A: CH_4 + 0.67H_2O + 0.16\ O_2 \rightarrow 1.08H_2 + 0.16CO_2 + 0.25CO + 0.58CH_4 + 0.42H_2O} \qquad \mathbf{0\ \frac{kJ}{mol}} \qquad \text{Equation 8.5}$$

$$\mathbf{B: CH_4 + 0.83H_2O + 0.17\ O_2 \rightarrow 1.19H_2 + 0.20\ CO_2 + 0.25CO + 0.56CH_4 + 0.53H_2O} \qquad \mathbf{0\ \frac{kJ}{mol}} \qquad \text{Equation 8.6}$$

$$\mathbf{C: CH_4 + 1.19H_2O + 0.20\ O_2 \rightarrow 1.41H_2 + 0.24\ CO_2 + 0.28CO + 0.47CH_4 + 0.82H_2O} \qquad \mathbf{0\ \frac{kJ}{mol}} \qquad \text{Equation 8.7}$$

$$\mathbf{D: CH_4 + 1.54H_2O + 0.23\ O_2 \rightarrow 1.65H_2 + 0.32\ CO_2 + 0.28CO + 0.40CH_4 + 1.09H_2O} \qquad \mathbf{0\ \frac{kJ}{mol}} \qquad \text{Equation 8.8}$$

Table **8** shows the H_2:CO ratio for each point for the chemical equilibrium reactions presented above compared to the results obtained assuming 100% methane conversion and considering only reaction stoichiometry.

Thermal Balance Points	Chemical Equilibrium	@ 100% CH_4 conversion
A	**4.27**	**2.15**
B	**4.84**	**2.87**
C	**5.01**	**4.27**
D	**5.90**	**-**

Table 8 : H_2:CO ratio for feed 1 at Chemical Equilibrium vs. H_2:CO ratio @ 100% CH_4 conversion

As can be seen on the table above the H_2:CO ratio is higher compared to the ratio obtained without considering equilibrium. This is because at low temperatures the formation of CO is not supported, CO decomposes to form solid carbon (C(s)) and CO_2. At higher temperatures the reverse reaction is favored.

$$\mathbf{2CO \leftrightarrow C + CO_2} \qquad \mathbf{-171\ \frac{kJ}{mol}} \qquad \text{Equation 8.9}$$

Figure 30 shows the conversion of methane over a temperature range 500K to 1300K at a steam to carbon ratio of 2.

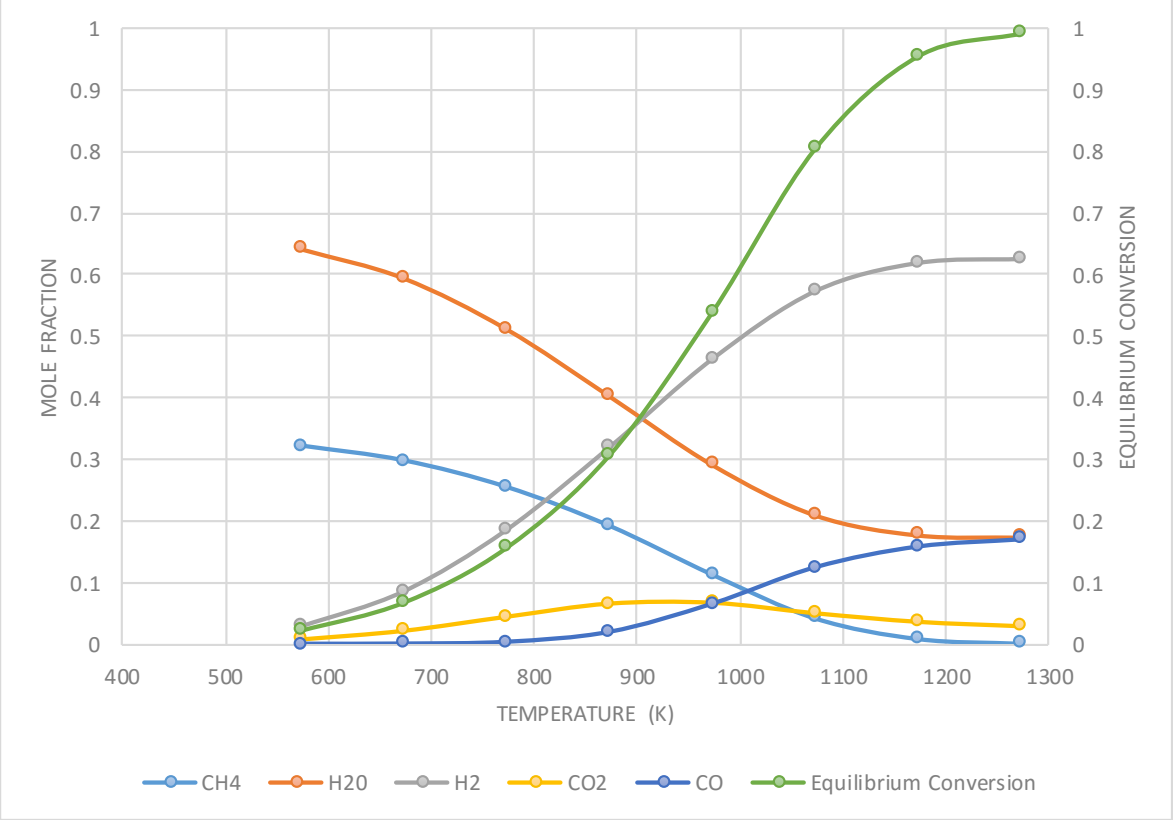


Figure 30 : Conversion of methane over a temperature range 500K to 1300K at a steam to carbon ratio of 2.

It can be seen on the graph above that the mole fraction of CO increases with an increase in temperature and the mole fraction of CO_2 begins to decreases at temperatures slightly greater than 900K. The equilibrium conversion of methane at the reformer conditions (T= 973 K and pressure of 8 bar) is 54%. A 99% conversion is obtained at a much higher temperature (T= 1273 K) which satisfies the ratio. However, operating at this temperature could damage the catalyst, to avoid damage temperatures should be kept below 1000K (Seo, et al., 2002)

On the other hand, the oxidation of methane at an oxygen to carbon ratio of 1 reports a much higher conversion of methane than partial oxidation as well as steam reforming. The expected reaction product at an oxygen to carbon ratio of 1 is CO_2 and H_2, however moles of CO_2 formed start to decrease at temperatures above 873K and moles of CO begin to increase as shown by the graph below. The conversion is 79% at the reformer operating conditions. As expected all the oxygen in the feed is used up and the mole fraction at the outlet stream is zero.

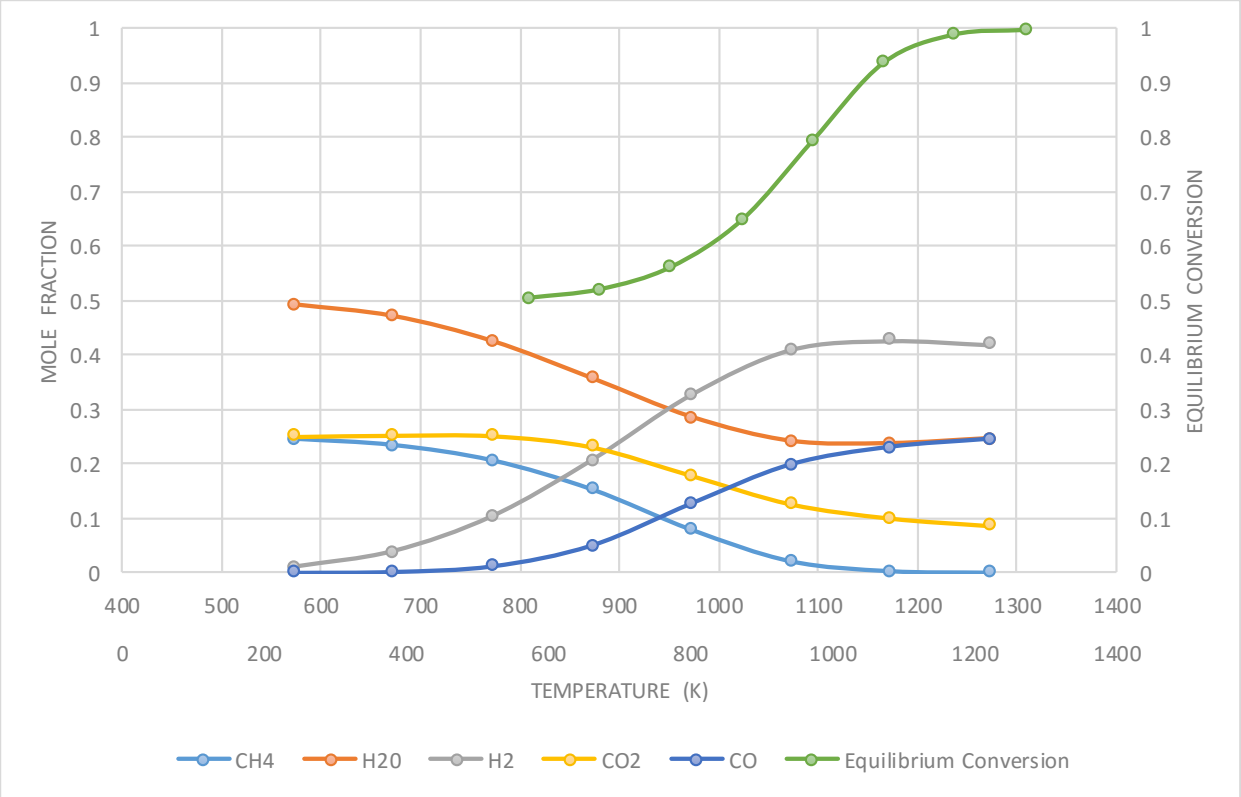


Figure 31 : Conversion of methane over a temperature range 500K to 1300K at an oxygen to carbon ratio of 1.

As a result of considering equilibrium, the thermal balance line has shifted to the extreme cold side of the TBL which was obtained without considering equilibrium. This is shown on figure 32 below.

7.1.2 DME synthesis using feed 1

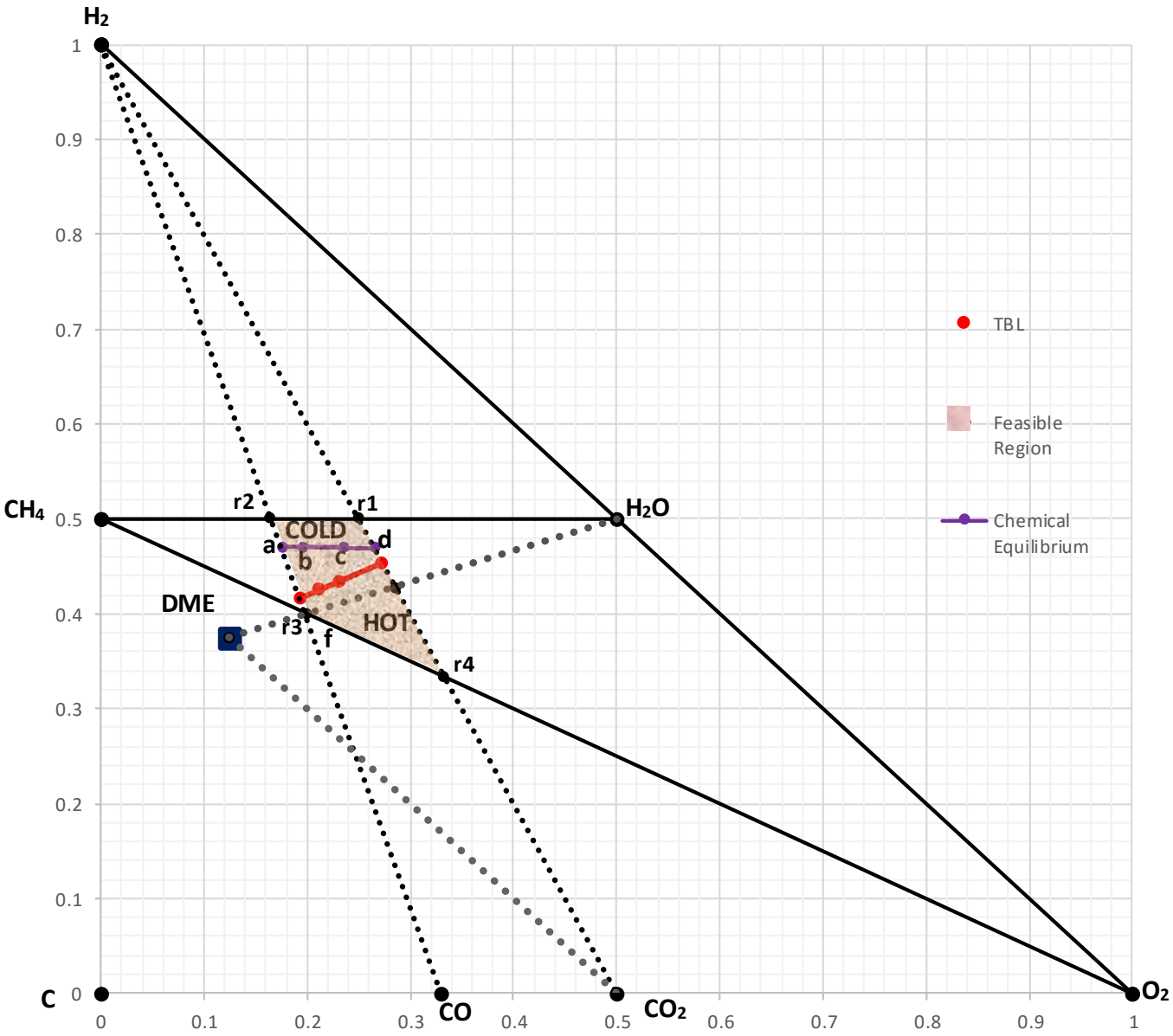


Figure 32 : Modelling Equilibrium– Feed 1

The ratio is too high for both DME synthesis via the JFE process as well as The Haldor Topsoe process. No value of alpha exists to find a linear combination of point A and D (the extreme points on the thermal balance line) which satisfies the ratio of H_2:CO = 1:1 or 2:1 on the TBL as well as within the stoichiometric region. Adjusting the ratio would require removing excess hydrogen from the feed.

Table **9** shows the amount of excess hydrogen for each point on the thermal balance line.

Thermal Balance Points	**Moles H_2 per mole methane**	**Excess hydrogen**
A	**1.08**	**0.58**
B	**1.19**	**0.70**
C	**1.41**	**0.85**
D	**1.65**	**1.09**

Table 9 : Thermal balance point A-D and amount excess hydrogen required

The points A – D are in the order of increasing excess hydrogen in the syngas. The most favorable points are those which require the removal of the least amount of hydrogen because it results in less process waste. The excess hydrogen can also be used downstream in other processes.

Option 1: Operating at thermal balance point A

$$\mathbf{A: CH_4 + 0.67H_2O + 0.16\ O_2 \rightarrow 1.08H_2 + 0.16CO_2 + 0.253CO + 0.58CH_4 + 0.42H_2O} \qquad \mathbf{0\ \frac{kJ}{mol}}$$ Equaton 8.10

Remove 0.57 moles hydrogen using a membrane separator in order to adjust the H_2:CO ratio to 2:1 and produce DME with methanol synthesis as an intermediate step. Remove all the inert species i.e. water, carbon dioxide and unreacted methane to get to point **f** and produce DME via the following equations,

$$\mathbf{0.51H_2 + 0.253CO \rightarrow 0.253CH_3OH}$$ Equation 8.11

$$\mathbf{0.253CH_3OH \rightarrow 0.127CH_3OCH_3 + 0.127H_2O}$$ Equation 8.12

The reaction moves away from the thermal balance line to the hot region on point $\mathbf{r_3}$, resulting in thermal inefficiencies. The yield of DME per mole methane is **0.125** with a carbon dioxide waste stream of **0.57 moles**. The process flow diagram is shown on

Figure **33**.

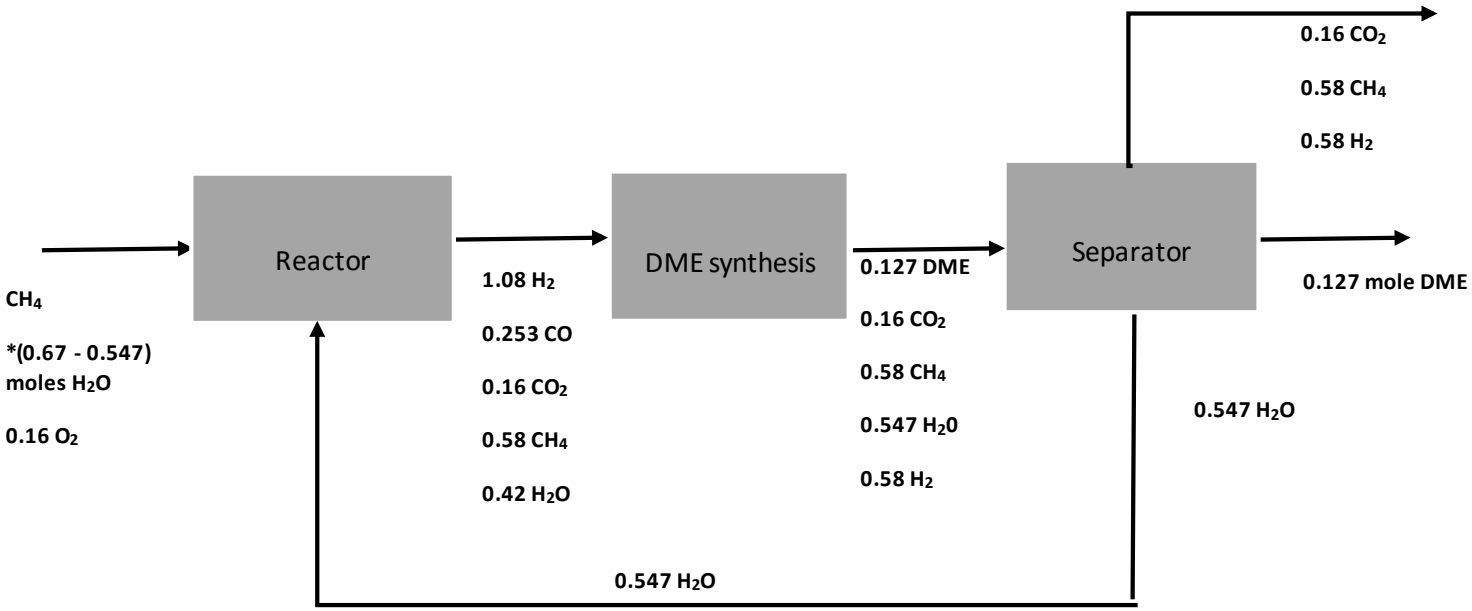


Figure 33 : Modelling Equilibrium - Process flow diagram for DME synthesis using feed 1 option 1

Option 2: Operating at thermal balance point B

The process is similar to the one above however this process requires removing more hydrogen than point A (0.7 moles), more water is also required to yield the same amount of DME as option 1.

Option 3: Operating at thermal balance point C

For this option the yield of DME per mole methane is **0.14** slightly higher than the options discussed above, however more water is required to achieve the yield.

Option 4: Operating at thermal balance point D

Point D has the same DME yield as option 3 above however the process produces more waste and requires more water to achieve the same yield.

7.1.3 Summary of all reaction routes

Table **10** shows a summary of all the options together with the amount of water required and waste produced/unreacted gases. All values are reported per mole of methane in the feed.

Options	**DME yield/mole methane**	**H_2O required in feed***	**Excess H_2**	**Unreacted gases (Including excess H_2)**	**ΔHrn (kJ/mol)**	**H_2:CO ratio**
1	0.127	0.12	0.57	1.33	0	2
2	0.123	0.18	0.70	1.45	0	2
3	0.14	0.22	0.85	1.57	0	2
4	0.14	0.32	1.09	1.81	0	2

Table 10 : Modelling Equilibrium Summary of options for feed 1

* H_2O required in feed is defined as total moles of water in the inlet stream less total amount of water in the recycle stream

*Total amount of water in the recycle stream = moles water produced + unreacted water (conversion is not 100%).

It can be concluded that the moles of CO in the syngas determine the yield of DME as well as the amount of H_2 which should be removed from the system. Option **3** and **4** have the highest DME yield but more process waste compared to option 1. However, the difference in DME yield and unreacted gas between the options is not significant and any one of the options can be considered All the above reactions take place at the thermal balance line and hence a zero heat of reaction.

7.2 Modelling Equilibrium feed 2

7.2.1 Analysing Equilibrium for feed 2

Feed 2 involves dry reforming and partial oxidation of methane. The reactions are shown below expressed per mole methane.

$$\mathbf{CH_4 + 3CO_2 \leftrightarrow 0.81H_2 + 1.84CO_2 + 1.82CO + 0.34\,CH_4 + 0.5H_2O} \qquad \mathbf{183\,\frac{kJ}{mol}}$$ Equation 8.13

$$\mathbf{CH_4 + CO_2 \leftrightarrow 0.56H_2 + 0.46CO_2 + 0.91CO + 0.63CH_4 + 0.17H_2O} \qquad \mathbf{98\,\frac{kJ}{mol}}$$ Equation 8.14

$$\mathbf{CH_4 + 1.5O_2 \rightarrow 0.65H_2 + 0.74CO_2 + 0.23CO + 0.03CH_4 + 1.29H_2O} \quad - \mathbf{555.8\,\frac{kJ}{mol}}$$ Equation 8.15

$$\mathbf{CH_4 + 0.5O_2 \rightarrow 0.72H_2 + 0.2CO_2 + 0.31CO + 0.49CH_4 + 0.29H_2O} - \mathbf{145\,\frac{kJ}{mol}}$$ Equation 8.16

The reaction of methane with oxygen at an oxygen to carbon ratio of 1.5 reports a much higher methane conversion (97%) than all the reactions at the reformer conditions specified. The expected product is CO and H_2O however at lower temperatures the products in high concentrations are H_2O and CO_2. This is because the total oxidation reaction resulting in this products is more favoured at lower temperatures than partial oxidation reactions. As the temperature increases to above 800K the concentration of H_2O and CO_2 begins to decrease and CO begins to form due to the mild exothermicity of its reaction. As the temperature increases further (beyond 1000K) partial oxidation of methane is favored than the total oxidation reactions because of its low exothermicity resulting in the formation of more CO and H_2 and the concentration of CO_2 continues to decrease until it is in equilibrium with H_2.

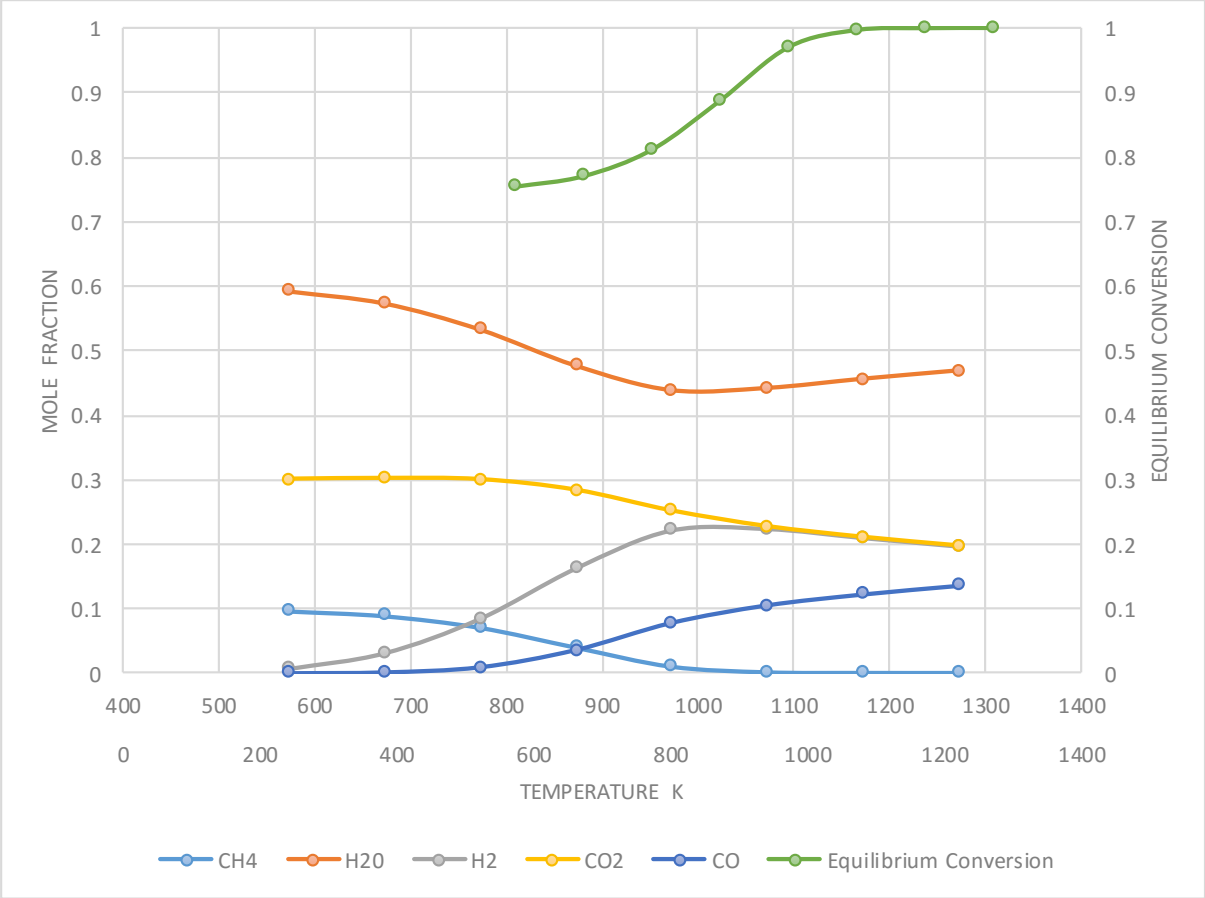


Figure 34 : Conversion of methane over a temperature range 500K to 1300K at an oxygen to carbon ratio of 1.5

Therefore, as a result of chemical equilibrium the product composition at the reactor exit is not only CO and H_2 for reaction r_3 predicted by reaction stoichiometry but also includes other products. This applies to all reactions r_1-r_4 resulting in the thermal balance line shifting to the extreme cold side of the original thermal balance line. This is represented on figure 34 above.

The thermal balance equations are shown below and expressed per mole methane.

$$\mathbf{A: CH_4 + 0.6CO_2 + 0.2\,O_2 \rightarrow 0.63H_2 + \ 0.35CO_2 + 0.67CO + 0.58CH_4 + 0.22H_2O} \qquad \mathbf{0\,\frac{kJ}{mol}}$$ Equation 8.17

$$\mathbf{B: CH_4 + CO_2 + 0.26\,O_2 \rightarrow 0.67H_2 + 0.59\,CO_2 + 0.95CO + 0.63CH_4 + 0.4H_2O} \qquad \mathbf{0\,\frac{kJ}{mol}}$$ Equation 8.18

$$\mathbf{C: CH_4 + 1.33CO_2 + 0.28\,O_2 \rightarrow 0.76H_2 + 0.93\,CO_2 + 0.97CO + 0.43CH_4 + 0.39H_2O} \qquad \mathbf{0\,\frac{kJ}{mol}}$$ Equation 8.19

$$\mathbf{D: CH_4 + 2.26CO_2 + 0.37O_2 \rightarrow 0.77H_2 + 1.57\,CO_2 + 1.42CO + 0.27CH_4 + 0.7H_2O} \qquad \mathbf{0\ \frac{kJ}{mol}}$$ Equation 8.20

The TBL has shifted to the left and also away from hydrogen resulting in a low H_2:CO ratio compared to the TBL obtained without considering equilibrium. The H_2:CO ratio for each thermal balance point is tabulated on the table below.

Thermal Balance Points	Chemical Equilibrium	@ 100% CH_4 conversion
A	**0.94**	**1.87**
B	**0.71**	**1.4**
C	**0.78**	**0.8**
D	**0.54**	**-**

Table 11 : H_2:CO ratio for feed 2 at Chemical Equilibrium vs. H_2:CO ratio @ 100% CH_4 conversion

7.2.2 DME synthesis using feed 2

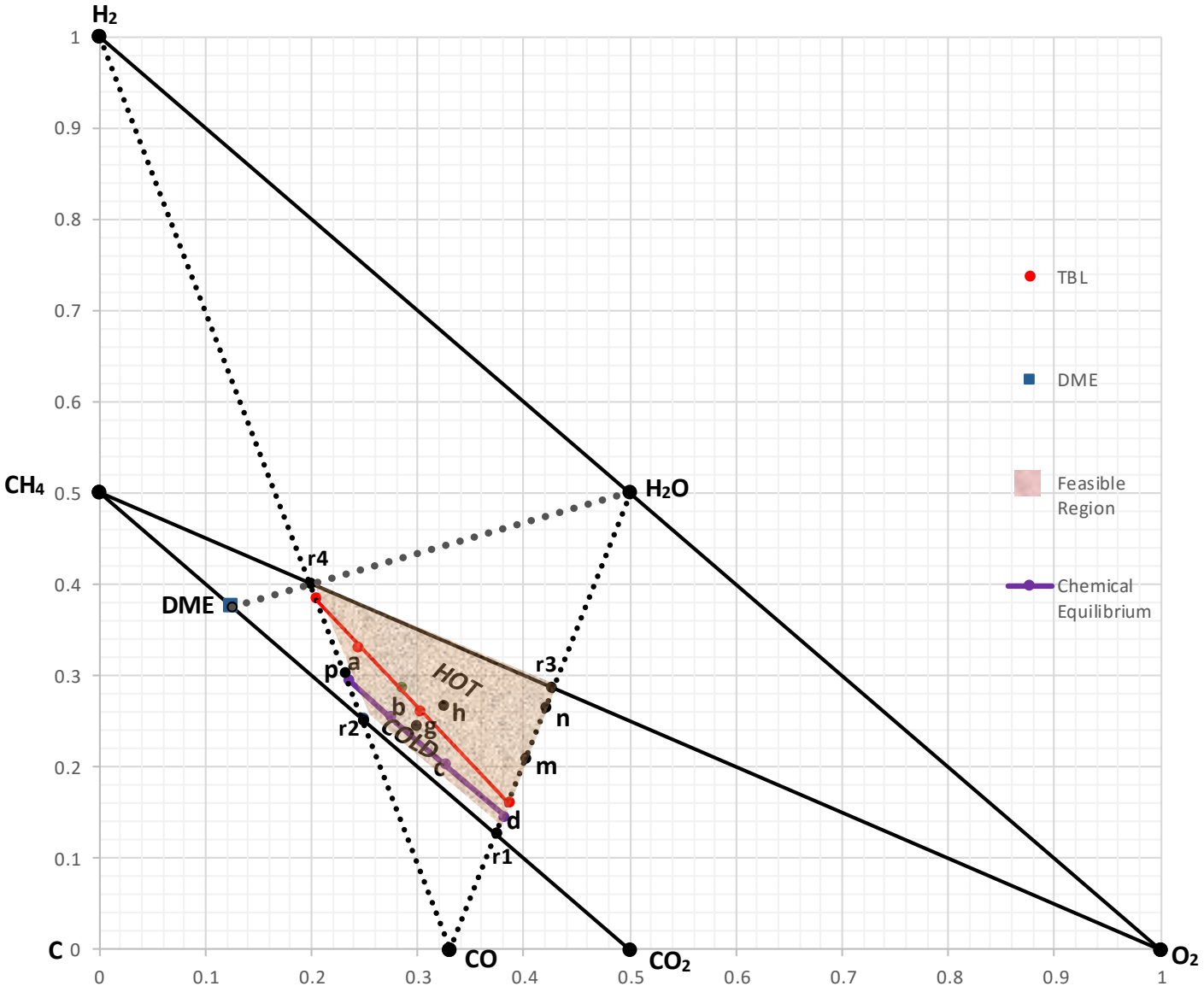


Figure 35 : Modelling Equilibrium – Feed 2

For DME synthesis the ratio of H_2:CO should be 1:1 or 2:1, in order to produce DME via the JFE process or the Haldor Topsoe process. This feed has ratios below 1. In order to produce DME via either of this routes will require operating away from the thermal balance line or finding a linear combination of the above thermal balance points which will result in the required ratio on the thermal balance line or within the stoichiometric region. No value of alpha exists to find a linear combination of point A and D (the extreme points on the thermal balance line) which satisfies the ratio of H_2:CO = 1:1 or 2:1 on the TBL. However, it is possible to meet

the ratio within the stoichiometric region by finding a linear combination of the reactions r_1-r_4, r_1-r_3, r_2-r_3, and r_2-r_4 which meets the ratio H_2:CO =1:1 or 2:1

Option 1a: Operating at the point **m o**n the extreme hot side of the TBL, obtained by a linear combination of $\mathbf{r_1}$ and $\mathbf{r_3}$ given by the following equation:

$$\alpha r_1 + (1-\alpha) r_3 \rightarrow 0.70 H_2 + 0.70 CO + \cdots + \cdots$$

For H_2:CO = 1:1 alpha = 0.3

Point **m** is given by:

$$\mathbf{m : CH_4 + 0.89CO_2 + 1.06O_2 \rightarrow 0.7H_2 + 1.07CO_2 + 0.7CO + 0.12CH_4 + 1.06H_2O} \qquad \mathbf{-338.7\ \frac{kJ}{mol}}$$ Equation 8.21

Remove all the inert species i.e. water, carbon dioxide and unreacted methane to get to point $\mathbf{r_2}$ and produce DME via the following equation,

$$\mathbf{0.7CO + 0.7H_2 \rightarrow 0.23CH_3OCH_3 + 0.23CO_2}$$ Equation 8.22

DME is separated from unreacted gases and some carbon dioxide recycled back to the reforming reactor. Excess methane is sent to feedstock storage. The process flow diagram is shown below. The yield of DME per mole methane is **0.23.**

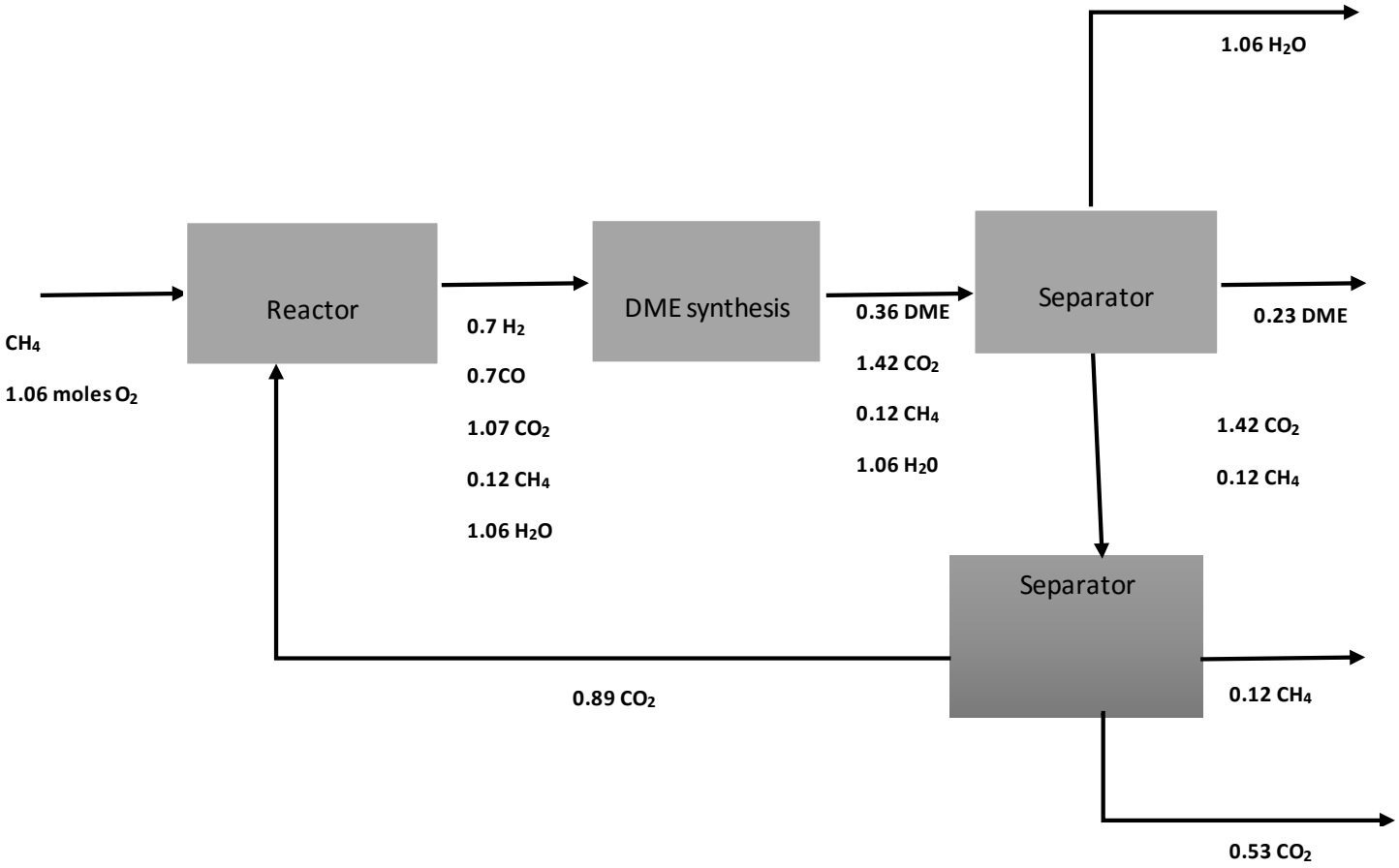


Figure 36 : Modelling Equilibrium - Process flow diagram for DME synthesis using feed 2 option 1

Option 1b: Operating at point **n** obtained by a linear combination of r_1 and r_3 given by the following equation for an H_2:CO ratio = 2:1:

$$\alpha r_1 + (1-\alpha) r_3 \rightarrow 0.66H_2 + 0.33CO + \cdots + \cdots$$

For H_2:CO = 2:1, alpha = 0.064

$$\mathbf{n: CH_4 + 0.19CO_2 + 1.4O_2 \rightarrow 0.66H_2 + 0.81CO_2 + 0.33CO + 0.05CH_4 + 1.24H_2O} \qquad \mathbf{-517.6\ \frac{kJ}{mol}}$$ Equation 8.23

Remove all the inert species, i.e. carbon dioxide, methane and water to get to point **r4** and produce DME via methanol dehydration at point **f**. Point **n** also lies on the extreme hot side of the thermal balance line resulting in thermal inefficiencies.

$$\mathbf{0.66H_2 + 0.33CO \rightarrow 0.33\ CH_3OH}$$ Equation 8.24

Dehydration of methanol

$$\mathbf{0.33\ CH_3OH \rightarrow 0.165CH_3OCH_3 + 0.165\ H_2O}$$ Equation 8.25

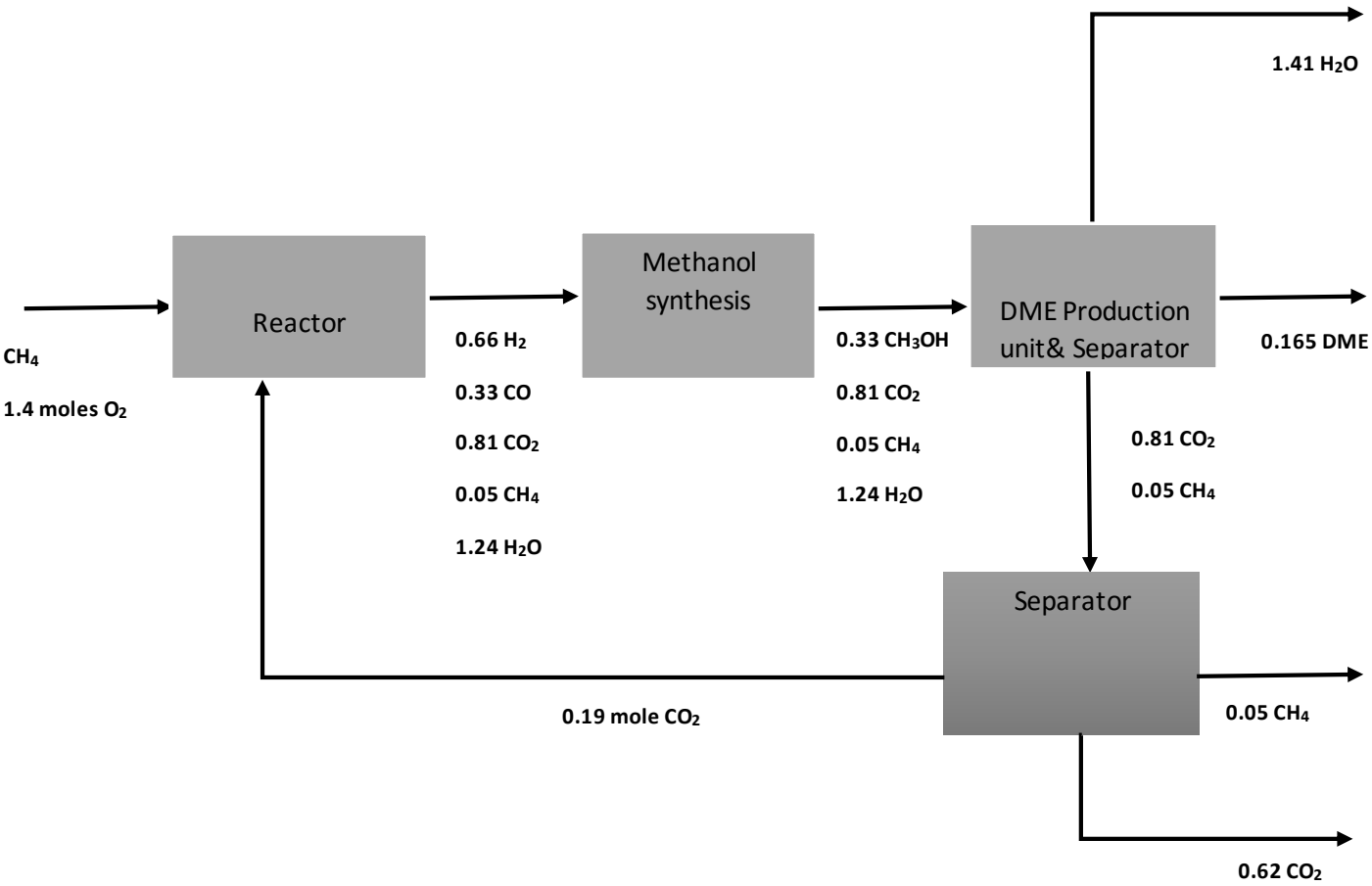


Figure 37 : Modelling Equilibrium - Process flow diagram for DME synthesis using feed 2 option 1b

Carbon dioxide is recycled back to the reformer reactor. The yield f DME per mole methane is **0.165.** Methane is sent to feedstock storage tank.

Option 2: Operating at point **g** obtained by a linear combination of r_1 and r_4.

The equation for point **g** is shown below:

$$\mathbf{g: CH_4 + 0.88CO_2 + 0.35O_2 \rightarrow 0.75H_2 + 0.68CO_2 + 0.75CO + 0.45CH_4 + 0.35H_2O} \qquad \mathbf{-63.7\frac{kJ}{mol}}$$ Equation 8.26

Remove carbon-dioxide, methane and water to get to point $\mathbf{r_2}$ and produce DME via the following reaction. Point **g** lies on the cold region of the TBL line, just close to the TBL, operating at this point is more efficient. When we move to point $\mathbf{r_2}$ we move towards the cold region which is less efficient than when operating on the thermal balance line where heat is neither lost nor required.

$$\mathbf{0.75CO + 0.75H_2 \rightarrow 0.25CH_3OCH_3 + 0.25CO_2}$$ Equation 8.27

The yield of DME per mole methane for this process is 0.25, the process flow diagram is similar to that of option 1 with a carbon dioxide recycle of 0.88 mole.

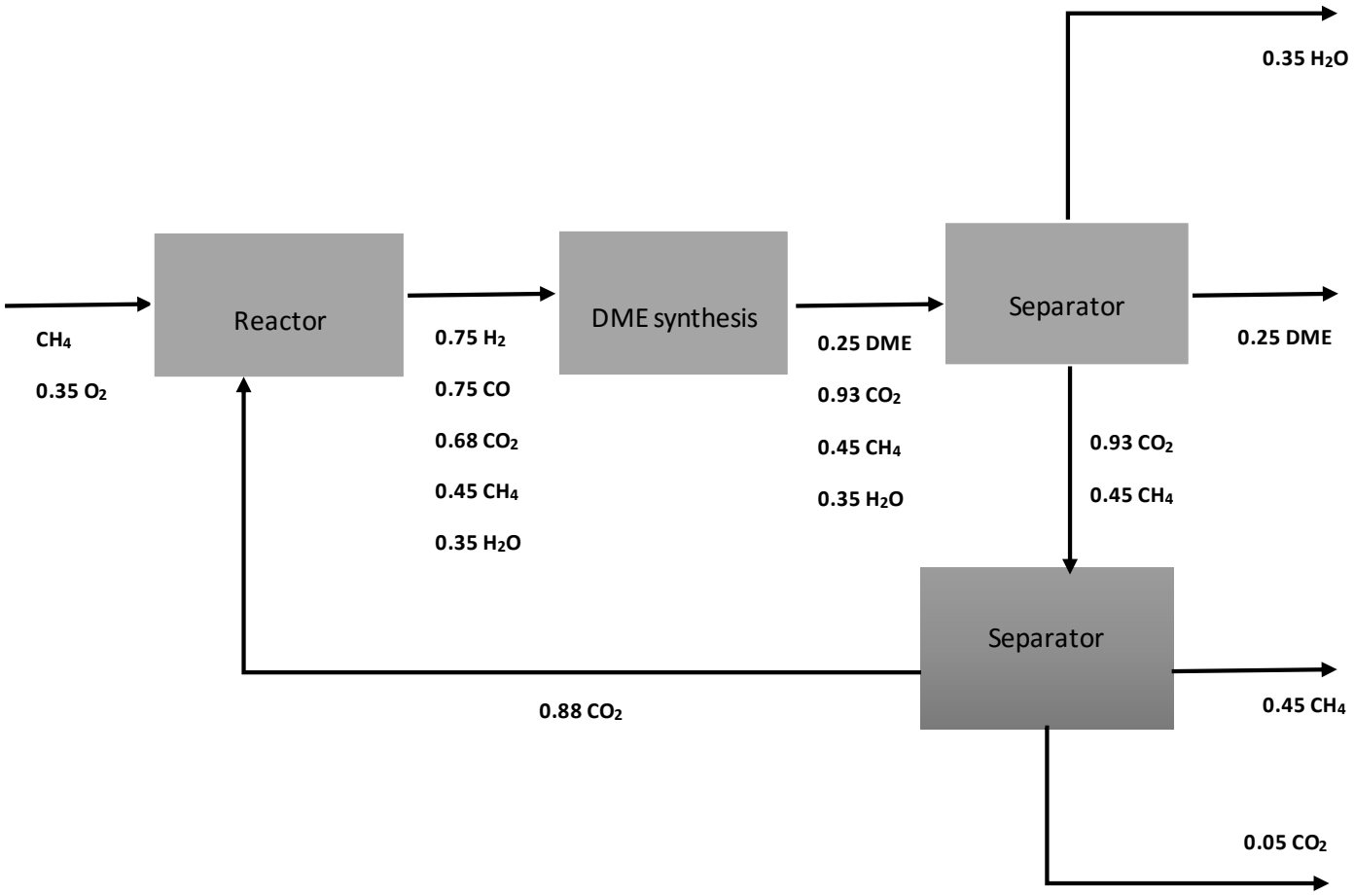


Figure 38 : Modelling Equilibrium - Process flow diagram for DME synthesis using feed 2 option 2

A value of alpha also exists to obtain a linear combination of r_1 and r_3 which satisfies the ratio H_2:CO = 2:1. However, the yield of DME for this route is always lower than the yield obtained for an H_2:CO ratio = 1:1. Therefore, it can be assumed that the yield for this route is less than 0.23.

Option 3: Operating at point **h** obtained by a linear combination of $\mathbf{r_2}$ and $\mathbf{r_3}$. Point h lies away from the TBL on the hot region.

Point **h** is given by the following equation:

$$\mathbf{h: CH_4 + 0.55CO_2 + 0.68O_2 \rightarrow 0.6H_2 + 0.59CO_2 + 0.6CO + 0.36CH_4 + 0.68H_2O}$$

$$\mathbf{-313.3\ \frac{kJ}{mol}} \qquad \text{Equation 8.28}$$

Remove all the non-reacting species to get to point $\mathbf{r_2}$ and produce DME and carbon-dioxide by the following route:

$$\mathbf{0.6CO + 0.6H_2 \rightarrow 0.2CH_3OCH_3 + 0.2CO_2} \qquad \text{Equation 8.29}$$

Process flow diagram is as follows:

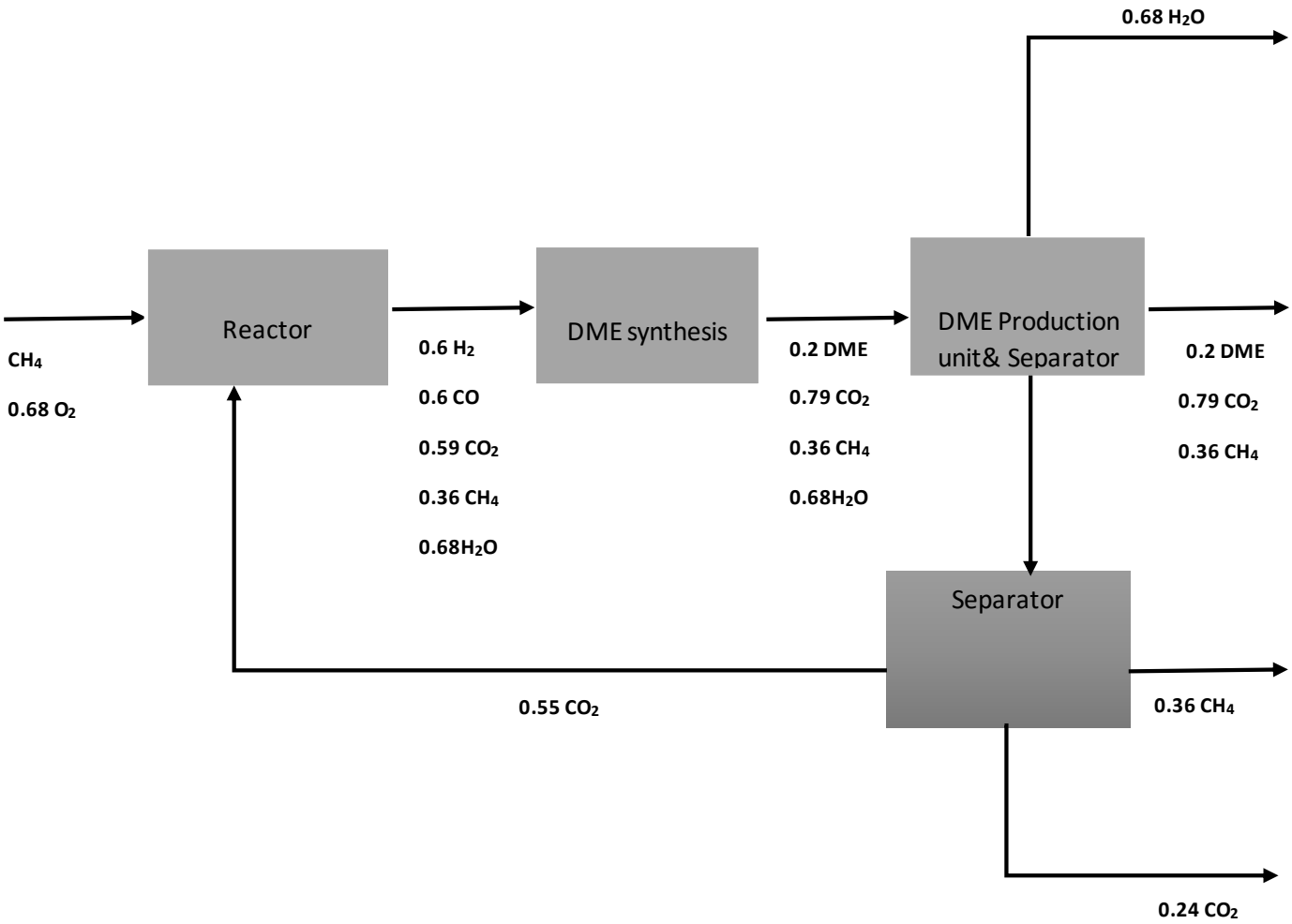


Figure 39 : Modelling Equilibrium - Process flow diagram for DME synthesis using feed 2 option 3

A value of alpha also exists to obtain a linear combination of r_2 and r_3 which yields an H_2:CO ratio of 2:1, however the yield of DME will be less than the yield obtained for a ratio of H_2:CO = 1:1. Therefore, it can be assumed that the yield for this case is less than **0.2.**

Option 4: Operating at point **p** obtained by a linear combination of r_2 and r_4 to satisfy the ratio H_2:CO of 1:1.

$$\mathbf{p: CH_4 + 0.55CO_2 + 0.23O_2 \rightarrow 0.64H_2 + 0.34CO_2 + 0.64CO + 0.57CH_4 + 0.23H_2O} \qquad \mathbf{31.1\ \frac{kJ}{mol}} \qquad \text{Equation 8.30}$$

Point P lies on the TBL and meets the ratio requirement. To get to point $\mathbf{r_2}$, i.e. operate on the DME and CO_2 line requires the removal of carbon dioxide, water and unreacted methane. DME is synthesised via the following reaction:

$$\mathbf{0.64CO + 0.64H_2 \rightarrow 0.213CH_3OCH_3 + 0.213CO_2} \qquad \text{Equation 8.31}$$

The yield of DME per mole methane is 0.21 with a 0.55 mole carbon dioxide recycle. The process flow diagram is similar to the one shown above. This process route also allows for DME to be synthesised via the Haldor Topsoe process however the yield is lower, below 0.21 mole DME per mole methane processed.

7.2.3 Summary of all reaction routes

The table below shows a summary of all options. All the values are expressed per mole DME

Options	**Yield DME/mole methane**	**CO_2 recycle**	**Unreacted gases**	**ΔHrn (kJ/mol)**	**Waste H_2O**	**H_2:CO**
1a	0.23	0.89	0.65	-338.7	1.06	1
1b	0.165	0.19	0.67	-517.6	1.41	2
2	0.25	0.88	0.5	-63.7	0.35	1
3	0.2	0.55	0.6	-313.3	0.68	1
4	0.21	0.55	0.57	31.1	0.23	1

Table 12 : Modelling equilibrium summary of options for feed 2

The yield of DME is higher for H_2:CO ratio of 1:1 than that of H_2:CO ratio of 2:1 as expected, option 2 has the highest DME yield per mole methane and has the least amount of unreacted gases. The amount of wastewater produced is also not as high, and it does not require heat input into the system. This makes it the most optimal option amongst the rest.

7.3 Modelling Equilibrium Feed 3

7.3.1 Analyzing Equilibrium for feed 3

The equilibrium thermal balance line for feed 3 lies on the line H_2-CO. It is slightly above the thermal balance line obtained at 100% methane conversion towards H_2 and slightly below towards the CO line (see Figure 42). As a result, point A has a higher H_2:CO ratio than the one obtained at 100% methane conversion and the point B a lower H_2:CO ratio as shown by Table **13**.

Thermal Balance Points	Chemical Equilibrium (H_2:CO)	@ 100% CH_4 conversion (H_2:CO)
A	**4.27**	**2.42**
B	**0.94**	**1.48**

Table 13 : H_2:CO ratio for feed 3 at Chemical Equilibrium vs. H_2:CO ratio @ 100% CH_4 conversion

Point A was obtained by balancing exothermic reaction r_3 with endothermic reaction r_2. Similarly point B was obtained by balancing endothermic reaction r_2 with exothermic reaction r_3. The thermal balance reactions are represented below.

$$\mathbf{A: CH_4 + 0.67H_2O + 0.16\ O_2 \rightarrow 1.08H_2 + 0.16CO_2 + 0.25CO + 0.58CH_4 + 0.42H_2O} \qquad \mathbf{0\ \frac{kJ}{mol}}$$ Equation 8.32

$$\mathbf{B: CH_4 + 0.6CO_2 + 0.2O_2 \rightarrow 0.63H_2 + 0.35\ CO_2 + 0.67CO + 0.58CH_4 + 0.22H_2O} \qquad \mathbf{0\ \frac{kJ}{mol}}$$ Equation 8.33

The reactions which were used to determine the thermal balance points are shown below:

$$\mathbf{CH_4 + CO_2 \leftrightarrow 0.56H_2 + 0.46CO_2 + 0.91CO + 0.63CH_4 + 0.17H_2O} \qquad \mathbf{98.2\ \frac{kJ}{mol}}$$ Equation 8.34

$$\mathbf{CH_4 + H_2O \leftrightarrow 1.26H_2 + 0.14CO_2 + 0.23CO + 0.63CH_4 + 0.49H_2O} \qquad \mathbf{70.6\ \frac{kJ}{mol}}$$ Equation 8.35

$$\mathbf{CH_4 + 0.5O_2 \rightarrow 0.72H_2 + 0.2CO_2 + 0.31CO + 0.49CH_4 + 0.29H_2O \quad -146\frac{kJ}{mol}}$$

Equation 8.36

Point A has a high H_2:CO ratio due to both reactions r_2 and r_3. Reaction r_3 represents the partial oxidation of methane, the expected products are CO and H_2 at 100% methane conversion. However, at the specified operating conditions not all the methane is converted and other products are formed (see Figure 40)

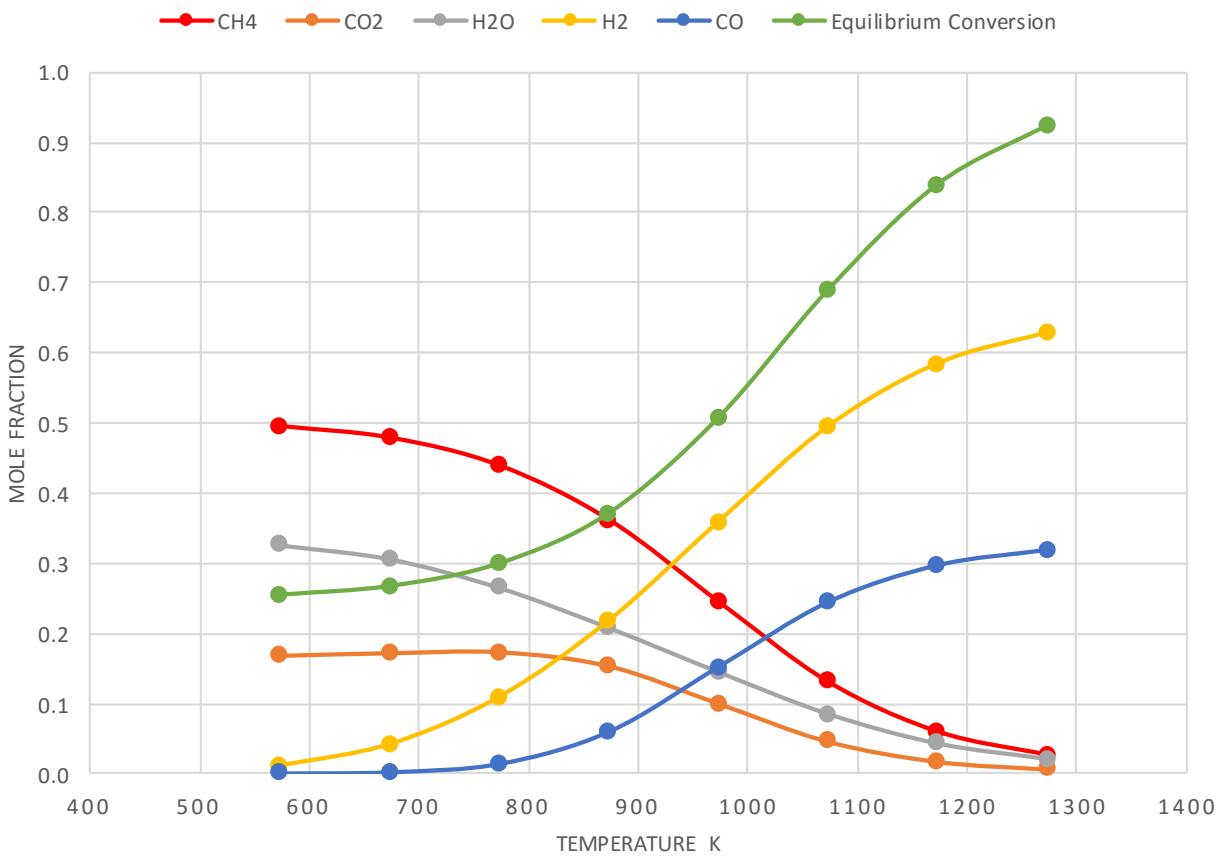


Figure 40 : Conversion of methane over a temperature range 500K to 1300K at an oxygen to carbon ratio of 0.5.

At lower temperatures the exothermic reaction (partial oxidation) which promotes the formation of H_2O and CO_2 is favored and the concentration of CO and H_2 is less than 5%. As the temperature increases the partial oxidation reaction is favoured thermodynamically and the concentration of CO and H_2 begins to increase however the concentration of CO does not increase at the same rate as H_2, as a result the H_2:CO ratio is high.

Similarly, the same temperature effect is observed for steam methane reforming resulting in point A having a high H_2:CO ratio affected by both reactions. It is also expected for steam reforming to produce syngas with a high H_2:CO ratio.

On the other hand, point B is obtained by balancing endothermic reaction r_1 with exothermic reaction r_3. The ratio of H_2:CO obtained at the specified reformer conditions is less than 1. This is more influenced by reaction r_1, the reaction of methane with carbon dioxide. At low temperatures the conversion of methane is low, this is because dry methane reforming is more prone to carbon deposition than other reforming reactions because of a low H/C ratio and the carbon deposition reaction is more favored at lower temperatures (Edwards & Maitra, 1995)

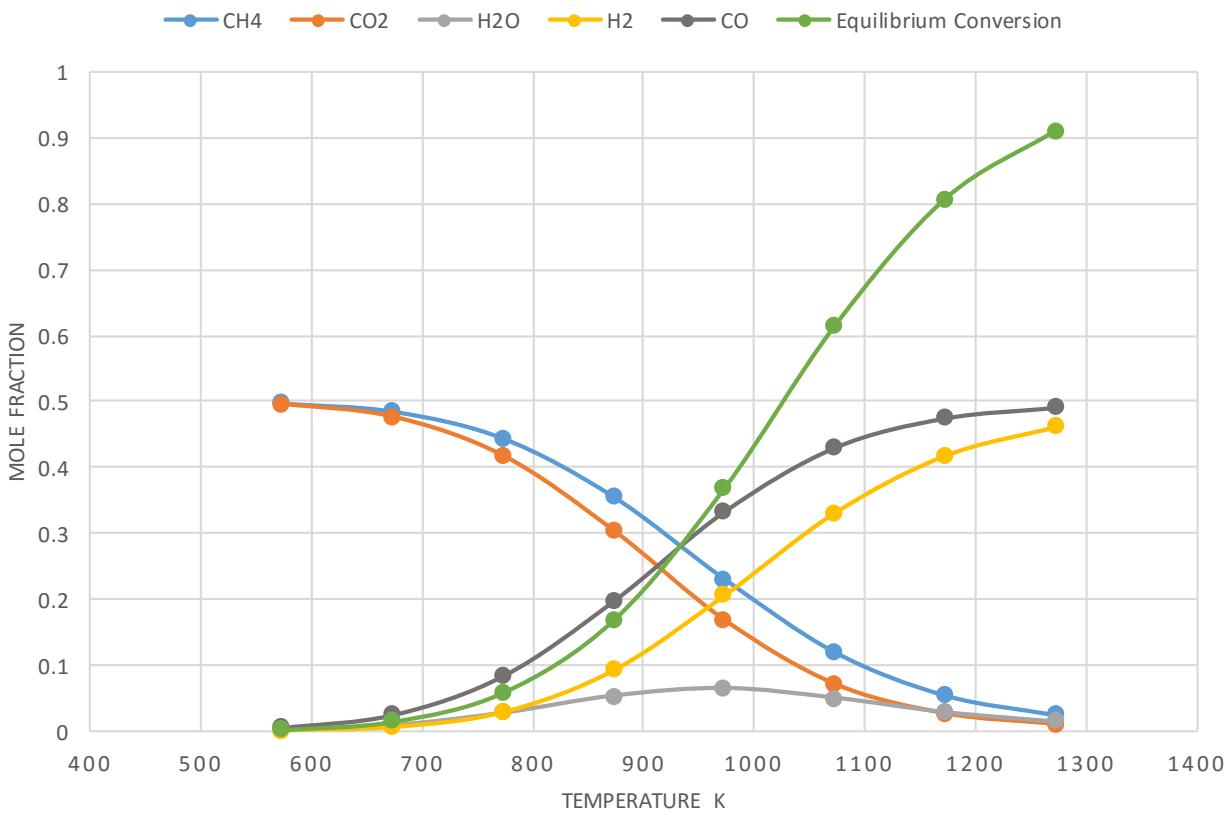


Figure 41 : Conversion of methane over a temperature range 500K to 1300K at a carbon dioxide to methane ratio of 1.

As the temperature increases the fraction of H_2 and CO increases, however H_2 does not increase at the same rate as CO. Hydrogen is consumed by reacting with carbon dioxide via the water gas shift reaction which is also favoured at lower temperatures compared to the main reaction. The desired ratio is achieved at higher temperatures where the selectivity is to H_2 and CO. The effect of reaction r_3 on point B is to push the ratio up to a value close to 1:1.

7.3.2 DME synthesis using feed 3

The graph below shows the thermal balance point A and B compared to the position of the thermal balance points obtained without considering equilibrium.

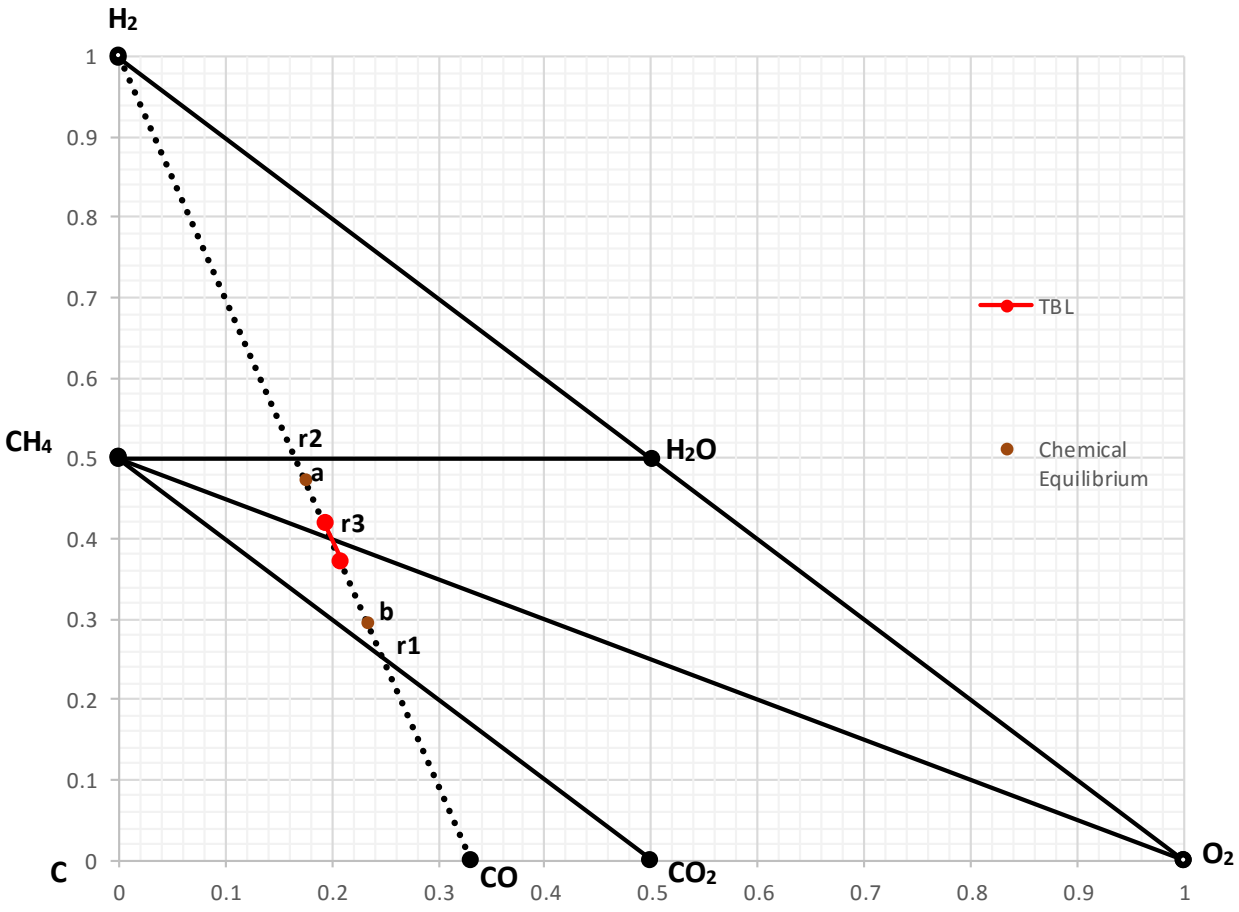


Figure 42 : Modelling Equilibrium – Feed 3

As can be seen on figure 42, the feasible region does not exist – the solution lies on the straight line H_2-CO. Therefore, DME cannot be synthesised using this feed type.

7.4 Comparison of Equilibrium results to Non-Equilibrium results

The objective for modelling chemical equilibrium was to take into consideration the other reactions which also take place during reforming reactions. These reactions where not taken into consideration when modelling non-equilibrium. Instead it was assumed that the reactions run to completion. The side reactions which take place affect the syngas composition and ultimately the H_2:CO ratio. The interesting thing to observe is that the biggest shift is on the H_2-CO line for both feed 1 and feed 2, which affects the H_2:CO ratio. Hence the reported ratios for equilibrium are either higher or lower than the non-equilibrium values. However, the yield of DME is affected largely by the fact that the reaction does not run to completion. With a new restriction the process flowsheets for DME synthesis were developed.

7.4.1 Comparing results for feed 1

The table below compares non-equilibrium results for feed 1 with equilibrium results. The yield of DME in the non-equilibrium scenario is higher than the yield of DME in an equilibrium scenario for all reaction routes considered.

Non-Equilibrium results for Feed 1

Options	**DME yield/mole methane**	**CO_2 recycle**	**CO_2 emissions**	**H_2O waste stream**	**Waste streams (H_2, CO)**	**ΔHrn (kJ/mol)**	**H_2:CO ratio**
1a	0.5	-	-	0.35	0.15	0	2
1b	0.5	-	-	0.5	-	-35.67	2
2a	0.5	-	-	0.18	0.32	0	2
2b	0.5	-	-	0.5	-	-76.82	2

Equilibrium results for Feed 1

Options	**DME yield/mole methane**	**H_2O required in feed***	**Excess H_2**	**Unreacted gases (Including excess H_2)**	**ΔHrn (kJ/mol)**	**H_2:CO ratio**
1	0.127	0.12	0.57	1.33	0	2
2	0.123	0.18	0.70	1.45	0	2
3	0.14	0.22	0.85	1.57	0	2
4	0.14	0.32	1.09	1.81	0	2

Table 14: Comparison of equilibrium and non-equilibrium results for feed 1

The yield of DME for the non-equilibrium results is higher than the yield of DME when equilibrium was considered. For the equilibrium results, the H_2:CO ratio is quite high, due to the thermal balance line shifting to the region of excess hydrogen. As a result, the ratio is not suitable for DME synthesis via the Haldor Topsoe process or the JFE process. To adjust the ratio to that suitable for DME synthesis required removing excess hydrogen resulting in a low DME yield compared to when equilibrium was not considered. The equilibrium reaction is however more thermally balanced than the non-equilibrium reactions.

7.4.2 Comparing results for feed 2

Non-Equilibrium results for Feed 2

Options	**DME yield/mole methane**	**CO_2 recycle**	**CO_2 emissions**	**H_2O waste stream**	**Waste streams (H_2, CO**)**	**ΔHrn (kJ/mol)**	**H_2:CO ratio**
1a	0.33	-	0.33	1	-	-277.5	1
1b	0.5	0.5	-	0.5	-	0	1
1c	0.67	0.67	-	-	-	247.3	1
2a	0.33	1	0.33	1	-	-236.4	1
2b	0.473	1.84	0.053	0.58	-	0	1
** 2c*	0.67	2.67	-	-	-	329.6	1
3a	0.5	-	-	0.5	0.07**	0	2
3b	0.5	-	-	0.5	-	-35.67	2

Equilibrium results for Feed 2

Options	**Yield DME/mole methane**	**CO_2 recycle**	**Unreacted gases**	**ΔHrn (kJ/mol)**	**Waste H_2O**	**H_2:CO**
1a	0.23	0.89	0.65	-338.7	1.06	1
1b	0.165	0.19	0.67	-517.6	1.41	2
2	0.25	0.88	0.5	-63.7	0.35	1
3	0.2	0.55	0.6	-313.3	0.68	1
4	0.21	0.55	0.57	31.1	0.23	1

Table 15: Comparison of equilibrium and non-equilibrium results for feed 2

For feed 2 the yield of DME for the equilibrium results is also lower than the yield for non-equilibrium results. In this case the thermal balance line has shifted to a region of low hydrogen resulting in a low H_2:CO ratio compared to non-equilibrium results. In conclusion the non-equilibrium results have a high DME yield/mole methane processed as would be expected, the

reaction runs to completion. The equilibrium reaction however is restricted and the yield is determined by the extent of reaction and the reactor conditions.

8. Conclusion

Different natural gas reforming technologies result in different syngas compositions. The critical factor is in obtaining the right composition for the desired end-use. As discussed in the literature review, the composition especially the ratio of H_2:CO is very important. Three different feeds were analysed using the ternary bond equivalent diagram in order to develop a conceptual design for DME synthesis. This feeds represented a combination of different natural gas reforming processes used in industry to produce syngas.

Feed 1 involved the reaction between methane, steam and oxygen. A combination of partial oxidation and steam reforming. The feed was restricted to a region within the C, H, O diagram by considering mass and energy balance. The region of operation for this feed type was hydrogen rich and as a result resulted in a syngas composition with an H_2:CO ratio greater than 2. The DME process for this feed type therefore followed the Haldor Topsoe process, with a DME yield of 0.5 mole DME per mole methane processed.

The difference with each process route for feed 1 is the separation required and the amount of waste produced from the process. The byproduct of all the reaction routes for this process is water. The most optimal process route had a DME yield of 0.5 mole DME per mole methane processed and 0.5 mole of water removed from the system.

Feed 2 involved the reaction between methane, oxygen and carbon dioxide. A combination of partial oxidation and dry reforming. The resultant H_2:CO ratio for this feed was less than 2 and it was operating within the CO rich region compared to feed 1. As a result of the ratio obtained with this feed type, the DME synthesis process followed both the Haldor Topsoe process as well as the JFE process. Different process routes resulted in different DME yield depending on the operating point within the C, H, and O diagram. The yield obtained with routes which followed the JFE process was higher than the yield obtained for routes which followed the Haldor Topsoe process and is expected and confirmed in literature. The yield of DME for feed 2 ranged from 0.33 to 0.67 DME per mole methane processed. The difference with each route is also the level of separation required, the carbon dioxide recycle stream, energy requirement and the amount of waste produced from the system.

The optimal DME process route for feed 2 has a DME yield of 0.67 mole per mole methane processed as well as a carbon dioxide recycle stream. We would expect the yield for feed 2 to be higher than that of feed 1 at the same temperature because with feed 1 methanol is produced

first and then water is removed to form DME. The other advantage for most process routes in feed 2 is that the by product is carbon dioxide along with the fact that it is easier to separate from DME than water.

Lastly, feed 3 involved a reaction between oxygen, carbon dioxide and water and the product distribution lies on the straight-line H_2-CO. The feasible region does not exist and therefore DME cannot be synthesised using this feed type.

When considering carbon deposition boundaries, feed 1 is not a feasible reaction route (at specified reaction parameters) due to the formation of carbon. For feed 2, all the optimal reaction routes operate in regions of no solid carbon formation therefore it is feasible to produce DME via these reaction routes.

When chemical equilibrium was considered the yield of DME decreased for both feed 1 and feed 2, due to a low methane conversion.

In conclusion by using the ternary bond diagram a flowsheet can be developed for the production of DME via different natural gas reforming processes. By considering mass and energy balance, carbon deposition boundaries as well as chemical equilibrium. The results of the analysis show that there are more process routes for the production of DME, and each route carries its own advantages and disadvantages. There will usually be a trade-off when selecting the optimal options.

References

1. Aasberg-Petersen, K., Christensen, T. S., Nielsen, C. S. & Dybkjær, I., 2002. Recent Developments in Autothermal Reforming and. *Fuel Chemistry Division Preprints,* 47(1), pp. 96-97.

2. Al-Sayari, S. A., 2013. Recent Developments in the Partial Oxidation of Methane to Syngas. *The Open Catalysis Journal,* Volume 6, pp. 17-28.

3. Ashcroft, A., Cheetham, A., Green, M. & Vernon, P., 1991. Partial Oxidation of Methane to synthesis gas using Carbon Dioxide. *Nature,* Volume 352, pp. 225-352.

4. ATKearney, 2013. *Southern Africa's Oil and Gas Opportunity,* Korea: A.T. Kearney, Inc.

5. Azizi, Z., Rezaeimanesh, M., Tohidian, T. & Reza, M. R., 2014. Dimethyl Ether : A review of technologies and production challenges. *Chemical Engineering and Processing,* Volume 82, pp. 150-172.

6. Bao, B., El-Halwagi, M. M. & Elbashir, N. O., 2010. Simulation, integration, and economic analysis of gas-to-liquid processes. *Fuel Processing Technology,* Volume 91, pp. 703-713.

7. Barelli, L., G. Bidini, F. & Servili, G. S., 2008. Hydrogen production through sorption-enhanced steam methane. *Energy,* Volume 33, pp. 554-570.

8. Battaerd, H. A. & Evans, D. G., 1979. An alternative representation of coal composition data. *Fuel,* Volume 58, pp. 105-108.

9. Bharadwaj, S. & Schmidt, L., 1995. Catalytic partial oxidation of natural gas to syngas. *Fuel Processing Technology ,* Volume 42, pp. 109-127.

10. BP, 2012. *BP Energy Outlook 2030,* s.l.: BP.

11. Cairns, E. J. & Tevebaugh, A. D., 1964. CHO Gas Phase Compositions in Equilibrium with Carbon,. *Chemical and Engineering Data,* 9(3), pp. 453-462.

12. Dennis, B. M. et al., 1991. Novel Technology for th synthesis of Dimethyl Ether from syngas. *Catalysis Today,* Volume 8, pp. 279-304.

13. Douglas, J. M., 1988. *Conceptual Design of Chemical Processes.*

14. Dybkjaer, I., 1995. Tubular reforming and autothermal reforming of natural. *Fuel Processing Technology,* Volume 42, pp. 85-107.

15. Economides, M. J. & Wood, D. A., 2009. The state of natural gas. *Journal of Natural Gas Science and Engineering,* Volume 1, pp. 1-13.

16. Eduardo, F. S., Lucia, G. A. & Claudio, M., 2005. Natural Gas Chemical transformations : The path to refining in future. *Catalysis Today,* Volume 101, pp. 3-7.

17. Edwards, J. H. & Maitra, A. M., 1995. The chemistry of methane reforming with carbon dioxide and. *Fuel Processing Technology*, Volume 42, pp. 269-289.

18. Florian, P. et al., 2011. CO2-based methanol and DME- Efficient technologies for industrial scale Production. *Catalysis Today*, Volume 171, pp. 242-250.

19. Ghosh, T. K., 1971. Change in coal macerals. *Letters to the Editor*, Volume 50, pp. 218-221.

20. Gradassi, M. J. & Green, W. N., 1995. Economics of natural gas conversion processes. *Fuel Processing Technology*, Volume 42, pp. 65-83.

21. Hall, T. J. et al., 1995. Catalytic synthesis of methanol and formaldehyde by. *Fuel Processing Technology 42 (1995) 151-178*, Volume 42, pp. 151-178.

22. International Association of DME, 2010. *IDA Fact Sheet no.2 : DME as a Transportation Fuel*. [Online] Available at: www.aboutdme.org [Accessed 14 November 2015].

23. Kaoru, F., Kenji, A., Tsutomu, S. & Hiro-o, T., 1984. Selective Synthesis of Dimethyl Ether from Synthesis Gas. *Chemistry Letters*, pp. 2051-2054.

24. Ki-Won, J., Hye-Soon, L., Hyun-Seog, R. & Sang-Eon, P., 2002. Catalytic Dehydration of Methanol to Dimethyl Ether (DME) over Solid-Acid Catalysts. *Korean Chemical Society*, 23(6), pp. 803-806.

25. Li, X. et al., 2001. Equilibrium modeling of gasification : a free eneergy minimization aproach and its application to a circulating fluidised bed coal gasifier. *Fuel*, Volume 80, pp. 195-207.

26. Lyubovsky, M., Roychoudhury, S. & LaPierre, R., 2005. Catalytic partial ‘‘oxidation of methane to syngas’’ at elevated pressures. *Catalysis Letters*, 99(3-4), pp. 113-117.

27. Mingting, X., Jack, L. H., Wayne, G. D. & Alak, B., 1997. Synthesis of Dimethyl Ether from Methanol over Solid-acid catalysts. *Applied Catalysis A: General*, Volume 149, pp. 289-301.

28. Miriam, S., Ruaa, A., Ulrich, A. & Manfred, D., 2011. Direct synthesis of Dimethyl Ether from carbon-monoxide-rich synthesis gas: Influence of dehydration catalyst and operating conditions. *Fuel Processing Technology* , Volume 92, pp. 1466-1474.

29. NaturalGas.org, 2013. *NaturalGas.org*. [Online] Available at: http://naturalgas.org/overview/background/ [Accessed 15 June 2014].

30. Olah, G. A., Goeppert, A. & Prakash, S. G., 2009. Chemical Recycling of Carbon Dioxide to Methanol and Dimethyl Ether : From Greenhouse Gas to Renewable, Environmentally Carbon Neutral Fuels and Synthetic Hydrocarbons. *Journal of Organic Chemistry*, 74(2), pp. 487-498.

31. Peer, M., Kamali, M. S., Mahdeyarfar, M. & Mohammadi, T., 2007. Separation of Hydrogen from Carbon Monoxide using a Hollow Fiber Polyimide Membrane: Experimental and Simulation. *Chemical Engineering and Technology,* 30(10), pp. 1418-1425.

32. Pillay, O., 2013. *Evaluation of processes for Landfill Gas Utilization, Dissertation.*

33. Prins, M., Ptasinski, K. & Janssen, G., 2003. Thermodynamics of gas-char reactions: First and Second law analysis. *Chemical Engineering Science,* Volume 58, pp. 1003-1011.

34. Rostrup-Nielsen, J. R. & Rostrup-Nielsen, T., 2001. *Large scale hydrogen production*.

35. Seo, Y., Shirley, A. & Kolaczkowski, S., 2002. Evaluation of thermodynamically favourable operating conditions for production of hydrogen in three different reforming technologies. *Journal of Power Sources,* Volume 108, pp. 213-225.

36. Shen, W.-J., Jun, K.-W., Choi, H.-S. & Lee, K.-W., 2000. Thermodynamic Investigation of Methanol and Dimethyl Ether synthesis from CO2 hydrogenation. *Journal of Chemical Engineering,* 17(2), pp. 210-216.

37. Simpson, A. & Lutz, A., 2007. Exergy analysis of hydrogen production via steam methane reforming. *International journal of hydrogen energy ,* Volume 32, pp. 4811- 4820.

38. Sorenson, S., 2001. Dimethyl Ether in Diesel Engines: Progress and Perspectives. *Journal of Engineering for Gas Turbines and Power,* Volume 123, pp. 652-658.

39. Souza, A. E. A. M. et al., 2008. Comparative evaluation between steam and Autothermal Reforming of Methane Processes to produce syngas. *Brazilian Journal of Petroleum and Gas,* 2(1), pp. 27-35.

40. Takashi, O., Norio, I., Tutomu, S. & Yotaro, O., 2003. Direct Dimethyle Ether Synthesis. *Journal of Natural Gas Chemistry,* 12(4), pp. 219-227.

41. Tavebaugh, A. & Cairns, E., 1965. Carbon deposition boundaries in the CHO system at several pressures. *Journal of Chemical and Engineering Data,* 10(4), pp. 359-362.

42. Tay, D. H. S., Ng, D. K. S., Kheireddine, H. & El-Halwagi, M. M., 2011. Synthesis of an integrated biorefinery via C-H-O ternary diagram. *Clean Techn Environ Policy,* Issue 13, pp. 567-579.

43. Troy, S. A., Rodney, B. A. & Howard, G. L., 2006. Dimethyl Ether (DME) as an alternative fuel. *Journal of Power Sources,* Volume 156, pp. 497-511.

44. Vakili, R., Vakili & Eslamloueyan, R., 2012. Optimal design of an industrial scale dual-type reactor for direct dimethyl ether (DME) production from syngas. *Chemical Engineering and Processing,* Volume 62, pp. 78-88.

45. Wang, L. et al., 2006. Influence of Reaction Conditions on Methanol Synthesis and WGS Reaction in the Syngas-DME Process. *Journal of Natural Gas Chemistry,* 15(1), pp. 38-44.

46. Wei, J., 1979. A stochiometric Analysis of coal Gasification. *Ind. Eng. Chem. Process Des,* 18(3), pp. 554-558.

47. Wei, W., Shengping, W., Xinbin, M. & Jinlong, G., 2011. Recent Advances in catalytic hydrogenation of carbon dioxide. *Chemical Society Reviews,* 40(7), pp. 3703-3727.

48. Yotaro, O. et al., 2006. *New Direct Synthesis Technology for DME (Dimethyl Ether) and its Application Technology,* s.l.: s.n.

49. Zhu, T. & Flytzani-Stephanopoulos, M., 2001. Catalytic partial oxidation of methane. *Applied Catalysis A: General,* Volume 208, pp. 403-417.

Appendix

Appendix A: Bond Equivalent percentages and using the CHO diagram

A1: Calculating the Bond Equivalent percentages

CO_2:

$$C = \frac{4x_C}{4x_C + x_{H_2} + 2x_{O_2}} = \frac{4*1}{4*1+0+2*2} = 0.5$$

$$O = \frac{2x_{O_2}}{4x_C + x_{H_2} + 2x_{O_2}} = \frac{2*2}{4*1+0+2*2} = 0.5$$

H_2O:

Oxygen bond equivalent percentage calculated as above using mole fraction of oxygen in water equal to 1.

$$H = \frac{x_{H_2}}{4x_C + x_{H_2} + 2x_{O_2}} = \frac{1*2}{4*0+1*2+2*1} = 0.5$$

A2: Using the CHO diagram to represent a separation process

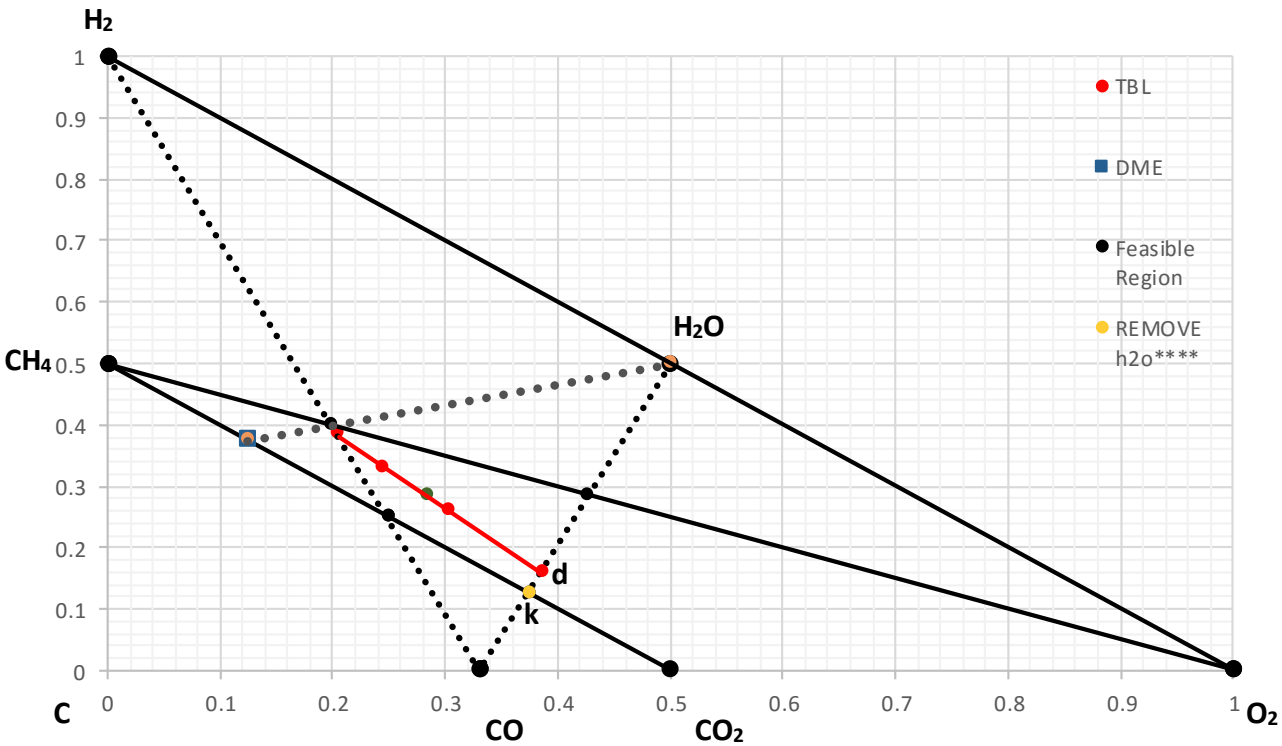


Figure 43 : Using the CHO diagram to represent a separation process

If a mixture is at thermal balance point D and would like to move to point k, the number of moles water to be removed from the system is calculated as follows:

Given the composition at point D (2.84 moles CO and 1 mole H_2O), the aim is to get to point k represented by the ratio CO:H_2O = 2:1

The current point is represented by the following BE percentages:

CO	H20	H2		
2.84	2.00	0.00		
	moles	**mole fraction**	**BE**	**BE%**
C	2.84	0.24	0.97	0.45
H	4.00	0.34	0.34	0.16
O	4.84	0.41	0.83	0.39
Sum	11.67	1.00	2.14	1.00

Table 16 : BE % for point D – Feed 2

The number of moles water to be removed to get to point k is obtained by solving the following equation.

Let α be the total number of moles removed from the system, therefore the ratio becomes:

$$\frac{CO}{H_2O} = \frac{2.84}{2-\alpha} = 2, solve\ for\ \alpha\ to\ satisfy\ the\ equation.$$

To satisfy the ratio the number of moles of water removed from the system is **0.575 moles**.

The new BE% at the new compositions is calculated as follows:

CO	H20	H2		
2.84	1.42	0.00		
	moles	mole fraction	BE	BE%
C	2.84	0.29	1.14	0.500
H	2.84	0.29	0.29	0.125
O	4.25	0.43	0.86	0.375
Sum	9.92	1.00	2.29	1.000

Table 17 : BE% for point K after removing 0.58 moles water from the composition at point D

This represents the BE% at point k

Appendix B: The thermal balanced lines

B1: Determining the thermal balanced line for Feed 1

$$\mathbf{CH_4 + 2H_2O \rightarrow 4H_2 + CO2} \qquad \mathbf{165\ \frac{kJ}{mol}} \qquad \text{Equation B1}$$

$$\mathbf{CH_4 + H_2O \rightarrow 3H_2 + CO} \qquad \mathbf{206\ \frac{kJ}{mol}} \qquad \text{Equation B2}$$

$$\mathbf{CH_4 + 0.5O_2 \rightarrow CO + 2H_2} \qquad \mathbf{-35.7\ \frac{kJ}{mol}} \qquad \text{Equation B3}$$

$$\mathbf{CH_4 + O_2 \rightarrow CO_2 + 2H_2} \qquad \mathbf{-318.\ \frac{6kJ}{mol}} \qquad \text{Equation B4}$$

Step 1: Balance endothermic reactions with exothermic reaction in order to obtain the thermal balanced line.

r1/r3	**4.63**
r2/r3	5.78
r1/r4	0.52
r2/r4	0.65

Table 18 : Balancing endothermic reactions with exothermic reactions for feed 1

Step 2: Therefore, to get the thermal balance point solve the following equation:

$$r1 + 4.63 \times r3 = 0 \frac{kJ}{mol}$$

Step 3: Calculate BE percentage for each element C, H and O in order to obtain the thermal balance point. The BE can be obtained by considering only the products. For this case it is hydrogen, carbon dioxide and carbon monoxide.

Reactions	CH4	H20	O2	H2	C02	CO
r1	1	2	0	4	1	0
r3	4.63	0.00	2.31	9.25	0.00	4.63

Sum	5.63	2.00	2.31	13.25	1.00	4.63

		mole	mole fraction	BE	BE %
	H	26.50	0.68	0.68	0.43
	C	5.63	0.15	0.58	0.36
	O	6.63	0.17	0.34	0.21
	Total	38.76	1.00	1.61	1.00

Table 19: Calculating BE percentage for Feed 1-point B

Therefore, **point B** is given by the point **(0.43,0.36,0.21)** on the CHO diagram.

Point D is obtained in the same manner by balancing r1 with r4

Reactions	CH4	H20	O2	H2	C02	CO
r1	1	2	0	4	1	0
r4	0.52	0.00	0.52	1.04	0.52	0.00
Sum	1.52	2.00	0.52	5.04	1.52	0.00

	Mole	mole fraction	BE	BE %
H	10.07	0.69	0.69	0.45
C	1.52	0.10	0.42	0.27
O	3.04	0.21	0.42	0.27
	14.62	1.00	1.52	1.00

Table 20: Calculating BE percentage for Feed 1-point D

Therefore, **point D** is given by the point **(0.45,0.27,0.27)** on the C,H, and O diagram

Thermal balance points A and C are obtained the same way

Feed 1: Thermal balance points summary

Points	C	H	O
A	0.39	0.42	0.19
B	0.36	0.43	0.21
C	0.33	0.43	0.23
D	0.27	0.45	0.27

Table 21: Thermal balance points for feed 1

B2: Thermal Balance points feed 2

$$CH_4 + 3CO_2 \rightarrow 4CO + 2H_2O \qquad 329.6\ \frac{kJ}{mol} \qquad \text{Equation B5}$$

$$CH_4 + CO_2 \rightarrow 2H_2 + 2CO \qquad 247\ \frac{KJ}{Kmol} \qquad \text{Equation B6}$$

$$CH_4 + 1.5O_2 \rightarrow CO + 2H_2O \qquad -519\ \frac{kJ}{Kmol} \qquad \text{Equation B7}$$

$$CH_4 + 0.5O_2 \rightarrow CO + 2H_2 \qquad -35.7\ \frac{kJ}{mol} \qquad \text{Equation B8}$$

Feed 2 thermal balance points were obtained the same way by balancing the above reactions. The summary for the points A-D is shown on the table below.

Points	C	H	O
A	0.43	0.35	0.22
B	0.45	0.27	0.28
C	0.45	0.26	0.29
D	0.45	0.16	0.39

Table 22: Thermal balance points for feed 2

B3: Thermal Balance points feed 3

$$CH_4 + CO_2 \rightarrow 2H_2 + 2CO \qquad 247.3\ \frac{kJ}{mol} \qquad \text{Equation B9}$$

$$CH_4 + H_2O \rightarrow 3H_2 + CO \qquad 206.18\ \frac{KJ}{Kmol} \qquad \text{Equation B10}$$

$$CH_4 + 0.5O_2 \rightarrow CO + 2H_2 \qquad -35.7\ \frac{kJ}{mol} \qquad \text{Equation B11}$$

Feed 3 thermal balance points were obtained the same way by balancing the above reactions. The summary for the points A-B is shown on the table below

Points	C	H	O
A	0.37	0.45	0.18
B	0.45	0.33	0.22

Table 23: Thermal balance points for feed 3

Appendix C: Testing for the value of alpha to adjust the H_2:CO ratio for each feed within the stoichiometric region

For feed 1

Obtain a linear combination for all reactions r_1 to r_4

Example – Between r_1 and r_2, find the value of alpha such that the ratio is 1 or 2,

$$\alpha r1 + (1 - \alpha) r2 \rightarrow H_2\,(3 + \alpha) + CO(1 - \alpha) + \alpha CO_2$$

and satisfies the condition $0 < \alpha < 1$

For this case the solution does not exist for both cases, α = -1, for H_2:CO =1:1 and α = -0.3 for H_2:CO = 2:1.

The same method was applied for all linear combinations and also for feed 2.

Appendix D: Carbon Deposition Boundaries

The carbon deposition boundaries were plotted by using data from Tay, et al., 2011, the data set is incomplete, as a result the data at the at the initial and end points were estimated from the graphs of carbon deposition boundaries from Tay, et al., 2011 (highlighted in red).

The carbon deposition boundaries are plotted on the graph below and the data shown on the table which follows.

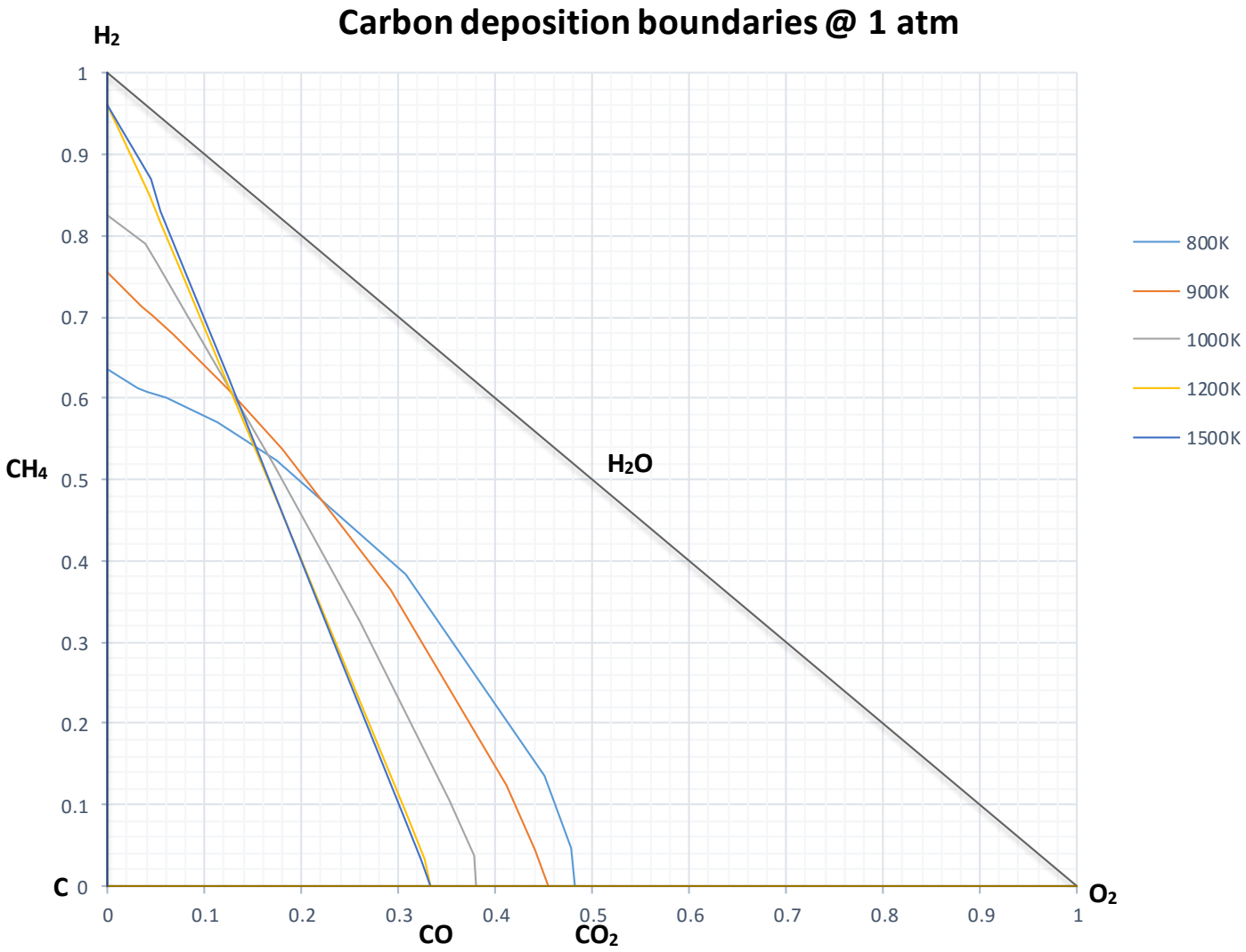


Figure 44 : Carbon deposition boundaries at 1 atm, represented as BE percentages of the equilibrium state

	Mole fraction - Tay, et al, 2011						Calculated BE%		
	H/O	xH2	x CO	xCO2	xH2O	xCH4	C	H	O
							0.518519	**0**	**0.481481**
800K	0.2	0.053	0.0862	0.75	0.1083	0.004	0.474086	0.047844	0.47807
	0.6	0.1331	0.0731	0.54	0.2309	0.025	0.4149	0.135038	0.450062
	2.5	0.3146	0.0428	0.18	0.3191	0.1394	0.308437	0.384178	0.307385
	6	0.4214	0.0244	0.06	0.2441	0.2501	0.300918	0.524334	0.174748
	10	0.4671	0.0164	0.03	0.182	0.3073	0.316368	0.56967	0.113961
	20	0.5088	0.009	0.01	0.1092	0.3647	0.340102	0.599964	0.059934
	30	0.5245	0.0062	0	0.0777	0.3876	0.351248	0.608258	0.040495
	40	0.5328	0.0048	0	0.0603	0.3999	0.357551	0.611833	0.030616
							0.363636	**0.636364**	**0**
							0.545455	0	0.454545
900K	0.2	0.0807	0.31	0.55	0.0614	0.0021	0.516015	0.043999	0.439987
	0.6	0.1996	0.2636	0.39	0.1293	0.0129	0.466208	0.123185	0.410606
	2.5	0.4575	0.1574	0.14	0.1769	0.0675	0.345509	0.363559	0.290932
	6	0.6046	0.0922	0.05	0.137	0.1179	0.283956	0.537033	0.179011
	10	0.6673	0.0631	0.02	0.1034	0.1437	0.265417	0.612114	0.122469
	20	0.7249	0.0354	0.01	0.0631	0.1695	0.254854	0.677406	0.067741
	30	0.7467	0.0247	0	0.0452	0.1799	0.25304	0.700207	0.046753
	40	0.7583	0.0189	0	0.0352	0.1855	0.252415	0.712058	0.035526
							0.244898	0.755102	0
							0.62069	**0**	**0.37931**
1000K	0.2	0.0901	0.6455	0.24	0.0232	0.0008	0.583789	0.037828	0.378383
	0.6	0.2243	0.5483	0.17	0.0491	0.0049	0.542117	0.105648	0.352235
	2.5	0.5211	0.3243	0.06	0.0675	0.0264	0.416102	0.324365	0.259533
	6	0.6936	0.1874	0.02	0.0519	0.0469	0.312654	0.515541	0.171806
	10	0.7676	0.1268	0.01	0.0389	0.0574	0.259279	0.617245	0.123476
	20	0.8354	0.0703	0	0.0235	0.068	0.205098	0.722565	0.072336
	30	0.861	0.0487	0	0.0167	0.0722	0.183235	0.765675	0.05109
	40	0.8745	0.0372	0	0.013	0.0745	0.171324	0.789233	0.039443
							0.173913	**0.826087**	**0**
							0.666667	**0**	**0.333333**
1200K	0.2	0.0901	0.8923	0.02	0.0021	0.0001	0.64085	0.032618	0.326532
	0.6	0.2284	0.7553	0.01	0.0045	0.0008	0.601529	0.091943	0.306528
	2.5	0.548	0.4373	0	0.0063	0.0047	0.467656	0.295735	0.236609
	6	0.739	0.2465	0	0.0048	0.0086	0.335625	0.498265	0.16611
	10	0.8208	0.1645	0	0.0035	0.0106	0.257158	0.619096	0.123746
	20	0.8953	0.0898	0	0.0021	0.0126	0.168183	0.756168	0.07565
	30	0.9232	0.0618	0	0.0015	0.0134	0.129204	0.816318	0.054478
	40	0.9379	0.0471	0	0.0012	0.0138	0.107143	0.850369	0.042488
							0.038835	**0.961165**	**0**
							0.666667	**0**	**0.333333**
1500K	0.2	0.0908	0.9085	0	0.0001	0	0.645003	0.032247	0.32275
	0.6	0.2304	0.7688	0	0.0003	0.0001	0.605891	0.090927	0.303182
	2.5	0.5543	0.4443	0	0.0004	0.0008	0.470713	0.29409	0.235198
	6	0.7482	0.25	0	0.0003	0.0014	0.33422	0.499402	0.166379
	10	0.8313	0.1667	0	0.0002	0.0017	0.251606	0.623711	0.124683
	20	0.9068	0.091	0	0.0001	0.0021	0.156681	0.766661	0.076658
	30	0.9352	0.0625	0	0.0001	0.0022	0.114341	0.830344	0.055315
	40	0.95	0.0476	0	0.0001	0	0.0871	0.869259	0.043641
							0.038835	**0.961165**	**0**

Table 24: Carbon deposition boundaries at 1 atm and temperature range 800K to 1500K **(Tay, et al., 2011)**